Segmentation et caractérisation des dunes sous-marines dans le Fleuve St-Laurent

Thèse

Willian Ney Cassol

Doctorat en sciences géomatiques
Philosophiæ doctor (Ph. D.)

Québec, Canada

Segmentation et caractérisation des dunes sous-marines dans le Fleuve Saint-Laurent

Thèse

Willian Ney Cassol

Sous la direction de :

Sylvie Daniel, directrice de recherche
Éric Guilbert, codirecteur de recherche

Résumé

Dans le Fleuve Saint Laurent, l'acquisition des données bathymétriques permet non seulement de produire des cartes de navigation, mais aussi d'appuyer toute activité visant à améliorer la compréhension de la dynamique du fond marin ainsi que des structures qui y sont présentes, notamment les structures sédimentaires telles que les dunes sous-marines. Ce travail de recherche est consacré à la segmentation et à la caractérisation des dunes sous-marines, tout en considérant la qualité des données acquises. En premier lieu, un modèle d'analyse de l'influence de la morphologie du fond marin sur la valeur de l'incertitude des données bathymétriques a été conçu. Une telle analyse permet de mieux connaître et comprendre l'influence du fond sur la valeur d'incertitude calculée par des approches classiques. Ainsi, la méthode proposée permet d'améliorer l'interprétation de la surface du fond et des structures qui y sont présentes. Par la suite, le projet a conçu et développé une méthode de segmentation des dunes à partir d'un Modèle Numérique Bathymétrique, adaptée au contexte fluviomarin. L'originalité de cette méthode repose sur l'utilisation d'un modèle conceptuel qui formalise l'identification des dunes sous-marines selon leurs saillances (i.e. ligne de crête et deux pieds de dunes). En effet, les dunes sont des structures floues sans une délimitation claire sur le fond marin. Dans la méthode proposée, les saillances sont identifiées à partir d'une analyse morphométrique du fond marin. Ensuite, une approche orientée-objet permet de générer les objets dunes à partir de ces saillances. La démarche associe chacune des lignes de crête aux pieds des dunes qui lui correspondent, permettant ainsi de circonscrire l'ensemble de la dune. L'approche orientée-objet offre une objectivité, répétabilité et robustesse à la segmentation, lui permettant de s'adapter au contexte variable des fonds. La méthode proposée a été validée avec les données bathymétriques de la Traverse Nord du Fleuve Saint Laurent, avec plus de 850 dunes segmentées et un taux de performance de 92% des dunes bien segmentées. Finalement, la dernière partie du projet a été consacrée à la caractérisation des dunes. Celle-ci repose également sur la formalisation des objets dunes. En considérant les saillances et la surface de la dune segmentée, la méthode conçue et développée calcule différents descripteurs morphologiques, sélectionnés à partir de la littérature. Pour valider la méthode de caractérisation proposée, plus de 1200 dunes ont été caractérisées dans neuf champs différents dans le contexte fluviomarin de la Traverse Nord du Fleuve Saint-Laurent. Ainsi, basé sur les méthodes de segmentation et de caractérisation des dunes, un outil qui permet de décrire de manière systématique autant les dunes individuelles que les champs où elles sont localisées à partir d'une surface modélisant le fond marin a été développé dans ce projet de recherche.

Abstract

In the Saint-Lawrence River, the acquisition of bathymetric data not only allows the production of navigation charts, but also supports different activities aiming to improve the knowledge related to the seafloor dynamics and the structures present on it, particularly sedimentary structures such as underwater dunes. This research work is dedicated to the segmentation and characterization of underwater dunes, considering the quality of the bathymetric data acquired. In the first place, a model was designed to estimate the influence of the seafloor morphology on the value of the uncertainty of bathymetric data. The analysis of such influence allows a better knowledge and understanding of the influence of the seafloor on the uncertainty value calculated by classical approaches. Therefore, the proposed model allows a better interpretation of the underwater structures as well as the seafloor surface. Afterwards, the project has designed and developed a method of dune segmentation from a Digital Bathymetric Model. This approach is adapted to the fluviomarine context. The originality of this method lies in the use of a conceptual model that formalizes the identification of underwater dunes considering their salient features (i.e. crest line, stoss trough and lee trough). Underwater dunes are fuzzy structures without a clear delineation on the seafloor. In the proposed method, the salient features are identified from a morphometric analysis of the seafloor. Then, an object-oriented approach is used to generate dune objects from these salient features. The approach matches each crest line with its respective troughs allowing to circumscribe the dune objects. This object-oriented approach offers objectivity, repeatability and robustness to the segmentation, allowing it to adapt to the variable context of the seafloor. The proposed method was validated with bathymetric data from the Northern Traverse of the Saint-Lawrence River, with more than 850 segmented dunes and a performance rate of 92% of well-segmented objects. Finally, the last part of the project was dedicated to the characterization of the dunes. This approach is also based on the formalization of dune object by the conceptual model. By considering the salient features and the entire surface of the segmented dunes, the designed and developed method calculates different morphological descriptors, selected from the literature. To validate the proposed characterization method, more than 1200 dunes were characterized in nine different dunes fields in the fluviomarine context of the Northern Traverse of the Saint-Lawrence River. Thus, a tool that allows a systematic way to describe both individual dunes and the fields where they are located has been developed in this project.

Table des matières

Liste des figures

Liste des tableaux

À mon épouse Vicky et à mon petit Ian

Comece do princípio...
e quando chegar ao fim, pare.
A lebre e o Chapeleiro. Alice in wonderland, 1951.

Remerciements

Avant d'exposer les résultats de mon projet de doctorat, je tiens à remercier toutes les personnes qui m'ont aidé et soutenu tout au long de ces derniers 3 ans et 6 mois.

Mes premiers mots de remerciement sont à ma directrice de recherche, Sylvie Daniel, et à mon codirecteur de recherche, Éric Guilbert. Votre encadrement et vision scientifique m'ont vraiment permis de comprendre le sens de la citation d'Isaac Newton « if I have seen further, it is by standing upon the shoulders of giants ».

Je tiens à remercier la confiance que Sylvie Daniel m'a accordée pour la réalisation de ce projet de recherche. J'ai vraiment apprécié votre disponibilité pour les nombreuses heures consacrées aux rencontres hebdomadaires qui ont permis de faire avancer le projet toujours dans la bonne direction. Également, vos corrections et suggestions toujours précises des documents produits au long de mon projet ont été bien appréciées, particulièrement dans la rédaction des articles scientifiques. Merci également pour toutes les opportunités que vous m'avez offertes pour la participation dans les rencontres de rassemblement de la communauté scientifique. Je me suis toujours senti encouragé par vous durant mon parcours doctoral, que ce soit dans la soumission des bourses, des présentations scientifiques, dans la participation à la vie étudiante ou encore dans l'enseignement académique. Je vous remercie de votre confiance vis-à-vis de mon implication dans l'école d'été 2019 et l'école d'automne 2021. Merci de vos bons conseils pour plusieurs questions existentielles liées à la vie académique. Merci énormément de votre support et encouragement.

Je tiens également à remercier mon codirecteur de recherche, Éric Guilbert. Je vous remercie de votre disponibilité pour avoir participé à toutes nos rencontres hebdomadaires et de vous être assuré que le projet était toujours dans la bonne direction. J'ai beaucoup apprécié la pertinence de vos commentaires et suggestions, que ce soit par rapport aux sujets de la recherche ou par rapport les documents rédigés durant mon doctorat. Vous m'avez aussi encouragé à participer de la vie étudiante et des différentes conférences, de faire la soumission pour les différentes bourses et pour ma participation dans l'enseignement académique. J'ai vraiment apprécié votre support et encouragement.

Je remercie Nathalie Debese d'avoir accepté d'être membre dans le comité d'encadrement de mon projet de recherche. Les commentaires et suggestions ont beaucoup contribué à l'avancement autant de mon projet que du premier article scientifique que compose cette thèse. Je vous remercie d'y avoir consacré du temps.

Julie Simard, Geneviève Béchard et Ian Church sont reconnus pour leurs travaux et contributions à la communauté scientifique et professionnelle. Je tiens à vous remercier vivement d'avoir accepté d'évaluer ce travail de recherche.

Sans le soutien financier je n'aurais pas été capable de poursuivre aux études doctorales. Pour cette raison je voudrais remercier le FRQNT (Fonds de Recherche du Québec – Nature et Technologies) et Mitacs Accélération d'avoir financé ce projet. J'ai reçu également du financement provenant des bourses d'études offertes par : le Fond Joncas, le Canadien National (CN), l'Association Canadienne de Sciences Géomatiques (ACSG), l'Association Géomatique Municipale du Québec (AGMQ) et les bourses à la réussite offertes par la Faculté de Foresterie, Géographie et Géomatique (FFGG). Merci énormément de m'avoir soutenu financièrement dans mes études doctorales.

Je n'aurais pas pu compléter mon projet sans avoir accès à la donnée. Je tiens ainsi à remercier le Service Hydrographique du Canada (SHC) qui a toujours été ouvert à fournir des données bathymétriques pour ce projet de recherche. Je remercie Groupe Océan, spécialement Sylvain Babineau, de m'avoir donné accès à une base de données formidable qui a permis la validation des méthodes proposées dans ce projet de recherche. Je tiens également à remercier le CIDCO (Centre de recherche et développement en cartographie côtière et océanique) pour les échanges et le stage réalisé durant la première phase du projet de doctorat.

Je tiens à remercier la FFGG et le Département des Sciences Géomatiques de l'Université Laval pour la disponibilité des différents logiciels utilisés dans cette recherche, de l'infrastructure et la disponibilité des ressources qui ont toujours répondu aux questions d'ordre administratif.

Je remercie le COMREN (Canadian Ocean Mapping Research Network) qui a financé ma participation aux conférences CHC-NSC 2018, USHydro 2019, CHC 2020, USHydro 2021 et CHC 2022. La participation à ces conférences a permis de rencontrer la communauté scientifique et professionnelle du domaine hydrographique.

Merci également aux experts qui ont participé à la validation des résultats obtenus à la troisième phase du projet, Sylvain Babineau et Marie-Ève Biron (Groupe Océan), Damien Pham Van Bang (INRS) et Gabriel Joyal (Garde côtière canadienne). Plus globalement, je tiens à remercier Marc Cocard et Stéphanie Bourgon pour les discussions liées aux résultats obtenus à la troisième phase du projet.

J'aimerais remercier mon ami et collègue Vincent Dupont. Tout d'abord, ta participation à la première et deuxième phase de mon projet a contribué directement à son avancement. Ensuite, les nombreuses discussions que nous avons eues sur les sujets les plus variés ont été vraiment appréciées. En plus, nous avons eu effectivement la chance de voyager à plusieurs conférences d'envergure dans le domaine et connaître un peu plus de l'Amérique du Nord. À Seattle, tu as pu constater que j'ai vraiment peur des hauteurs. Merci pour ton support et encouragement, autant dans mon projet que pour monter le Space Needle.

Je tiens également à remercier les collègues de l'AGREGE de m'avoir fait confiance pour les représenter dans les différents postes du conseil exécutif de l'association. Plus spécifiquement, j'aimerais remercier Pauline Perbet, Reza Mahmoudi Kouhi, Olivier Stocker, Olivier Matte, Thanh Huy Nguyen, Philippe Blais, Niloufar Haghighatgou et Juzer Noman pour les belles discussions sur nos projets et la vie étudiante.

Merci à mon épouse, Vicky Binette. Tu m'as supporté dans la décision de poursuivre aux études doctorales. Tu as toujours été présente et compréhensive en m'écoutant et me donnant des forces dans toutes les périodes de stress, de fatigue et d'euphorie. Merci de m'avoir supporté malgré les soupers tardifs et les fins de semaines courtes, sans beaucoup de vacances. Merci à mon petit Ian, qui depuis 7 mois m'encourage tous les jours avec des sourires et des petites morsures!

Pai, mãe, Matheus, muito obrigado pelo apoio que vocês sempre me deram, mesmo estando do outro lado da América. Également, merci à ma famille élargie de votre encouragement tout au long de mon doctorat.

De modo geral, agradeço três pessoas que ajudaram a despertar o meu interesse pela pesquisa científica: os professores Dr. Luis A. K. Veiga e Dra. Maria Aparecida Z. Zanetti e ao Pe. Aleixo W. De Souza. Vocês foram os primeiros a acreditar em meu potencial e a me financiar em projetos de pesquisa. Muito obrigado.

Je tiens à remercier Dieu de m'avoir donné les forces de compléter ce projet de doctorat.

Finalement, merci à tous ceux et celles qui ont contribué à la réalisation de ce projet.

Avant-propos

Cette thèse contient trois articles scientifiques soumis dans des revues à comité de lecture. Les articles sont intégrés dans les chapitres 1, 2 et 3 respectivement.

Le chapitre 1 contient l'article « Cassol, W. N., Daniel, S., Guilbert, É. and Debese, N. **An empirical study of the influence of seafloor morphology on the uncertainty of bathymetric data**. *Marine Geodesy,* 2022. https://doi.org/10.1080/01490419.2022.2075499 ». Cet article a été soumis le 28 septembre 2021 à la revue *Marine Geodesy* et a été publié le 18 mai 2022. Quelques changements ont été apportés entre la version publiée dans la revue scientifique et le chapitre de la thèse. Ils concernent la transformation de l'article en chapitre de thèse. Le titre de l'article est devenu le titre du chapitre 1. Également, les sections et sous-sections ainsi que les figures et tableaux ont été numérotés selon le format adopté pour le document de thèse.

Le chapitre 2 contient l'article « Cassol, W. N., Daniel, S. and Guilbert, É. **A segmentation approche to identify underwater dunes from digital bathymetric models**. *Geosciences*, 2021, 11, 361. https://doi.org/10.3390/geosciences11090361 ». Cet article a été soumis le 23 juin 2021 à la revue *Geosciences* et a été publié le 25 août 2021. Quelques changements ont été apportés entre la version publiée dans la revue scientifique et le chapitre de la thèse. Ils concernent la transformation de l'article en chapitre de thèse. Le titre de l'article est devenu le titre du chapitre 2. Également, les sections et sous-sections ainsi que les figures, les tableaux et les références ont été numérotés selon le format adopté pour le document de thèse.

Le chapitre 3 contient l'article « Cassol, W. N., Daniel, S. and Guilbert, É. **An approach for the automatic characterization of underwater dunes in fluviomarine context**. *Geosciences*, 2022, 12, 89. https://doi.org/10.3390/geosciences12020089 ». Cet article a été soumis le 20 janvier 2022 à la revue *Geosciences* et a été publié le 16 février 2022. Quelques changements ont été apportés entre la version soumise à la revue scientifique et le chapitre de la thèse. Ils concernent la transformation de l'article en chapitre de thèse. Le titre de l'article est devenu le titre du chapitre 3. Également, les sections et sous-sections ainsi que les figures, les tableaux et les références ont été numérotés selon le format adopté pour le document de thèse.

Statut de l'auteur et sa contribution : Willian Ney Cassol, auteur de cette thèse, est le premier auteur des trois articles mentionnés précédemment. Dans les trois articles, il a contribué à la conceptualisation, au développement de la méthodologie, à la validation des méthodes proposées, à la génération et à l'analyse des résultats ainsi qu'à l'écriture, révision et édition de tout le contenu des articles sous la supervision de sa directrice de recherche et de son codirecteur de recherche.

Introduction

Mise en contexte

Le Fleuve Saint-Laurent draine un bassin versant de plus d'un million de km^2 le long de son parcours d'approximativement 550 km entre les Grands Lacs Laurentiens et la Ville de Québec, avec un débit moyen annuel de 12.600 m^3/s, le deuxième plus grand en Amérique du Nord (Hudon et Carignan, 2008). Étant donné sa localisation stratégique, c'est un axe de développement majeur du Québec et une importante porte d'entrée de marchandises au Canada. Avec une voie navigable achalandée et un environnement dynamique, la sécurisation de la navigation est un enjeu crucial, rendant impératif l'acquisition de données bathymétriques (i.e. de profondeur) qui permettent de déterminer la configuration générale du fond marin. La connaissance de la morphologie du fond marin est également utilisée dans l'étude des habitats marins (Van Dijk et al., 2012) et dans les modèles de simulation hydrologique et de transport de sédiments. Ces derniers sont requis dans le cadre des études portant sur l'érosion côtière et la prévention du risque d'inondation dans les zones côtières. De telles opérations d'acquisition et ultérieurement de traitement de données bathymétriques s'inscrivent dans le domaine de l'hydrographie. Ce dernier est le domaine des sciences appliquées qui traite du mesurage et de la description des éléments physiques des océans, mers, fleuves et tout environnement fluviomarin, ainsi que des changements de la surface du fond marin dans l'intérêt premier de sécuriser la navigation et appuyer toute activité humaine dans l'environnement maritime et fluvial (OHI, 2011).

Dans le Saint Laurent, l'acquisition des données bathymétriques permet non seulement de produire des cartes de navigation, mais aussi d'appuyer toute activité visant à améliorer la compréhension de la dynamique du fond marin ainsi que des structures qui y sont présentes, notamment les structures sédimentaires. Celles-ci ont une grande diversité de formes et de dimensions. Leur formation et leur évolution sont liées aux conditions météorologiques et hydrodynamiques, aux sédiments transportés par le courant et à l'interaction du sédiment transporté avec la surface du fond marin (Drapeau, 1992; Boggs, 2006; Garlan, 2007; Nichols, 2009). Les dunes sous-marines sont un exemple de ces structures ayant des hauteurs variables allant de 7,5 cm à plus de 5 m, et des largeurs variant entre 60 cm et plus de 100 m sur la surface du fond marin (Ashley, 1990). Elles sont fréquemment identifiées en utilisant une surface modélisant le fond marin construite à partir de données bathymétriques. Tel que mentionné par Lucieer et al. (2016), la résolution de la surface du fond marin générée à partir des données bathymétriques est intimement liée à leur incertitude.

Les méthodes d'identification et de caractérisation des dunes sous-marines à partir de ces surfaces sont peu automatisées, même si les informations concernant ces dunes ont une multitude d'applications. Ce travail est encore essentiellement effectué manuellement par les différents utilisateurs des données bathymétriques. Il s'avère en général fastidieux, subjectif, imprécis et peu adapté à de gros flux de données. Ainsi, quelques

initiatives de recherche ont été menées afin d'automatiser le procédé d'identification des dunes au moyen d'approches de segmentation (Debese et al., 2016; Di Stefano and Mayer, 2018; Ogor, 2018, Lebrec et al., 2022). Néanmoins, ces méthodes considèrent la segmentation des dunes sous-marines dans un contexte marin plutôt que fluviomarin, caractéristique du Fleuve Saint-Laurent. Il existe des différences significatives entre les dunes formées dans ces deux contextes, comme par exemple, leur disposition sur la surface du fond marin ou encore le dynamisme lié à leur évolution sur le fond. Ainsi, le besoin d'une méthode efficiente et objective de segmentation et de caractérisation des dunes sous-marines adaptée au contexte fluviomarin du Fleuve Saint-Laurent reste à combler. Une telle méthode permettrait, entre autres, de mieux comprendre la dynamique morpho-sédimentaire des environnements fluviomarins et de mettre à jour les informations associées à la navigation et à la maintenance des voies navigables.

Problématique

La segmentation et la caractérisation des dunes sous-marines est effectuée à partir de la surface modélisée du fond marin. En général, cette modélisation s'appuie sur des données bathymétriques acquises à partir d'une plateforme hydrographique. Celle-ci est composée de plusieurs capteurs, à savoir d'au moins un récepteur GNSS (*Global Navigation Satellite System*), d'une centrale inertielle et d'un sondeur acoustique. Différents sondeurs peuvent être considérés lors de l'acquisition des données bathymétriques. Celui qui est le plus employé pour la modélisation du fond est le sondeur multifaisceaux. Une sonde pour mesurer la vitesse du son dans la colonne d'eau doit être associée à ce dernier. Les données acquises par la plateforme hydrographique permettent de générer un nuage de points géoréférencés où chaque point dispose d'une coordonnée *X, Y, Z* représentative de la surface du fond marin. La Figure 0.1 schématise la plateforme hydrographique ainsi que les différents capteurs qui la composent.

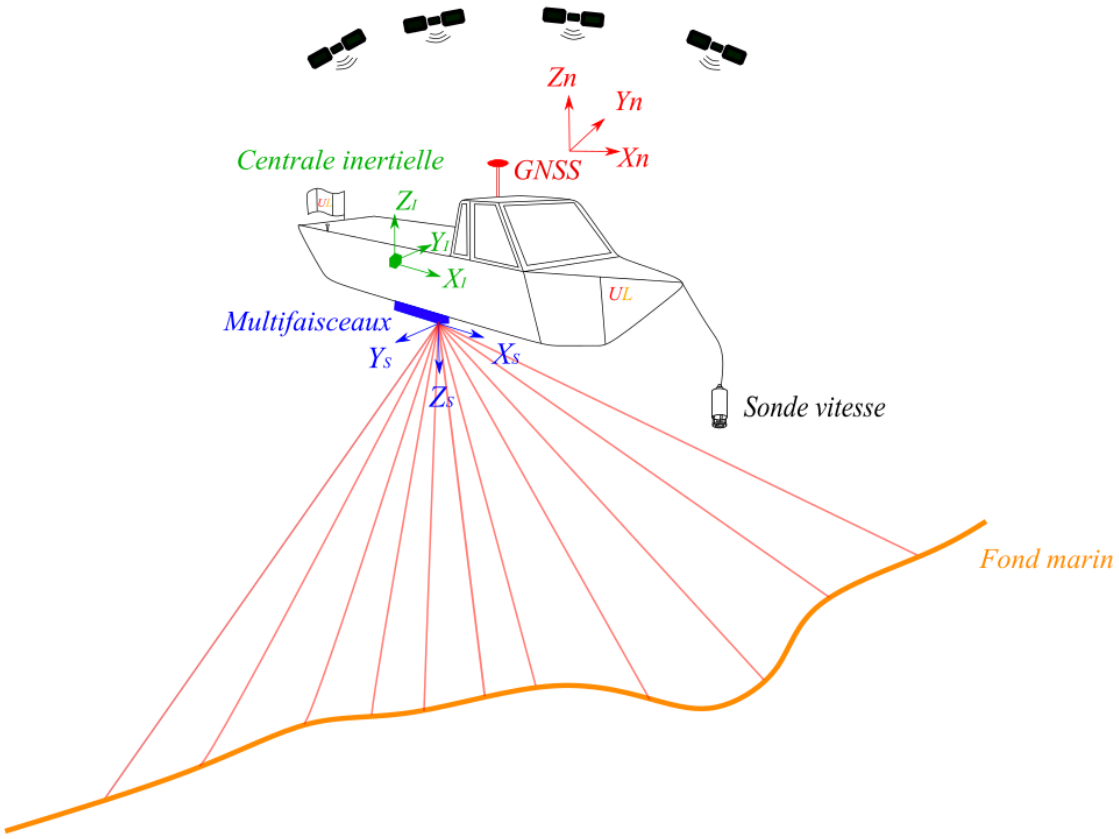

Figure 0.1 – Capteurs composant un système d'acquisition de données bathymétriques embarqués sur un navire hydrographique.

Le géoréférencement des points (aussi appelés points de sonde ou points bathymétriques) est réalisé en utilisant le modèle de géoréférencement direct. Chaque mesure acquise a une valeur d'incertitude associée qui est propagée aux coordonnées des points représentant la surface du fond marin. Le modèle le plus courant dans la littérature pour estimer l'incertitude associée aux données bathymétriques acquises avec des systèmes multifaisceaux est celui défini par Hare (1995), et intitulé TPU (*Total Propagated Uncertainty*). Cette valeur d'incertitude est un facteur déterminant lors de la définition de la résolution d'un Modèle Numérique Bathymétrique (MNB), comme mentionné par le Service Hydrographique du Canada (SHC, 2012). Le MNB est une grille régulière qui modélise la surface du fond à partir du nuage de points bathymétriques. La propagation de l'incertitude par le modèle de TPU est bien maîtrisée dans la littérature et implémentée dans les différents logiciels de traitement des données bathymétriques. Néanmoins, peu d'études ont été effectuées concernant l'influence de la morphologie du fond sur la valeur de l'incertitude des données bathymétriques. Hughes Clarke (2018) a identifié la morphologie du fond comme un facteur contributeur pour la résolution du MNB, spécifiquement les dénivelés du fond marin et les angles rasants associés au levé des données bathymétriques. Le manque de connaissance sur l'influence de la morphologie sur l'incertitude des données bathymétriques est

un enjeu étant donné les fausses interprétations du fond marin et des structures qui y sont présentes qu'il peut induire, ayant ainsi un impact direct sur la segmentation des dunes à partir des MNB.

Comme indiqué précédemment, la segmentation et la caractérisation des dunes sont essentiellement effectuées manuellement, le plus souvent en considérant le fond marin modélisé par un MNB. Les dunes, tout comme d'autres formes de relief, sont des objets flous, sans une délimitation claire sur le fond marin. Ainsi, l'identification des dunes dans le MNB est subjective et liée au contexte de l'utilisateur. Différentes approches ont été proposées pour segmenter les dunes dans le contexte marin (ex. Debese et al., 2016; Ogor, 2018; Di Stefano and Mayer, 2018). Néanmoins, elles ne formalisent pas explicitement les éléments constitutifs d'une dune sous-marine, ce qui permettrait alors de les identifier objectivement dans le MNB. De plus, la proximité et l'adjacence entre les dunes peuvent s'avérer un problème lors de l'identification de leurs éléments constitutifs. Également, d'autres structures sédimentaires peuvent se superposer sur les dunes sous-marines (e.g. rides), ce qui peut nuire à leur segmentation.

La caractérisation des dunes segmentées est effectuée à l'aide de différents descripteurs morphologiques (e.g. Di Stefano and Mayer, 2018; Ogor, 2018; Lebrec et al., 2022). La caractérisation des dunes est importante, car elle peut mettre en évidence des différences dans les conditions environnementales affectant certaines régions du fond marin et conditionnant la formation et l'évolution de ces structures sur le fond marin. Néanmoins, l'estimation de ces descripteurs varie, dépendamment de leur définition, comme cela est discuté par Van Der Mark and Blom (2007), Gutierrez et al. (2013) et Ogor (2018). Ainsi, il reste des progrès à faire relatifs aux descripteurs morphologiques afin que leur définition et leur mise en œuvre puisse se faire de manière robuste et répétable à partir de la surface numérique du fond marin.

Question de recherche

Compte tenu du besoin d'une méthode efficiente et objective de segmentation et de caractérisation des dunes sous-marines adaptée au contexte fluviomarin et des problématiques inhérentes aux démarches visant à le combler, la question de recherche à laquelle ce projet de doctorat se consacre est la suivante : Comment, à partir des données bathymétriques, segmenter et caractériser les dunes sous-marines présentes dans des environnements fluviomarins, tout en considérant un formalisme explicite des dunes et l'influence de la morphologie du fond dans la valeur de l'incertitude des données acquises?

Revue de littérature

Afin d'apporter des éléments de réponse à la question de recherche, une revue de littérature portant sur les travaux en lien avec les problèmes identifiés est proposée dans cette section.

Modèle de géoréférencement direct

Comme indiqué précédemment, les données bathymétriques sont acquises avec une plateforme hydrographique composée de différents capteurs (cf. Figure 0.1). Afin d'obtenir un nuage de points géoréférencés, les mesures acquises sont géoréférencées par le modèle de géoréférencement direct, tel que proposé par Hare (1995), et utilisé par Debese (2013), Naankeu Wati et al. (2016) et Seube et Keyetieu (2017). Sa forme simplifiée est donnée dans l'équation (0.1).

$$X_n(t) = P_n(t) + C_I^n(t)(C_S^I M_S(t) + b_I) \qquad (0.1)$$

Où :

- X_n représente les coordonnées géoréférencées du point de sonde levé par le système d'acquisition;
- $P_n(t)$ représente le vecteur des coordonnées géographiques de la plateforme ($x_{\mathrm{P_n}}, y_{\mathrm{P_n}}, z_{\mathrm{P_n}}$) mesuré par le récepteur GNSS dans le repère de navigation local n;
- $C_I^n(t)$ est la matrice de transformation entre le repère de navigation local n et le repère de la centrale inertielle (IMU) I qui contient les angles d'attitude de la plateforme (φ, Θ, ψ);
- C_S^I est la matrice de transformation entre le repère de l'IMU I et le repère du sondeur multifaisceaux S qui contient les angles de montage entre ces deux systèmes (φ_b, Θ_b ,ψ_b);
- $M_S(t)$ représente le vecteur qui contient les coordonnées des points sondés dans le repère du multifaisceaux S ;
- b_I représente le vecteur contenant les valeurs des bras de levier entre l'IMU et le multifaisceaux ;
- t représente le temps d'acquisition associé aux mesures enregistrées par les différents capteurs. Cette valeur est considérée dans la synchronisation des capteurs. Elle est également considérée dans l'estimation de la latence existante entre les capteurs telle que définie par Bjorn et Einar (2006) et Naankeu Wati et al. (2016).

Veuillez noter que les angles présents dans la matrice C_S^I et les valeurs de bras de levier contenus dans le vecteur b_I sont déterminés par la calibration du système d'acquisition des données. Également, dans l'équation (0.1), un seul récepteur GNSS est considéré pour simplifier l'équation, mais il est possible d'ajouter d'autres récepteurs GNSS, ainsi que d'autres mesures effectuées par d'autres capteurs lors de l'acquisition des données.

Incertitude des données bathymétriques

Différents travaux dans la littérature ont abordé l'estimation de l'incertitude liée aux données bathymétriques. Hare (1995) a effectué le développement d'un modèle mathématique qui permet l'estimation de l'incertitude des données bathymétriques (i.e. TPU) acquises avec un sondeur multifaisceaux. Ce modèle estime l'incertitude de

chaque point sondé par le système d'acquisition en utilisant la loi de propagation des variances-covariances. Ainsi, le modèle considère l'équation de géoréférencement direct (0.1), les mesures acquises et leur incertitude associée. Également, le modèle considère les paramètres de montage du système estimés par calibration, tel que les angles de montage et les bras de levier. Afin de simplifier l'équation de géoréférencement (0.1), on peut considérer $M_n = C_I^n(t)\, C_S^I M_S\,(t)$ et $b_n = C_I^n(t)\, b_I$ pour obtenir l'équation (0.2).

$$\mathrm{X_n} = \mathrm{P_n} + \mathrm{M_n} + \mathrm{b_n} \quad (0.2)$$

En considérant l'équation (0.2), l'incertitude ($\mathcal{V}$) des points sondés (X_n) est estimée par l'équation (0.3).

$$\mathcal{V}X_n = \mathcal{V}P_n + \mathcal{V}M_n + \mathcal{V}b_n \quad (0.3)$$

Le modèle décrit par l'équation (0.3) considère :

- Les mesures de la position de la plateforme, c'est-à-dire, les coordonnées GNSS ($x_{\mathrm{P_n}}, y_{\mathrm{P_n}}, z_{\mathrm{P_n}}$), et les incertitudes associées. Elles interviennent dans la matrice de variance-covariance $\mathcal{V}P_n$,

- Les angles d'attitude mesurés par la centrale inertielle (φ, Θ, ψ) ; Les angles de montage (φ_b, Θ_b ,ψ_b) ; La distance sondée et l'angle de pointage, présents dans le terme M_S et calculés en considérant le temps du trajet aller-retour du signal acoustique ($t_{\boldsymbol{\rho}}$) et la vitesse du son dans l'eau, ces derniers étant mesurés par, respectivement, le sondeur multifaisceaux et la sonde de vitesse du son dans l'eau ; les incertitudes associées à ces mesures sont également considérées. Toutes deux interviennent dans la matrice de variance-covariance $\mathcal{V}M_n$,

- Les angles d'attitude mesurés par la centrale inertielle (φ, Θ, ψ), les bras de levier (a_X, a_Y ,a_Z) entre la centrale inertielle et le sondeur multifaisceaux ainsi que les incertitudes associées à ces mesures. Elles interviennent dans la matrice de variance-covariance $\mathcal{V}b_n$.

L'estimation de l'incertitude des données bathymétriques par le modèle proposé par Hare (1995) considère uniquement le système hydrographique. Autrement dit, dans ce modèle, l'incertitude des points sondés est estimée à partir des mesures acquises par les différents capteurs composant le système hydrographique, les paramètres de montage du système et l'incertitude associée aux mesures acquises et aux paramètres de montage. L'incertitude des mesures acquises peut être soit fournie par les fabricants des capteurs, soit estimée dans la phase de post-traitement des données, tandis que l'incertitude des paramètres de montage est estimée lors du processus de calibration du système hydrographique. Ainsi, la morphologie du fond n'intervient pas dans l'estimation de l'incertitude des données bathymétriques dans le modèle proposé par Hare (1995). Néanmoins, Hughes Clarke (2018) souligne que la qualité de la détection du fond marin, plus spécifiquement, la distance

mesurée entre le fond et le système d'acquisition, peut être variable en fonction de l'angle d'incidence du faisceau. Peu de travaux ont investigué cet enjeu dans le domaine hydrographique (Hare, 2001, Lurton, 2003; Lurton and Augustin, 2010). Par contre, dans le domaine géospatial, plusieurs travaux liés au LiDAR (Light Detection And Ranging) aéroporté traitent de l'influence de la morphologie du terrain sur la qualité des données acquises. L'acquisition des données LiDAR aéroporté repose sur les mêmes principes que celle effectuée avec un sondeur multifaisceaux à savoir que le LiDAR mesure l'angle et le temps de parcours bidirectionnel d'une impulsion transmise. Ces études ont proposé des modèles permettant d'évaluer explicitement la contribution de la morphologie du terrain sur la valeur d'incertitude des données acquises (Schaer et al., 2007; Goulden, 2009; Goulden and Hopkinson, 2010). Basé sur différents travaux, Cassol (2018) a proposé un modèle pour évaluer l'influence de la morphologie du terrain dans les nuages de points LiDAR acquis par des systèmes de cartographie mobile.

Formation des dunes sous-marines

Les dunes sous-marines sont les structures sédimentaires les plus récurrentes sur le fond marin dans le contexte fluviomarin. Elles ont une importance fondamentale dans le transport des sédiments tout en ajoutant une résistance dans l'écoulement du chenal de navigation (Venditti, 2013 ; Hendershot et al., 2016). La formation d'une dune sous-marine débute avec la présence d'une irrégularité sur le fond marin qui affecte le courant provoquant une perturbation dans le dépôt sédimentaire. Cette perturbation crée des zones d'érosion-dépôt et par conséquent crée d'autres irrégularités sur le fond marin. Les irrégularités initiales sont des ondulations et la croissance des dunes est la conséquence de l'accumulation de sédiments dans ces irrégularités. Ainsi, la morphologie des dunes est similaire à la morphologie des ondulations initiales (Ferret, 2011).

Une dune présente sur le fond marin a une pente douce face au courant culminant dans la ligne de crête de cette structure. Ensuite, les sédiments transportés par traction sur la dune tombent dans le côté en pente raide de la dune. Ainsi, l'extension de cette structure sédimentaire est délimitée par le début de l'irrégularité sur la surface du fond, aussi appelé pieds des dunes, tel qu'illustré à la Figure 0.2. Ces zones correspondent à des zones de changement d'accumulation de sédiments (adapté de Nichols, 2009 ; Garlan, 2007 ; Thibaud et al, 2013). Il existe une corrélation entre la vitesse du courant et la granulométrie des sédiments transportés pour la formation des dunes tel que décrit par Nichols (2009). En effet, les dunes sont formées par des sédiments tels que le sable fin et les graviers avec une granulométrie entre approximativement 0,1 mm et plus de 1,0 mm. La ligne de crête de ces structures sédimentaires est normalement perpendiculaire à la direction principale du courant, bien que des variations pouvant aller jusqu'à 20° peuvent être observées (Garlan, 2007). La largeur des dunes varie de 60 cm jusqu'à plus de 100 m et leur hauteur varie de 7,5 cm à plus de 5 m, tout dépendamment du contexte de formation de cette structure (Ashley, 1990).

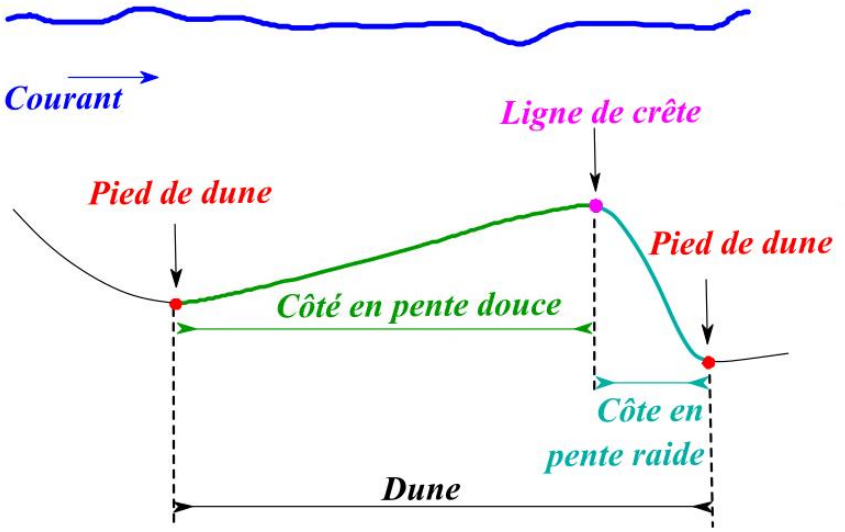

Figure 0.2 – Dune en profil avec la ligne de crête, les pieds de dune et les côtés en pente douce et pente raide.

Segmentation des dunes sous-marines

Différentes approches ont été proposées dans la littérature pour segmenter les dunes sous-marines en considérant un modèle de la surface du fond généré à partir des données bathymétriques. Debese et al. (2016) proposent une méthode de segmentation des dunes en considérant la morphométrie géodésique. Cette analyse morphométrique de la surface du fond marin a pour objectif d'extraire les saillances des dunes sous-marines, à savoir les lignes de crête et les pieds des dunes. Cette approche considère la surface du fond modélisée par un TIN (*Triangulated Irregular Network*). Tel que mentionné précédemment, une des difficultés liées à la segmentation des dunes est son identification sur la surface du fond marin. En effet, différentes structures sédimentaires y sont présentes, telles que les rides. Ainsi, pour faire face à la présence des rides, Debese et al. (2016) ont proposé un filtre anisotrope pour préserver les dunes et éliminer les autres structures présentes sur la surface modélisée. Une autre méthode a été proposée par Ogor (2018) en considérant la surface du fond marin modélisée par un TIN. Dans ce travail, l'identification des lignes de crête des dunes a été effectuée par une analyse morphométrique du fond en considérant la géométrie différentielle. Une fois les lignes de crête identifiées, elles ont été utilisées comme régions d'amorce pour circonscrire les segments associés aux dunes.

Di Stefano et Mayer (2018) proposent une méthode de segmentation des dunes divisée en trois étapes. La première étape effectue une classification morphométrique du MNB en utilisant l'algorithme des Géomorphons (Jasiewwicz and Stepinski, 2012). L'objectif de cette première étape est l'extraction des lignes de crête des dunes. La deuxième étape est l'identification de régions correspondant à des dunes à partir des lignes de crête identifiées dans l'étape précédente et d'une analyse et agrégation de classes Geomorphons spécifiques. Une fois extraite la région associée à la dune, la troisième étape réalise l'identification des deux côtes de la dune

(i.e. pente douce et pente raide). Dans une approche qui considère également le fond marin modélisé par un MNB, Lebrec et al. (2022) ont proposé également une méthode de segmentation des dunes. Cette approche est divisée en deux étapes. La première est l'identification et la segmentation de la ligne de crête des dunes à partir d'une analyse de voisinage des maximums et minimums locaux. La deuxième étape consiste à générer un nombre élevé de profils perpendiculaires à la ligne de crête identifiée. Ces profils visent à affiner la position de la ligne de crête et identifier les limites des dunes (i.e. pieds des dunes). Ensuite, la région représentative de la dune est générée par association de chaque ligne de crête aux pieds de dunes qui lui correspondent.

Les méthodes décrites dans le précédent paragraphe sont généralement identifiées comme des approches orientées-objet. Les objets sont alors définis comme des régions discrètes d'une grille qui sont cohérentes vis-à-vis d'un critère prédéfini. Ils correspondent à des objets du monde réel, tels qu'une dune sous-marine, qui ont des formes et des dimensions associées (Blaschke, 2010; Benz et al., 2004; Castilla et al., 2002). Les approches orientés-objet sont normalement divisées en deux étapes. La première est la segmentation de l'image ou de la surface ayant comme résultat des régions homogènes constituées des pixels ou cellules connectés. Les régions peuvent être elles-mêmes agrégées afin de constituer un objet à part entière (Dragut and Blaschke, 2006; d'Oleire-Oltmanns et al., 2013). Une limite associée à cette première étape est la définition des paramètres pour segmenter les différentes régions, qui peut être relativement arbitraire lorsque les objets à extraire sont difficiles à délimiter. Ensuite, la deuxième étape est la classification des objets segmentés. Celle-ci considère différents descripteurs calculés pour les objets segmentés afin de les classifier dans différentes classes d'intérêt. Les approches orientées-objet sont fréquemment utilisées en imagerie ou dans le domaine géospatial (Diesing and Thorsnes, 2018).

Caractérisation des dunes sous-marines

Différents descripteurs morphologiques peuvent être utilisées pour la caractérisation des dunes sous-marines. Leur définition et leur pertinence sont variables tout dépendamment du domaine de recherche et des phénomènes à étudier. Différents travaux dans la littérature discutent de ces descripteurs morphologiques associés à ces structures sédimentaires (Ashley, 1990; Berné et al., 1993 ; Le Bot, 2001; Knaapen, 2005 ; Van Der Mark and Blom, 2007; Ferret, 2011; Franzetti et al., 2013; Ogor, 2018).

Concernant les descripteurs morphologiques associés aux dunes, ce sont des mesures géométriques estimées à partir des saillances des dunes (i.e. ligne de crête et pieds des dunes). Ainsi, il est possible d'estimer la direction de migration des dunes en considérant les points de début et de fin de la ligne de crête (Knaapen, 2005). Parmi les autres mesures définies dans la littérature, on retrouve : la profondeur de la dune (Van Der Mark and Blom, 2007; Ferret, 2011), la largeur (Berné, 1991; Let Bot, 2001; Ogor, 2018) et la hauteur des dunes, la largeur et les angles associés à chaque côté de la dune (Van Der Mark and Blom, 2007; Lebrec, 2022). Les

dunes peuvent également être caractérisées par trois indices, calculés en considérant les mesures géométriques décrites précédemment : l'indice de symétrie, l'indice de pente, l'indice de sinuosité (Ferret, 2011; Ogor, 2018; Lebrec, 2022).

Les champs de dunes peuvent être également caractérisés par deux descripteurs morphologiques. Le premier descripteur de champs est l'espacement entre les dunes localisées dans un même champ (Le Bot, 2001 ; Ogor, 2018). Ce descripteur est estimé à partir de la distance géométrique entre les lignes de crête des deux dunes consécutives dans un même champ. Le deuxième descripteur est la densité des dunes dans un champ (Ashley, 1990). Celui-ci correspond à la fraction de la surface du fond marin relative au champ qui est couverte par les dunes sous-marines.

Discussion

Il est possible de faire plusieurs constats à la suite de cette revue de la littérature. Le premier concerne la qualité des données bathymétriques acquises. Les modèles d'estimation de l'incertitude couramment utilisés impliquent l'incertitude liée aux mesures faites par les capteurs composant la plateforme hydrographique. Cependant, il existe une influence de la morphologie du fond marin sur l'incertitude des données bathymétriques, comme cela a été référencé dans plusieurs travaux. Cette influence doit donc être prise en compte dans le modèle. C'est d'ailleurs ce qui se fait déjà dans les modèles d'estimation de l'incertitude proposés dans le domaine du LiDAR aéroporté.

En termes de segmentation, parmi les approches pouvant s'appliquer au contexte fluviomarin, plusieurs travaux se sont révélés performants pour l'identification des dunes sous-marines sur un MNB en adoptant une approche orientée-objet. Celle-ci s'appuie sur l'identification des saillances des dunes, telles que les crêtes ou les côtés en pente. Cependant, bien que ces travaux fassent intervenir souvent les mêmes éléments, les méthodes proposées sont peu adaptables à des contextes changeants en termes de dimension, forme ou adjacences des dunes, faute d'une formalisation explicite de leur définition.

Pour ce qui est de la caractérisation des dunes, on constate que la littérature compte déjà de nombreux descripteurs morphologiques associés aux dunes et estimés à partir de leurs saillances. Néanmoins, l'identification de ces saillances reste subjective, les dunes étant des objets flous sans une délimitation claire sur le fond marin. Ainsi, la caractérisation des dunes doit également s'appuyer sur une formalisation explicite des dunes et de leurs saillances afin de pouvoir s'appliquer de manière objective et répétable dans différents contextes de formation des dunes.

Hypothèse

Afin de résoudre le problème soulevé dans la question de recherche, l'hypothèse suivante a été établie : un modèle d'estimation de l'incertitude intégrant une composante morphologique et une méthode orientée-objet basée sur la détection des saillances des dunes sous-marines permet de les segmenter et de les caractériser au moyen de descripteurs morphologiques objectifs et adaptés à l'environnement fluviomarin, tout en considérant l'influence de la morphologie du fond dans la valeur de l'incertitude des données acquises.

Objectifs

L'objectif général de cette recherche est de concevoir et développer une méthode de segmentation des dunes sous-marines orientée-objet qui permette la caractérisation efficiente et objective des dunes en considérant la qualité des données acquises.

Afin d'atteindre l'objectif général de cette recherche, celui-ci est articulé selon les objectifs spécifiques suivants :

- Objectif spécifique 1 : conception d'un modèle d'analyse de l'influence de la morphologie du fond marin sur la valeur de l'incertitude-type composée relative aux données bathymétriques qui considère non seulement les mesures et les incertitudes-types des capteurs du système d'acquisition et de la plateforme elle-même, mais aussi la morphologie du fond marin. Ce modèle vise à mieux évaluer la résolution spatiale adéquate pour la surface générée à partir des données bathymétriques ainsi que l'interprétation des structures présentes sur celle-ci;

- Objectif spécifique 2 : conception et développement d'une méthode orientée-objet de segmentation de la surface numérique représentant le fond marin pour l'identification des dunes sous-marines. Cette méthode vise également l'identification des saillances des dunes à partir d'un modèle conceptuel. Dans cette méthode les dunes sont considérées comme des entités individuelles devant être circonscrites sur le modèle numérique représentant le fond marin.

- Objectif spécifique 3 : conception et développement d'une méthode de caractérisation des dunes sous-marines au moyen de descripteurs morphologiques impliquant les saillances des dunes.

Méthodologie

La démarche méthodologique du projet de doctorat est articulée selon les trois objectifs spécifiques énoncés précédemment et synthétisée par le diagramme de la Figure 0.3.

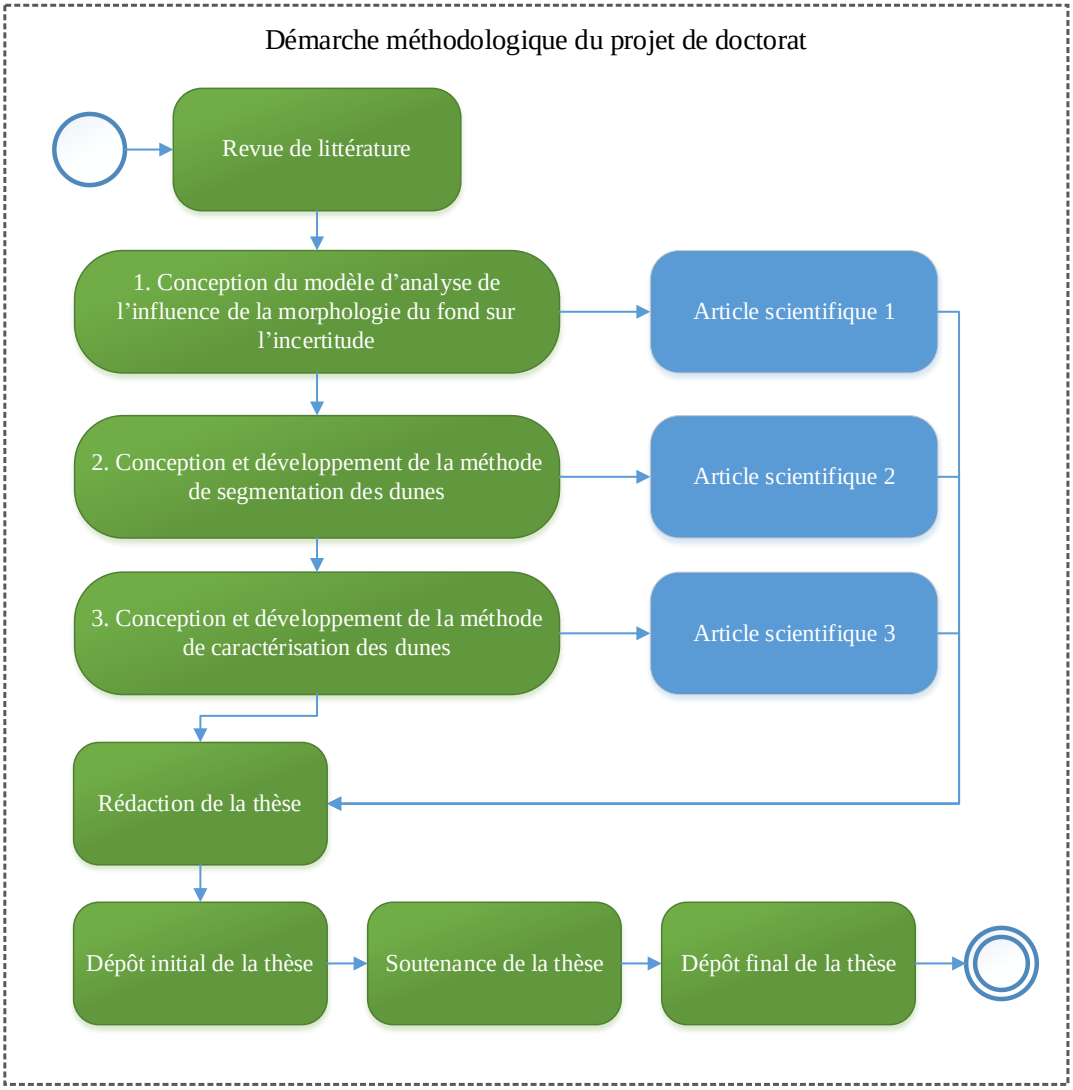

Figure 0.3 – Diagramme de démarche méthodologique du projet de doctorat.

Le projet a débuté avec une revue de littérature approfondie de chaque problématique associée au projet. Cette étape est cruciale afin de mieux circonscrire les verrous scientifiques et proposer des méthodes adaptées pour atteindre les objectifs spécifiques. Malgré qu'elle ne soit mentionnée qu'une seule fois dans le diagramme, la revue de littérature s'est faite de manière continue tout au long du doctorat. Les étapes 1, 2 et 3 sont détaillées dans les prochaines sections. Chacune s'est conclue avec la rédaction d'un article scientifique qui a été intégré à la présente thèse. L'implémentation du modèle mathématique proposé à l'étape 1, et de l'approche de segmentation et caractérisation proposée aux étapes 2 et 3 a été effectuée dans l'environnement Matlab (les algorithmes sont détaillés à l'aide des diagrammes dans l'Annexe A).

Conception du modèle d'analyse de l'influence de la morphologie du fond sur l'incertitude des données bathymétriques

Le premier objectif spécifique est étroitement lié à la génération du MNB à partir du nuage de points bathymétriques. Le nuage de points est calculé à partir des mesures acquises. Ainsi, chaque point du nuage a une valeur d'incertitude associée. Cette valeur est utilisée comme référence pour la détermination de la résolution du MNB. Pour estimer l'influence de la morphologie du fond marin sur la valeur d'incertitude des points bathymétriques, un modèle mathématique a été développé à partir du modèle de TPU proposé par Hare (1995). Il prend en considération les mesures bathymétriques acquises, leur incertitude et des paramètres représentant la morphologie du fond marin. Le modèle proposé a été validé à partir de données bathymétriques multifaisceaux simulées et réelles. Il a ainsi été possible d'analyser l'influence de la morphologie du fond sur l'incertitude des données géoréférencées à partir du nouveau modèle mathématique proposé. Le diagramme de la Figure 0.4 synthétise les étapes associées à l'accomplissement du premier objectif spécifique.

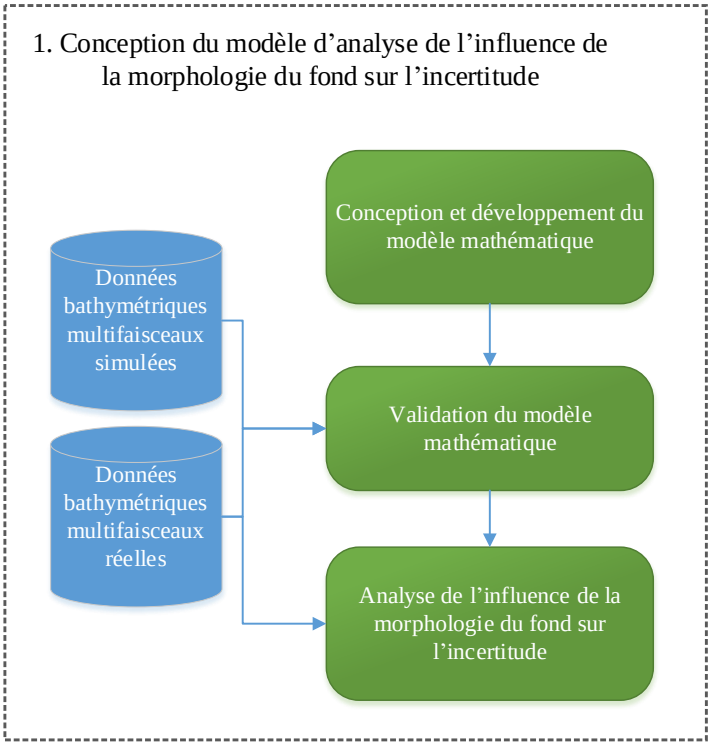

Figure 0.4 - Diagramme de la démarche méthodologique pour l'accomplissement du premier objectif spécifique.

Conception et développement de la méthode de segmentation des dunes

La première étape de l'élaboration de la segmentation des dunes sous-marines selon l'approche orientée-objet a consisté à établir un modèle conceptuel qui explicite les éléments saillants d'une dune sous-marine. Ensuite, une analyse morphométrique du MNB généré à partir des données bathymétriques a été effectuée. Cette

analyse visait l'extraction des saillances des dunes définies au préalable par le modèle conceptuel. Puis les objets dunes ont été formés en s'appuyant sur le calcul d'attributs associés aux lignes de crêtes et à leur appariement avec les pieds de dunes correspondants. L'approche proposée a été validée avec des MNB des différents secteurs de la Traverse Nord du Fleuve Saint-Laurent. La Figure 0.5 synthétise les étapes associées à l'accomplissement du deuxième objectif spécifique.

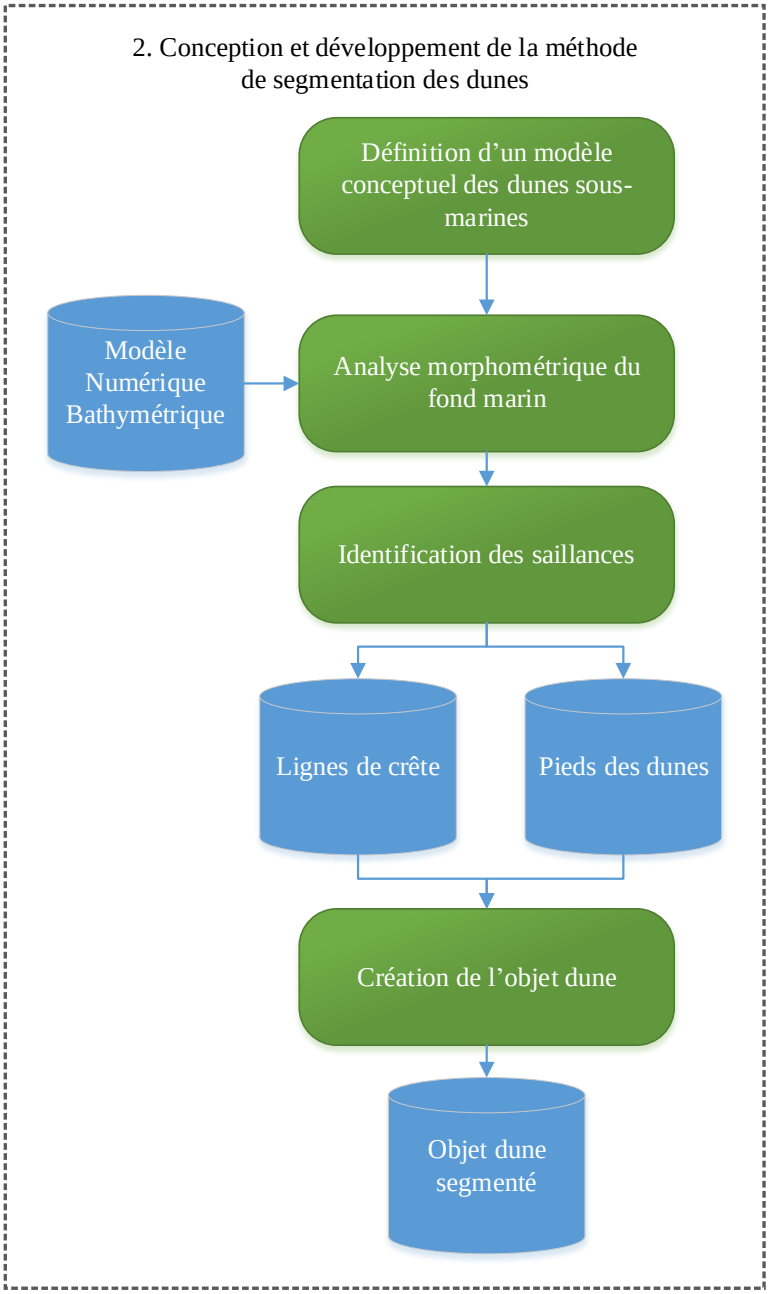

Figure 0.5 - Diagramme de la démarche méthodologique pour l'accomplissement du deuxième objectif spécifique.

Conception et développement de la méthode de caractérisation des dunes

La première étape de la caractérisation des dunes a consisté à appliquer le modèle conceptuel des dunes sous-marines, défini pour la segmentation, au calcul de différents descripteurs morphologiques des dunes et des champs où elles sont localisées. Ce calcul a impliqué non seulement le MNB, mais également les saillances des dunes et l'objet dune lui-même. Une sélection des descripteurs a été réalisée à partir de la littérature en fonction de leur pertinence vis-à-vis du contexte fluviomarin. L'approche de caractérisation des dunes a abouti à un ensemble de descripteurs pour chaque dune individuelle ainsi qu'à des descripteurs associés aux champs de dunes. La validation de l'approche proposée a été effectuée en utilisant les MNB des secteurs du chenal de navigation de la Traverse Nord du Fleuve Saint-Laurent La Figure 0.6 synthétise les étapes associées à l'accomplissement du troisième objectif spécifique.

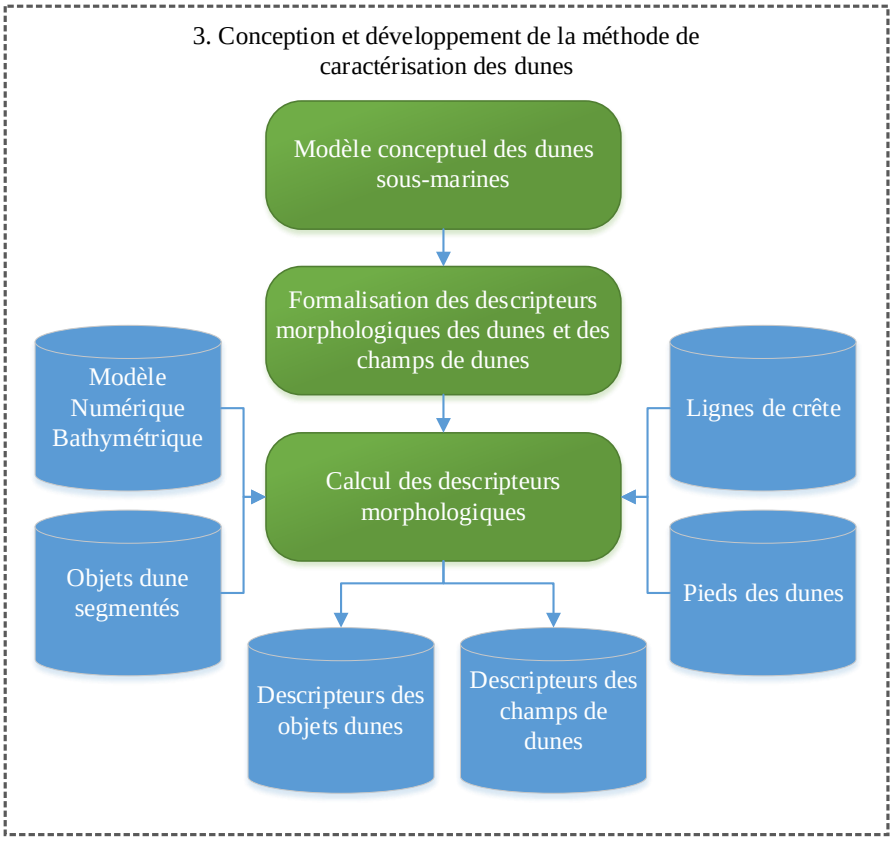

Figure 0.6 - Diagramme de la démarche méthodologique pour l'accomplissement du troisième objectif spécifique.

Structure de la thèse

L'introduction de la thèse visait à présenter le projet de recherche ainsi que la problématique, la question de recherche, l'hypothèse, l'objectif général et les objectifs spécifiques et la démarche méthodologique. Le chapitre 1 est consacré au modèle mathématique conçu pour l'estimation de l'influence de la morphologie du fond sur la

valeur d'incertitude des données bathymétriques. Le chapitre 2 aborde la méthode orientée-objet de segmentation des dunes sous-marines alors que le chapitre 3 aborde la méthode de caractérisation des dunes et des champs où elles sont localisées. Finalement, le dernier chapitre de la thèse est dédié aux conclusions générales de cette recherche, à ses contributions, aux retombées attendues ainsi qu'aux perspectives liées aux différentes directions de recherche envisageables.

Chapitre 1 An empirical study of the influence of seafloor morphology on the uncertainty of bathymetric data

1.1 Résumé

L'estimation de l'incertitude liée aux données bathymétriques est essentielle pour déterminer la qualité des données acquises. Cette estimation est basée sur la propagation de la covariance en considérant le modèle classique de géoréférencement des données bathymétriques. L'estimation de l'incertitude en utilisant le modèle de *Total Propagated Uncertainty* (TPU) est bien décrite dans la littérature. Basé sur ce modèle, cet article propose une analyse de l'influence morphologique du fond marin sur la valeur de l'incertitude des points sondés. Une meilleure compréhension de l'influence de la morphologie du fond marin sur la valeur d'incertitude des données bathymétriques permettrait d'améliorer le traitement et l'interprétation du fond marin ainsi que des structures qui y sont présentes.

1.2 Abstract

The estimation of the uncertainty related to bathymetric data is essential in determining the quality of the data acquisition. This estimation is based on the covariance propagation considering the classical sounding georeferencing model. The estimation of the uncertainty using the Total Propagated Uncertainty (TPU) model is well described in the literature. Developing on this model, this study introduces an analysis of the morphological influence of the seafloor on the uncertainty value of the sounded points. Advancing the comprehension of the influence of the seafloor on the uncertainty value of the bathymetric data would improve the processing and interpretation of the seafloor surface as well as the structures present on the seafloor.

1.3 Introduction

Bathymetric data are primarily used in the production of nautical charts to ensure safe navigation. However, bathymetric data also allows for the study of the seafloor morphology such as for the identification of sedimentary structures on the seafloor (Debese et al., 2016; Di Stefano and Mayer, 2018) and their spatial-temporal evolution (Thibaud et al., 2013). They can also be used for the maintenance of navigation channels, such as for dredging (Lecours et al., 2016), or to contribute to the temporal monitoring of marine habitats (van Dijk et al., 2012). In these different contexts, the bathymetric measurements are equally as important as their associated uncertainty. The International Hydrographic Organization (IHO) has published minimum standards regarding the uncertainty of bathymetric data. The IHO proposes a classification of data in different orders according to the depth, uncertainties (vertical and horizontal), and use of this data (IHO, 2020). The estimated uncertainty of the sounded

points is directly propagated to the deliverables built from the surveyed bathymetric data and can drastically influence the decisions relying on these information sources (Chapter III, Debese, 2013).

Calder and Mayer (2003) proposed a method known as CUBE (Combined Uncertainty and Bathymetric Estimator) to identify the georeferenced soundings with the highest probability of being the seafloor surface, which has rapidly become an industry standard. CUBE uses the bathymetric measurements acquired and their *a priori* precision to create a depth estimate. The soundings provided by the depth estimation using CUBE can then be used to model the seafloor as a Digital Bathymetric Surface (DBM). The uncertainty related to georeferenced points composing the DBM can then be used to define the resolution of the grid, as recommended by the Canadian Hydrographic Service standards for post-processing bathymetric data (CHS, 2012). The most common model that estimates the uncertainty related to bathymetric data is well described in the literature (Hare, 1995). Even if several variations of the model exist (Byrne and Schmidt, 2015), they generally involve the same parameters related to the measurements recorded by the sensors belonging to the data acquisition system (Hare et al., 2011; Naankeu Wati et al., 2016). However, few studies have investigated the influence of seafloor morphology on the uncertainty estimation of georeferenced data. Although recent studies have indicated an impact of seafloor morphology on the uncertainty of bathymetric data. Tidd (2005) conducted a study on how the variations of the seafloor topography affects the resolution and uncertainty of the MultiBeam EchoSounder (MBES) data. The study not only mentions the variations of the seafloor, but also the impact of seafloor object orientation and geometry. Hughes Clarke (2018) identified the seafloor morphology as a contributor to the limit associated to the resolution of the seafloor surface. Specifically, the author underlined the seafloor slope and the obliquity of the sounding beam as influencing parameters. Amante and Eakins (2016) have also identified the influence of the terrain and the cell sampling density as a limit associated to the accuracy of the DBM production. Therefore, it would be beneficial to understand the consequences of the variation of seafloor morphology on the estimation of the uncertainty of bathymetric data. Furthermore, this information would also improve the interpretation of the seafloor surface, especially in the presence of artifacts. Therefore, the objective of this paper is to propose a complementary approach to the common model to estimate the influence of the seafloor morphology on the uncertainty value.

This paper is organized into four sections. The first section is a complete overview on bathymetric data uncertainties. It consists of the description of the bathymetric survey system, the georeferencing model, the uncertainty sources of bathymetric data and, the classical Total Propagated Uncertainty (TPU) model as found in the literature. The second section presents the mathematical model proposed to analyze the influence of the seafloor morphology on the uncertainty value. The third section provides results of the experiments conducted to access the influence of seafloor morphology on the data uncertainty using simulated and real datasets. The

fourth section proposes a discussion deepening the analysis of the results and the use of the proposed model. A synthesis of conclusions and perspectives for future research concludes this paper.

1.4 Bathymetric data uncertainty

1.4.1 Georeferencing model

The bathymetric acquisition system consists of, at least, a GNSS (Global Navigation Satellite System) receiver, an IMU (Inertial Measurement Unit) and an acoustic sounder. In this paper, the considered acoustic sounder is the MultiBeam EchoSounder (MBES). The MBES is associated with a sound velocity probe that measures the speed of sound in the water column as well as the sound velocity probe at the sonar head. Each sensor has its own reference frame, the sensors and their respective frames can be observed in Figure 1.1.

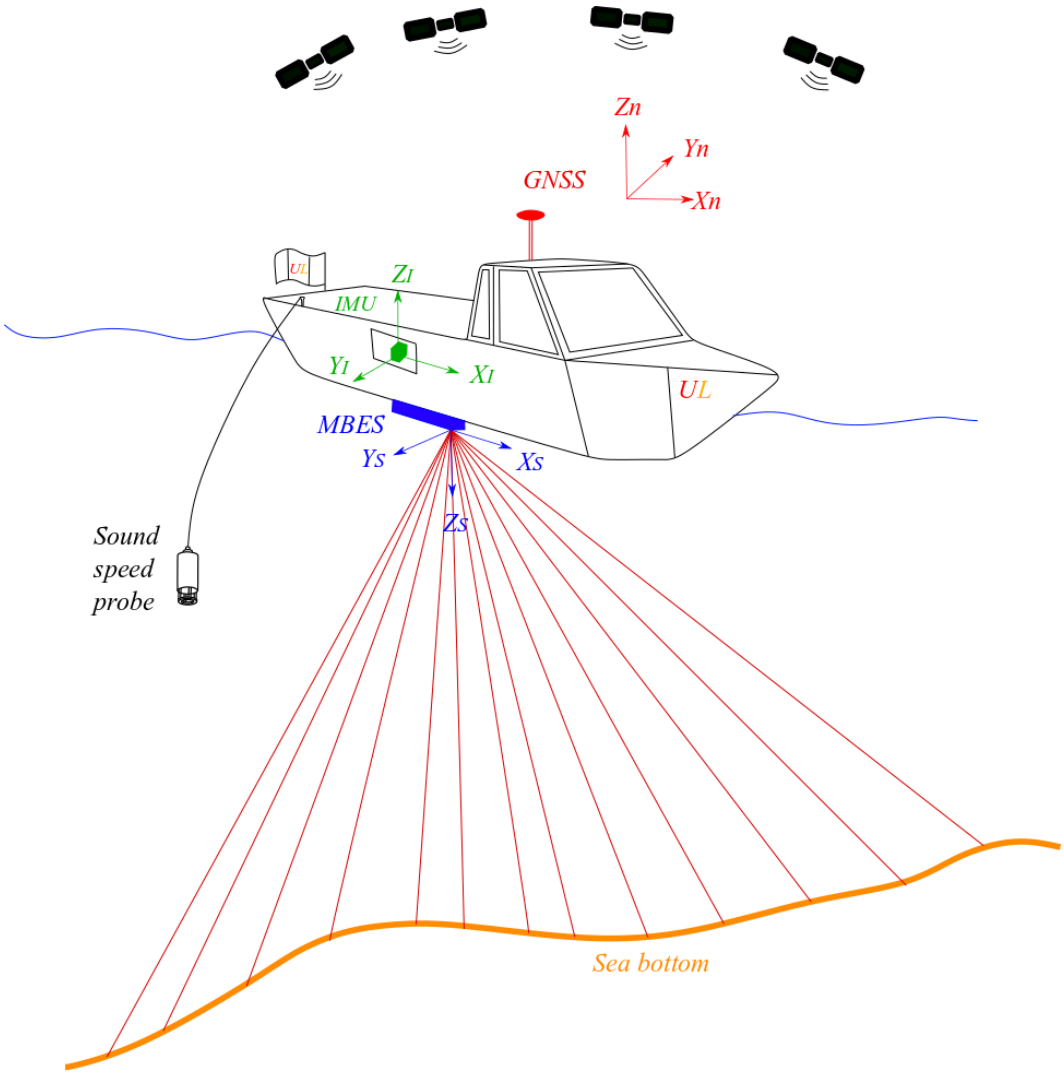

Figure 1.1 - Sensors and frames of a MBES data acquisition system embedded on a vessel.

The data acquired by the different sensors of the acquisition system can be georeferenced using the sounding georeferencing model given in equation (1.1). This model is the simplified form of the model proposed by Hare (1995) and used by Debese (Chapter II, 2013), and Seube and Keyetieu (2017).

$$X_n(t) = P_n(t) + C_I^n(t)(C_S^I M_S(t) + b_I) \qquad (1.1)$$

where:

- X_n is the georeferenced sounding from the measurement acquired by the acquisition system;
- $P_n(\mathrm{t})$ is the vector of geographic coordinates $(x_{\mathrm{P_n}}, y_{\mathrm{P_n}}, z_{\mathrm{P_n}})$ measured by the GNSS receiver in the local navigation frame n;
- $C_I^n(t)$ is the transformation matrix between the local navigation frame n and the IMU frame I using the attitude angles (roll - φ, pitch - Θ, heading - ψ);
- C_S^I is the transformation matrix between the IMU frame I and the MBES frame S using the boresight angles (φ_b, Θ_b ,ψ_b);
- $M_S(\mathrm{t})$ is the vector related to the sounding coordinates measured in the MBES frame S ;
- b_I are the lever-arms vector between the IMU and the MBES;
- t is the acquisition time associated to the measurements recorded by the sensors. The time (t) is used for the synchronization of the sensors. This time is also considered in the estimation of the latency between the sensors as defined by Bjorn and Einar (2005) and Naankeu Wati et al. (2016).

The model described in (1.1) considers the IMU and GNSS receiver are collocated. The COG (Center Of Gravity) is generally established arbitrarily as the reference of the boat frame. The boresight angles (φ_b, Θ_b ,ψ_b) used in $\mathrm{C_S^I}$ can be determined by the patch test as described by Godin (1998), which implies a predetermined pattern of survey lines. The $\mathrm{b_I}$ vector is determined before the survey through the calibration of the acquisition system. This vector contains the distances between the different sensors on the survey vessel.

The M_S vector consists of the sounding coordinates in the S frame calculated from the range (ρ) measurements made by the MBES. This distance can be expressed, in a simplified form, by the multiplication of the sound speed in the water column (s_{speed}) by half of the travel-time ($\frac{t_\rho}{2}$) as mentioned by Lurton (2003). The s_{speed} is measured by the sound velocity probe in the water column. The water column can be modeled by different layers and a refraction occurs when the sound wave goes through a new layer. Hence, the sound wave does not follow a rectilinear trajectory (Beaudoin et al., 2009). Nevertheless, in this paper, for the sake of simplicity, the rectilinear trajectory of the sound wave is adopted and the following expression of ρ is used: $\rho = \mathrm{s_{speed}} \frac{\mathrm{t_\rho}}{2}$.

It is worth mentioning the modelling could be more precise by re-computing the equivalent path assuming a single sound velocity (Hare, 1995).

1.4.2 Measurement uncertainties and mathematical model

Several works in the literature addressed the estimation of the uncertainty related to bathymetric data. Hare (1995) documented the mathematical developments of an uncertainty model for bathymetric data acquired by MBES systems (TPU model). In this model, the uncertainty value of each sounded point is estimated using the law of propagation of uncertainty (Joint Committee for Guides in Metrology, 2008). This law propagates the uncertainties in the georeferencing model given in (1.1) considering the bathymetric measurements and their variance-covariance values. The uncertainty model also considers the installation parameters of the sensors in the acquisition system, as the lever-arms and boresight angles estimated by calibration process and their variance-covariance values. The simplified version of the georeferencing model (1.1) can be rewritten as (1.2), to lighten the mathematical developments proposed in this section.

$$\mathrm{X_n} = \mathrm{P_n} + \mathrm{M_n} + \mathrm{b_n} \quad (1.2)$$

Where:

- $M_n = C_I^n(t)\, C_S^I M_S\,(t)$;
- $b_n = C_I^n(t)\, b_I$.

As a result, the estimated uncertainty values ($\mathcal{V}$) of the georeferenced points X_n are given by (1.3):

$$\mathcal{V}X_n = \mathcal{V}P_n + \mathcal{V}M_n + \mathcal{V}b_n \quad (1.3)$$

The uncertainties estimated in (1.3) are calculated considering:

- the position measurements, namely the GNSS positions ($x_{\mathrm{P_n}}, y_{\mathrm{P_n}}, z_{\mathrm{P_n}}$) and their uncertainties; they are expressed in the P_n variance-covariance matrix (noted $\mathcal{V}P_n$),
- the attitude measurements recorded by the IMU (φ, Θ, ψ), the boresight angles (φ_b, Θ_b ,ψ_b), the sounding distance and pointing angle in the M_S, that are calculated with the travel-time ($t_{\boldsymbol{\rho}}$) and the s_{speed}, recorded, respectively, by the MBES and the sound speed probe and the uncertainties related to these measurements; they are expressed in the $M_n$variance-covariance matrix (noted $\mathcal{V}M_n$),

- the attitude measurements recorded by the IMU (φ, Θ, ψ), the lever-arms (a_X, a_Y ,a_Z) between IMU and MBES and the uncertainties related to these measurements; they are expressed in the $\mathrm{b_n}$ covariance matrix (noted $\mathcal{V}b_n$),

If latencies are considered in the uncertainty model, the latency between the GNSS receiver and the IMU should be included in $\mathcal{V}P_n$, while the latency between the IMU and the MBES should be included in $\mathcal{V}M_n$ and $\mathcal{V}b_n$. In addition, the speed of the platform (Sp_X, Sp_Y ,Sp_Z) should be considered in $\mathcal{V}P_n$, while the angular velocities of the platform (ω_1, ω_2 ,ω_3), measured by the IMU, should be considered in $\mathcal{V}M_n$ and $\mathcal{V}b_n$. The detailed development of the uncertainty model with the latency considerations can be found in Cassol (2018).

The uncertainties associated to the bathymetric measurements can be either provided by the sensor nominal accuracy, included in the manufacturer technical specifications, or estimated in the data post-processing phase. The bathymetric measurements are recorded by the acquisition system, but their full content may not be easily made available to the hydrographer. Although they are depending on certain information for instance, the format of the acquisition files and the software tools available to read these files. As an example, the hydrographer cannot easily access the IMU recorded values of angular velocities (ω_1, ω_2 ,ω_3). Hence, in this case it is not possible to consider the latency value between the IMU and the MBES in the uncertainty estimation. However, this latency shall be considered in the development of the uncertainty model.

1.5 Proposed uncertainty value related to the seafloor morphology

This paper aims to evaluate the influence of the seafloor morphology on the uncertainty of bathymetric data. To evaluate this influence, the uncertainty model given by (3) should also consider the seafloor morphology. This morphological influence on the uncertainty has seldom been investigated in the hydrography field. Hughes Clarke (2018) mentioned that the seafloor detection may vary in the "resulting quality of range estimation as a function of incidence angle". To this aim, the author proposed to consider a morphological parameter associated with the incidence angle of the georeferenced point. The incidence angle γ is the angle computed between the normal vector (unit vector $\hat{n}$) of a georeferenced point X_n and the vector supporting the beam ρ, as shown in Figure 1.2. A normal can be estimated and associated to each sounded point by considering the plan formed by its neighbours, as shall be further discussed. Please note that the grazing angle of the acoustic beams may also be considered further in this paper. The grazing angle is the complementary angle of the incidence angle. In this Figure, the normal vector of the sounding in the MBES frame $\hat{u}_S$ is also represented. More work has been carried out in the field of airborne LiDAR (Light Detection And Ranging) on a similar topic. The airborne LiDAR is an analogous sensor to the hydrographic system involving a MBES. These works have integrated a contribution of the terrain morphology on the uncertainty value. Studies by Schaer et al. (2007), Goulden (2009) and Goulden and Hopkinson (2010) can be mentioned as examples. Relying on these works, Cassol (2018) proposed a model

to assess the morphological uncertainty in LiDAR point clouds recorded with mobile mapping systems. Such a model has been used as the foundation of the model described in this section.

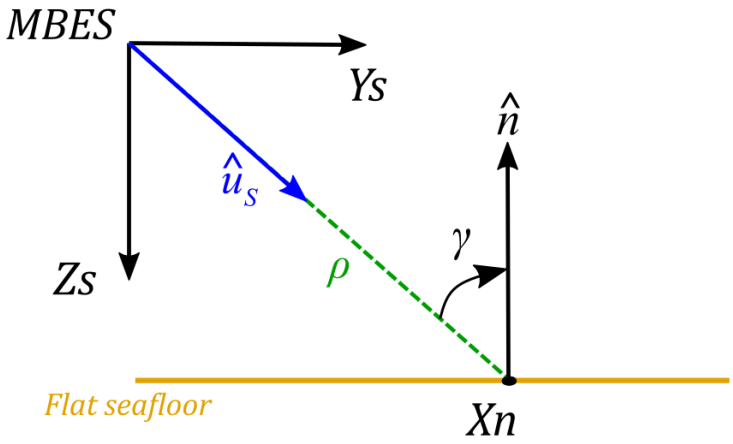

Figure 1.2 - Incidence angle considered in the estimation of the morphological uncertainty.

To consider the morphological component of the error, we propose to decompose the sounding error $\delta\rho$ as the sum of two components ($\delta\rho_m$ and $\delta\rho_i$). As a result, the measured sounding range ρ_m can be expressed as in (1.4).

$$\rho_m = \rho + \delta\rho_m + \delta\rho_i \quad (1.4)$$

Where:

- ρ_m is the measured distance between the MBES and the seafloor;
- ρ is the measured distance between the MBES and the seafloor without errors;
- $\delta\rho_m$ is the measurement error related to the sensors of the bathymetric acquisition system;
- $\delta\rho_i$ is the morphological error related to the seafloor morphology.

The measurement error $\delta\rho_m$ and its related uncertainty are already included in the $\mathcal{V}M_n$ term in the uncertainty model (3). The morphological error $\delta\rho_i$, introduced in this paper, is related to the incidence angle γ between the sounding and seafloor. This term is not included in (1.3). Hence, the sounding error can be expressed as $\delta\rho = \delta\rho_m + \delta\rho_i$. The uncertainty model assumes a flat seafloor, as shown in Figure 1.2. However, if this assumption is not true, the positioning errors related to the sounded point will occur related to the incidence angle error. Indeed, the normal associated to the sounded point shall differ if the seafloor is flat, sloping or display some morphological pattern. Therefore, the term $\delta\rho_i$ can be regarded as the morphological error. Let us denote

by $\mathcal{v}_{\delta\rho_m}$, the uncertainty related to the sounding error $\delta\rho_m$. Similarly, we denote by $\mathcal{v}_{\delta\rho_i}$ the uncertainty related to the morphological error $\delta\rho_i$.

We propose a mathematical model to estimate the influence of the seafloor morphology on the sounded points, also called morphological uncertainty ($\mathcal{v}_{\delta\rho_i}$). This morphological uncertainty shall be further considered in the uncertainty model of the sounded points. To simplify the mathematical demonstrations, the parameters and the measurements considered in (1.3) will be represented by $\chi\ (\varphi, \theta, \psi, t, \varphi_b, \theta_b, \psi_b, \rho)$. The error associated to the measurement ρ is $\delta\rho_i$ to develop the morphological uncertainty term, since $\delta\rho_m$ is already considered in $\mathcal{V}M_n$ in (1.3). Note that the measurements and uncertainties related to the MBES and to the sound speed probe are already considered in $\mathcal{v}_{\delta\rho_m}$ and should not be considered in the morphological uncertainty ($\mathcal{v}_{\delta\rho_i}$) estimation.

To develop the morphological uncertainty term, we assume that the seafloor neighbourhood of the sounded point X can be represented by a plane surface $S(X) = 0$ with S a linear equation. This neighbourhood is considered to be possible to associate a normal to each sounded point. Since S is a plane, its general expression considering the georeferenced point X is represented in (1.5) where the coordinates of the georeferenced point X are represented by (x, y, z).

$$S(X) = s_1 x + s_2 y + s_3 z + s_4 \qquad (1.5)$$

Considering (1.5), a sounding X belonging to the surface is georeferenced using the parameters χ, therefore $S(X(\chi)) = 0$. To estimate the morphological uncertainty, we assume that if we have a small variation δ in the χ parameters $\delta\chi$, the surveyed point still belongs to S, or in other words $S\big(X(\chi + \delta_\chi)\big) = 0$. Figure 1.3 illustrates this assumption using an example involving a small variation in roll angle $\delta\varphi$.

Given the plane seafloor assumption for the area near the georeferenced point, the derivative of $S(X(\chi)) = 0$ according to χ can be expressed by (1.6).

$$\frac{d}{d\chi} S(X(\chi)) d\chi = 0 \qquad (1.6)$$

The equation (1.6) can be rewritten as (1.7).

$$\frac{d}{dX} S(X) dX \frac{d}{d\chi} X(\chi) d\chi = 0 \qquad (1.7)$$

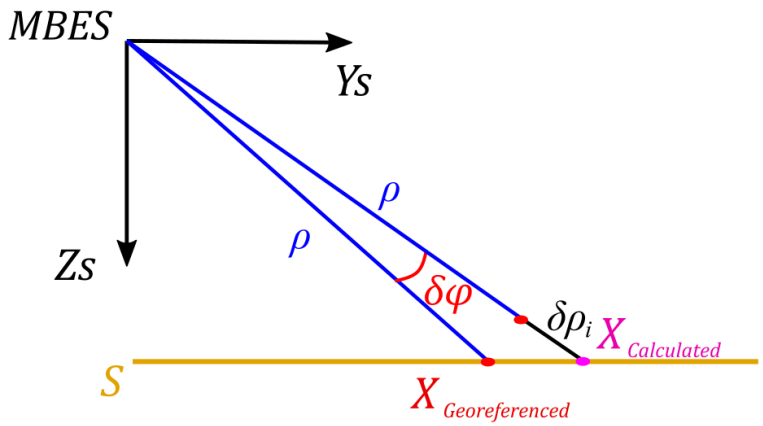

Figure 1.3- Represents the position of the sounded point in order to estimate the morphological error. We consider that, even with a small variation in the georeferencing parameters (i.e. roll angle - $\delta\varphi$), the sounding belongs to a plane surface on the seafloor.

In (1.7), $\frac{d}{dX}S(X)dX$ represents the gradient of S according to X and $\frac{d}{d\chi}X(\chi)$ is the Jacobian matrix of X according to χ.

The partial derivative of S according to the coordinates of X (1.5) is $\frac{dS}{dX} = (s_1, s_2, s_3)$. This derivative represents the normal of the local plane. The derivative can also be denoted by $\hat{n} = (s_1, s_2, s_3)$. This normal $\hat{n}$ relates to the seafloor morphology of the georeferenced point. Accordingly, replacing $\frac{d}{dX}S(X)dX$ by $\hat{n}$, (1.7) becomes (1.8).

$$\hat{n} \cdot \frac{d}{d\chi}X(\chi)d\chi = 0 \qquad (1.8)$$

Please note that the " · " represents the scalar product in (1.8). The morphological term of our proposed model is strongly related to the normal vector ($\hat{n}$) estimated for each sounding. There are different ways to estimate the normal from a group of soundings. In this paper, the normal estimation proposed by Dupont (2020), involving a robust PCA (Principal Component analysis) method, is used. We considered a plan formed by the 10 nearest neighbours to estimate the normal vector ($\hat{n}$) to associate with each sounded point. This estimation involved all the recorded points acquired on the survey, and not only the points of the swath. Equation (1.8) can be rewritten using the parameters included in χ and their partial derivatives. The resulting equation is expressed by (1.9).

$$\hat{n} \cdot \left(\frac{\partial X}{\partial \varphi}\delta\varphi + \frac{\partial X}{\partial \theta}\delta\theta + \frac{\partial X}{\partial \psi}\delta\psi + \frac{\partial X}{\partial t}\delta t + \frac{\partial X}{\partial \varphi_b}\delta\varphi_b + \frac{\partial X}{\partial \Theta_b}\delta\Theta_b + \frac{\partial X}{\partial \psi_b}\delta\psi_b + \frac{\partial X}{\partial \rho}\delta\rho_i\right) = 0 \quad (1.9)$$

Based on (1.9), the morphological error $\delta\rho_i$ can be estimated considering the parameters $(\varphi, \theta, \psi, t, \varphi_b, \theta_b, \psi_b)$ and the normal $\hat{n}$ as shown by (1.10).

$$\delta\rho_i = \frac{-\hat{n}\cdot(\frac{\partial X}{\partial\varphi}\delta\varphi+\frac{\partial X}{\partial\theta}\delta\theta+\frac{\partial X}{\partial\psi}\delta\psi+\frac{\partial X}{\partial t}\delta t+\frac{\partial X}{\partial\varphi_b}\delta\varphi_b+\frac{\partial X}{\partial\theta_b}\delta\Theta_b+\frac{\partial X}{\partial\psi_b}\delta\psi_b)}{\hat{n}\cdot\frac{\partial X}{\partial\rho}} \qquad (1.10)$$

To simplify the notations in equation (1.10), we represent the ratio of the scalar product of the normal vector and partial derivative vector to the scalar product of the normal and partial derivative by the coefficients a_i (for example $a_1 = \frac{-\hat{n}\cdot\frac{\partial X}{\partial\varphi}}{\hat{n}\cdot\frac{\partial X}{\partial\rho}}$). With this simplification, the equation can be rewritten as (1.11).

$$\delta\rho_i = a_1\delta\varphi + a_2\delta\theta + a_3\delta\psi + a_4\delta t + a_5\delta\varphi_b + a_6\delta\Theta_b + a_7\delta\psi_b \qquad (1.11)$$

Using (1.11) and the uncertainties related to the parameters in χ (noted $\upsilon_{xx}$where *xx* represents one of the χ parameters) except the sounding range, the uncertainty related to $\delta\rho_i$ is given by (1.12):

$$\upsilon^2_{\delta\rho_i} = {a_1}^2\upsilon_{\delta\varphi}{}^2 + {a_2}^2\upsilon_{\delta\theta}{}^2 + {a_3}^2\upsilon_{\delta\psi}{}^2 + {a_4}^2\upsilon_{\delta t}{}^2 + {a_5}^2\upsilon_{\delta\varphi_b}{}^2 + {a_6}^2\upsilon_{\delta\theta_b}{}^2 + {a_7}^2\upsilon_{\delta\psi_b}{}^2 \quad (1.12)$$

Therefore, the georeferencing model (1.2) can be written as (1.13) only for the estimation of the morphological uncertainty. In this equation, the term $\delta\rho_m$ is considered in M_n term and $\delta\rho_i$ is added to estimate the morphological uncertainty.

$$X_n = P_n + M_n + b_n + \delta\rho_i C_I^n \; C_S^I \hat{u}_S \quad (1.13)$$

The term $\delta\rho_i C_I^n \; C_S^{bI}\hat{u}_S$ in (1.13) can be simplified as S_n. The term S_n allows for the observation of the contribution of the morphological uncertainty value to each coordinate of X_n according to $\hat{u}_S$. Similarly, as the uncertainty values in (1.3), the morphological uncertainty is computed using the law of propagation of covariance. The covariance matrix of S_n (denoted $\mathcal{V}S_n$) associated to the georeferenced point X_n considering the morphological uncertainty $\upsilon^2_{\delta\rho_i}$ is expressed in (1.14).

$$\mathcal{V}S_n = \upsilon^2_{\delta\rho_i}(C_I^n \; C_S^I \; \hat{u}_S)(C_I^n \; C_S^{bI} \; \hat{u}_S)^T \quad (1.14)$$

The morphological uncertainty of a georeferenced point can be estimated using (1.14). This estimation uses only the measurements that can have an influence on the morphological uncertainty. With this new morphological uncertainty term now defined, we can update the uncertainty model. It can be expressed as the covariance matrices P_n, M_n, b_n and S_n as given by (1.15).

$$\mathcal{V}X_n = \mathcal{V}P_n + \mathcal{V}M_n + \mathcal{V}b_n + \mathcal{V}S_n \quad (1.15)$$

This updated uncertainty model will be used to assess the impact of the seafloor on the uncertainty of the georeferenced points. To this end, the values provided by the original uncertainty model (1.3) will be compared to the values provided by the updated model (1.15). The relative difference between the uncertainty values will be computed to highlight the significance of the morphology contribution to the uncertainty budget.

1.6 Application of the proposed uncertainty model to simulated and real datasets

In this section, we applied the uncertainty model proposed in (1.15) on simulated and real datasets. The simulated datasets were used to develop the proposed model. Then, we applied the model on a real dataset to better understand the influence of the seafloor morphology on the uncertainty value related to the bathymetric data. Please note that, in the following, the normal vector of each sounding is considered when estimating the uncertainty related to the seafloor morphology. In addition, the sensor nominal accuracy was used as the uncertainty related to the measurements. This may not be applicable in real hydrographic survey contexts, where such uncertainties may be recorded and made available in survey files.

1.6.1 Simulated datasets

Two simulated datasets were built to apply and validate the uncertainty model proposed in (1.15). The first one is a flat seafloor and the second one is a seafloor composed of underwater dunes. Profiles related to these two simulated seafloor surfaces are illustrated in Figure 1.4.

The sensors considered in the simulation are the same as the ones on the Helen Irene Battle vessel of the CHS (Canadian Hydrographic Service). This acquisition system was used to acquire the real dataset which will be further discussed. The sensors are as follows: the SP90m and PosMV OceanMaster as positioning system and IMU, the Kongsberg EM2040 as MBES, the AML MicroX (AML Oceanographic) as surface speed sensor and the profiler BaseX of AML as sound velocity profiler. The *a priori* uncertainties and parameters of the sensors are given by the manufacturers and presented in Table 1.1.

To better understand the influence of the seafloor morphology on the uncertainty of the sounded points, we calculated the uncertainty values using the model described in (1.3). This uncertainty value associated to the georeferenced point shall be considered in this paper as the 3D combination of the uncertainty related to the coordinates x, y, z. For the flat simulated seafloor, the minimal uncertainty value can be observed at the nadir sounding with a value of 12.6 cm. The values increase up to the outer soundings to a maximal uncertainty value of 17 cm, as it was expected. Considering the dune-simulated seafloor, the minimal uncertainty value of 12.1 cm is also at nadir soundings. The uncertainty values increase up to the outer soundings to a maximal

uncertainty value of 16.1 cm. As expected, by using the uncertainty model without taking into account the seafloor morphology (i.e. model described in equation 1.3), the same behaviour and uncertainty range of values are observed for the two datasets.

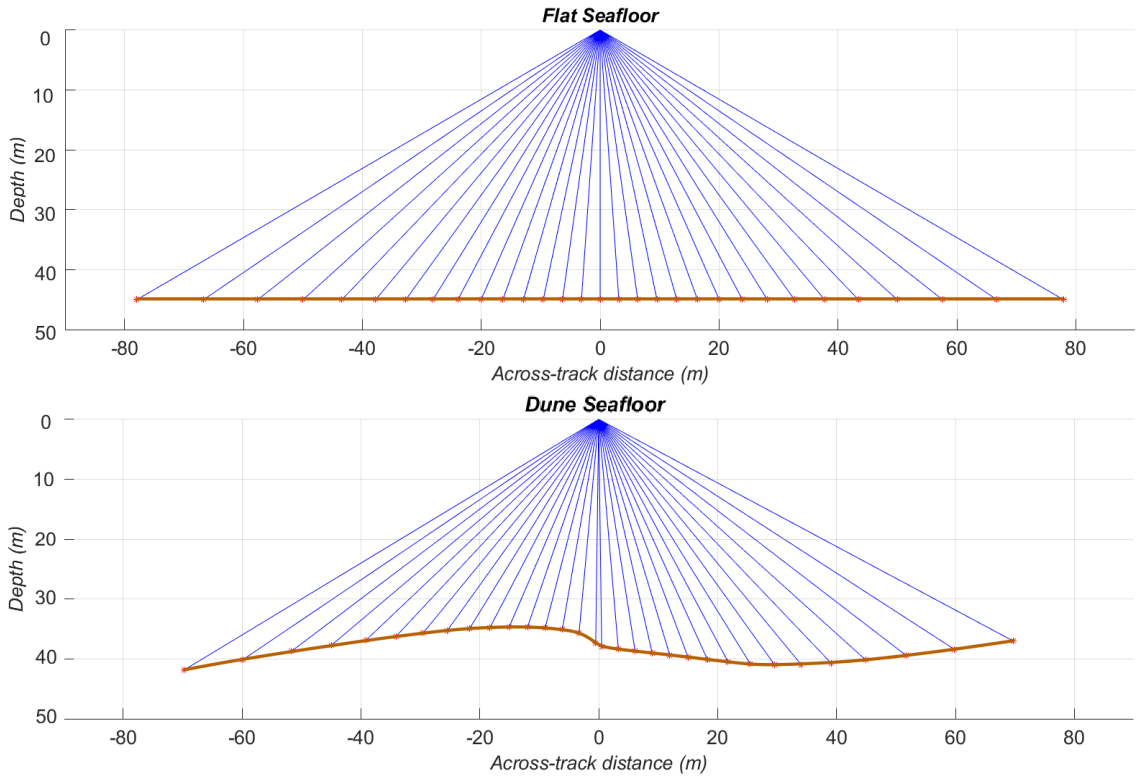

Figure 1.4 - Simulated datasets. The maximum depth is 45m with a swath angle of 120° represented by soundings every 4° (equiangular acquisition mode). On the top, a simulated flat seafloor profile. On the bottom, a simulated dune profile oriented in the direction of the river current (same direction as Y_S), which is perpendicular to the direction of swath track line.

The uncertainties were also estimated considering the seafloor morphology using the proposed model in (1.15). For the flat seafloor, the minimal uncertainty value is at nadir with a value of 12.7 cm. The uncertainty values increase up to the outer beams to a maximal value of 23.3 cm at the highest grazing beam. The minimum value of uncertainty for the dune seafloor using (1.15) is 12.2 cm. This value was not estimated for the nadir beam, but for the acoustic beam measuring the crest of the dune (located in the nadir area in Figure 1.4). Nonetheless, the uncertainty value at nadir is still low with a value of 12.5 cm. The maximal uncertainty can be observed at the outer beams with a value of 26.9 cm.

POSITIONING SYSTEM UNCERTAINTIES	
MEASUREMENT	*A priori* uncertainty
x_{P_n}, y_{P_n} [1]	(5cm+1ppm×baseline length)
z_{P_n}	(8cm+1ppm×baseline length)
φ , Θ [2]	0.01°
ψ [2]	0.02°
MBES AND SOUND SPPED PROBE UNCERTAINTIES	
RAW RANGE RESOLUTION[3]	10.5 mm
MAXIMAL ANGULAR COVERAGE[3]	170°
SOUND SPPED PROBE [4]	0.025m/s
SENSORS INSTALLATION PARAMETERS UNCERTAINTIES	
φ_b, θ_b, ψ_b [5]	0.05°
a_X, a_Y ,a_Z [5]	1,5 cm

Table 1.1 - A priori uncertainties and parameters of the acquisition system sensors given by the manufacturers. [1](Spectra Geospatial, 2020), [2] (Applanix, 2019), [3](Kongsberg, 2021), [4](AML Oceanographic, 2020), [5] considered values for the survey involving the survey platform Hele Irene Battle.

Comparing the uncertainty values calculated using (1.3) and (1.15), we observed no significant difference at the nadir soundings. However, there is a significant difference on the value of uncertainty calculated for the outer beams. For the flat seafloor, this difference is 6.3 cm and for dune seafloor, the difference is 10.8 cm. The difference between the uncertainty estimated with (1.3) and (1.15) can be observe on Figure 1.5.

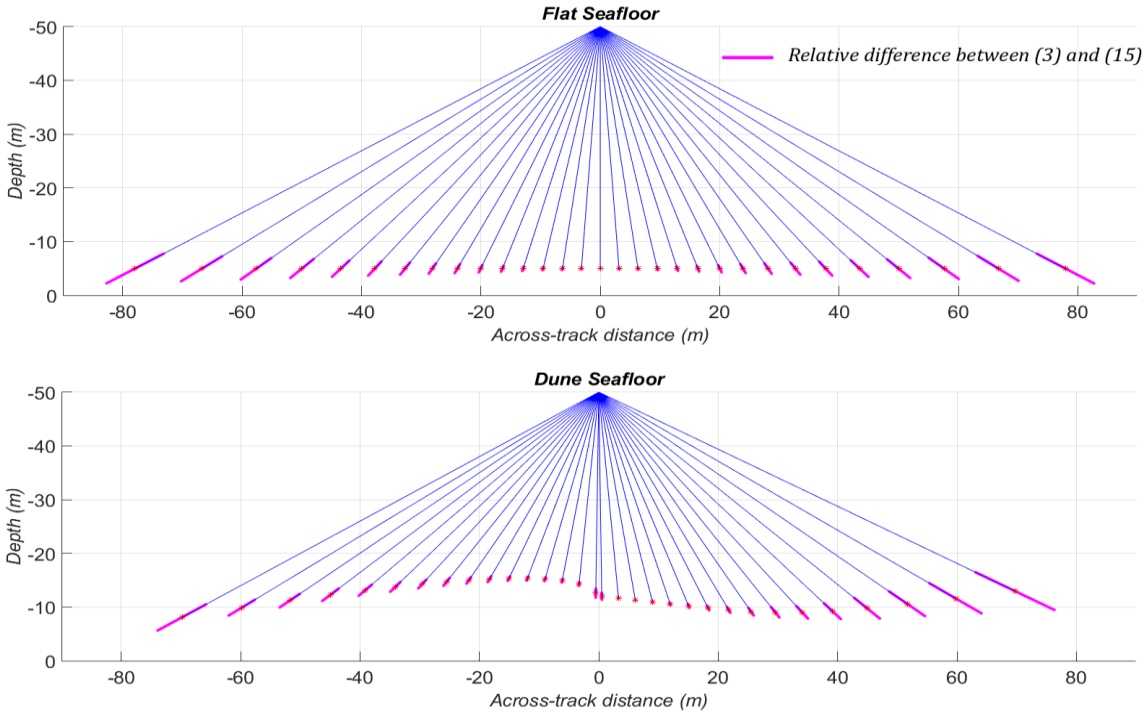

Figure 1.5 - Relative difference between the uncertainty computed using (3) and (15) representing the influence of the seafloor morphology on the uncertainty value. This difference is due to the $\mathcal{V}S_n$ term and can be observed in magenta for each simulated beam sounding (blue lines). The morphological uncertainty estimated by $\mathcal{V}S_n$ term has an exaggeration scale of 100 in relation to the soundings distance.

In order to better observe the influence of the seafloor morphology on the uncertainty illustrated on Figure 1.5, we classified the relative difference between the classical and the proposed model (i.e. $[(1.15) - (1.3)]/(1.15)$) according to five classes namely: 0-1%; 1.0 – 5%; 5.0 – 15%; 15.0 – 30%; 30.0 – 100%. The result can be observed on Figure 1.6.

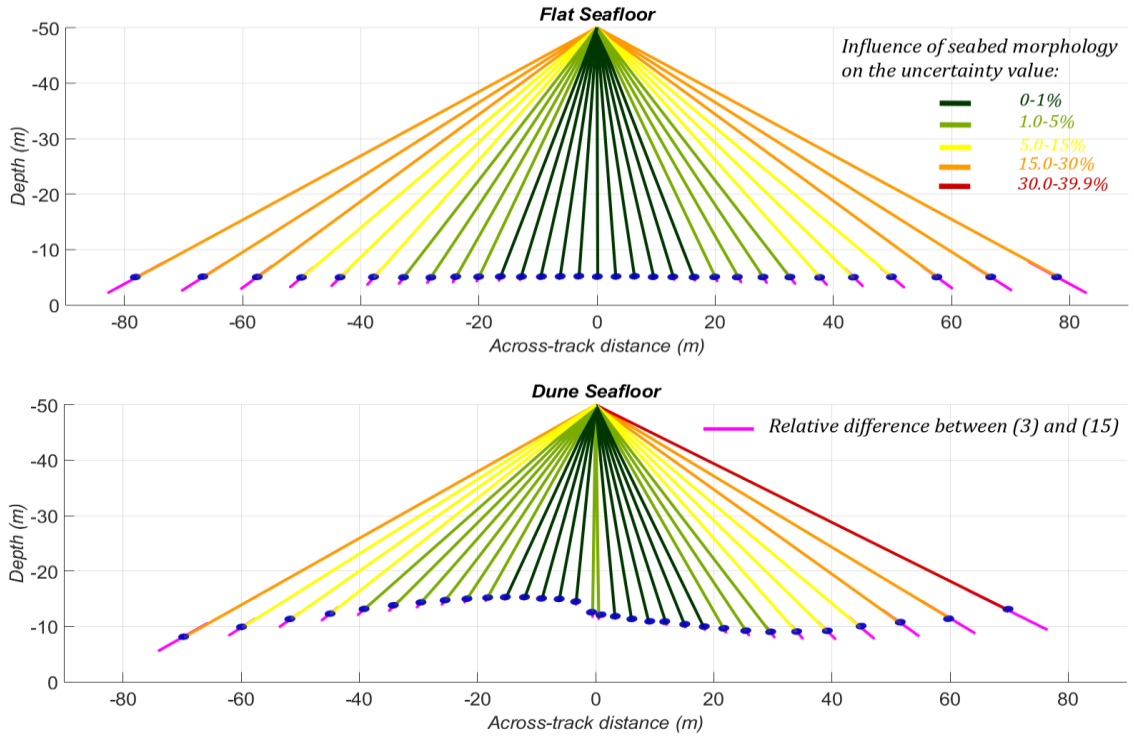

Figure 1.6 - Relative difference between the uncertainty computed using (3) and (15) representing the influence of the seafloor morphology on the uncertainty value. The relative difference is converted in percentage and presented as a magenta segment attached to the simulated points (blue). The morphological uncertainty estimated by the $\mathcal{V}S_n$ term has an exaggeration scale of 100 in relation to the soundings distance.

As previously mentioned, and shown in Figure 1.6, the relative difference is negligible in the flat simulated seafloor with an influence of the seafloor morphology under 1% in the nadir beams. In the outer beams of the swath, this difference is between 15% and 20% and in the outermost beam, approximately 27% of the uncertainty value comes from the morphological uncertainty. For the dune seafloor, the relative difference is still negligible at nadir with a value of approximately 2%. As mentioned earlier, the lowest influence of the seafloor morphology on the uncertainty value is located at the dune crest. Indeed, for this sounding, the uncertainty value is lower than 1%. The influence of the seafloor morphology estimated by the relative difference between (1.3) and (1.15) increases up to approximately 40% for the outermost beam (i.e. red beam on Figure 1.6). This influence is between 15% and 25% in the grazing beams located on the border of the swath (i.e. orange beams on Figure 1.6). These values shall be further discussed in the fourth section of the paper.

1.6.2 Real dataset

After applying the proposed model considering the seafloor morphology (1.15) on simulated datasets, the model was tested on a real dataset. This dataset was acquired on the sector G14 of the Northern Traverse of the Saint

Lawrence River, near the Orléans Island (Eastern Canada). The sector of this navigation channel includes many underwater sedimentary structures, such as underwater dunes. The survey involved nine lines in the Southwest-Northeast direction. The paper focuses on two selected zones of the G14 sector (i.e. zones A and B), which have relevant morphological characteristics. Nevertheless, the proposed method is scalable to larger areas. The data acquisition system was embedded in the Helen Irene Battle vessel of the CHS. The sensors used in this acquisition are the same as the ones described in the previous section with their *a priori* uncertainties and parameters described in Table 1.1. As previously mentioned, the normal vector associated to each sounded point was estimated using a robust PCA method as proposed by Dupont (2020). The DBMs of the zones A and B can be observed in Figure 1.7. Both DBMs surfaces were computed with processed bathymetric data (e.g. celerity correction, processing of the vessel trajectory) without post-processing filtering.

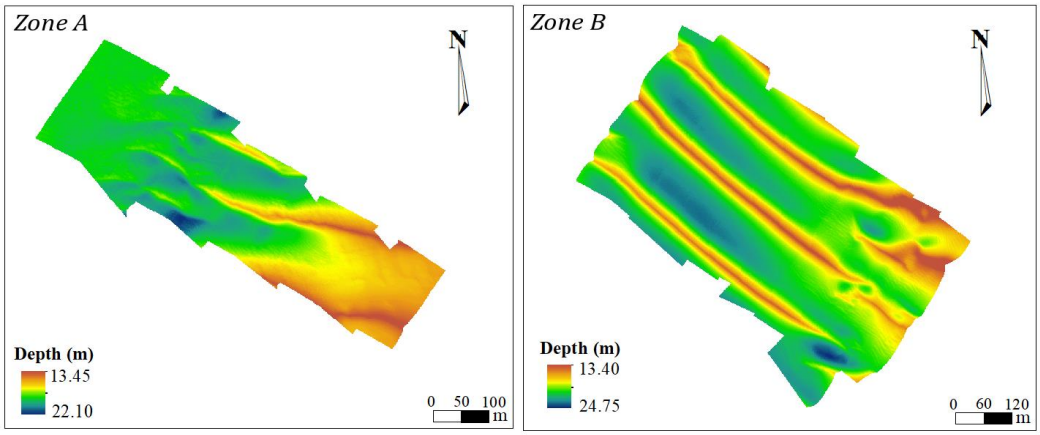

Figure 1.7 - DBM of zones A and B of the sector G14 of the Northern Traverse of the Saint-Lawrence River. The cell resolution is 1 m. The DBM is computed considering the mean values of the soundings in each cell.

Both surfaces shown in Figure 1.7 present sedimentary structures (e.g. underwater dunes) on the seafloor surface. Zone A has a minimum depth of 13.45 m and a maximum depth of 22.10 m. In this zone, we can observe the presence of dunes in the eastern side and a relatively flat seafloor in the western side of the zone. Zone B has a similar depth with a minimum of 13.40 m and a maximum depth of 24.75 m. These surfaces shall be used to illustrate the influence of the seafloor morphology on the uncertainty value. Therefore, the uncertainty was estimated for both zones, with the proposed uncertainty model (1.15). The calculated uncertainty values are presented in Figure 1.8. This figure also illustrates the survey lines and the crest lines of the dunes aiming to highlight the influence of the seafloor morphology on the uncertainty value. Please note that the computational cost to estimating the influence of the seafloor on the uncertainty from both zones is relatively high (i.e. around twenty hours including the estimation of the normal by the robust PCA method for about 7 million sounded points using a computer with 12 GB RAM and Intel Core i7-3770 @ 3.40GHz CPU).

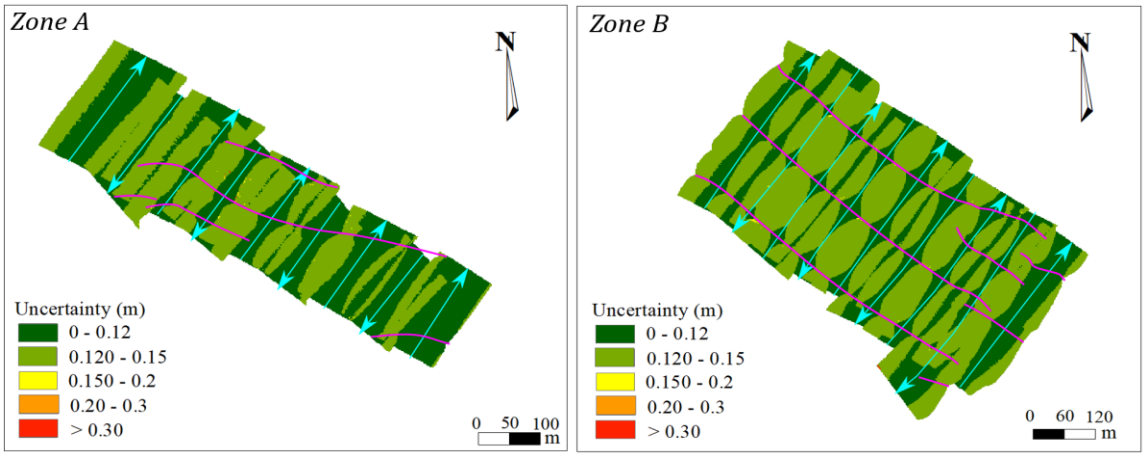

Figure 1.8 - Uncertainty values computed with the proposed model including the seafloor morphology, the survey lines (cyan lines) and crest lines of the dunes (magenta). The mean value of the uncertainty was considered at each cell to represent the uncertainty value. The cell resolution is 1 m.

The uncertainty values for both zones are generally inferior to 15 cm with a few isolated soundings with a superior value, but it is not critical on the survey. Similarly, to the simulated datasets, a preliminary estimation of the uncertainty was carried out using the model described in (1.3) for the dunes real datasets. It can be observed that some areas in the center of zone A have an uncertainty greater than 15 cm. The influence of the morphological parameter on the estimation of the uncertainty is clearly shown in Figure 1.8. In fact, in the western flat area of zone A, it can also be observed that the minimum uncertainty value is located in the near-nadir area of the survey line. The uncertainty is increasing with the grazing angle of the soundings in the swath. In the center of the zone A, we can observe the effect of the seafloor morphology, with the minimum uncertainty on the near-nadir area and in the crest line of the dune. This influence is more significant in zone B, where the uncertainty values have minimum values in the near-nadir area and near the crest line of the dunes. The classified relative difference for the real dataset can be observed in Figure 1.9. Please note that different classes were used to highlight the relative difference between (3) and (15), namely: 0-1%; 1.0 – 5%; 5.0 – 10%; 10.0 – 15%; 15.0 – 100%.

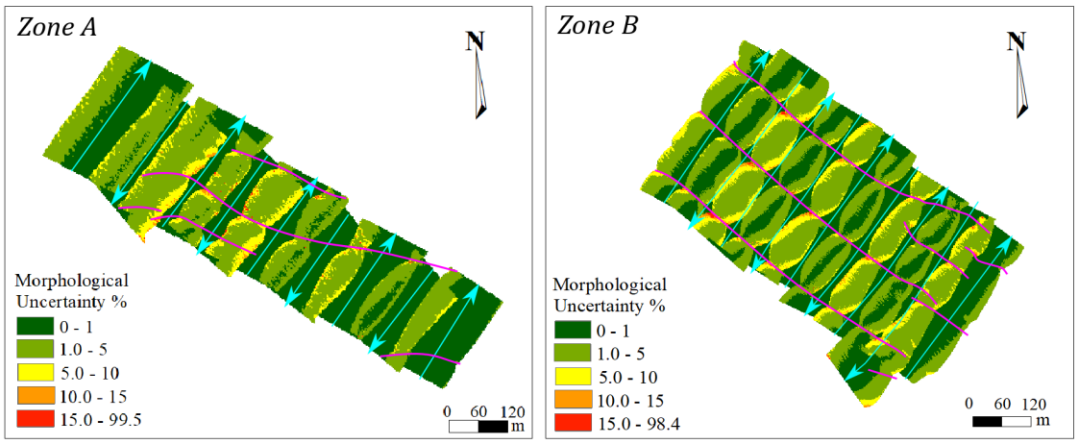

Figure 1.9 - The influence of the seafloor morphology on the uncertainty considering the underwater dune context, the survey lines (cyan lines) and crest lines of the dunes (magenta). The mean value of the relative uncertainty was considered at each cell. The cell resolution is 1 m.

The morphological influence on the uncertainty value is more spatially variable in the underwater dune context. We can compare the flatter areas of zone A (eastern and western areas) with the dune seafloor. For flat seafloor areas, close to the nadir, the majority of the surface cells has a contribution lower than 1%. This value of relative difference increases with the grazing angle in the outer beams of the swath. In the dune areas, specifically, in zone A, the relative uncertainty is ranging between 5% and 15% in the outer beams of the swath over the dunes. The relative difference of some cells of the DBM is superior to 15% being related to noisy points considered in our analysis. Noisy points often yield errors in the normal estimation, which is associated to the sounded points considered in the proposed model. In zone B, the influence of the morphological parameter is more significant. A higher spatial variability of the uncertainty values is observed. The influence of the morphological parameter is lower than 1% in the near nadir area and near the crest lines of the dunes. This is due to the fact that the crest lines are closer to the survey platform and do not present acute grazing-angle beams. The relative uncertainty increases up to 15% in the outer beams of the swath, especially in the valley zone between the dunes, where the sounding beams present an acute incidence angle. Thus, this is where the morphological parameter has the stronger impact.

1.7 Discussion

This section aims to further discuss the results presented in the previous section and the strength and limitations of the proposed complementary model. The influence of the seafloor on the uncertainty value, estimated by the relative difference between (1,3) and (1.15), was negligible in the beams at nadir of the simulated and the real datasets. In both datasets, this influence increases on the outer beams of the swath. This growth is related to the grazing angle between the beam and the seafloor surface. Since this influence is directly associated to the

seafloor morphology, higher values could be located anywhere on the swath, not necessarily on the outer beams. The relationship between the seafloor morphology (i.e. normal associated to the sounded point) and the morphological uncertainty proposed in this paper can be observed in Figure 1.10, where the difference between the sounding range uncertainties $\upsilon_{\delta\rho_m}$ and $\upsilon_{\delta\rho_i}$ considered in (1.15) are presented.

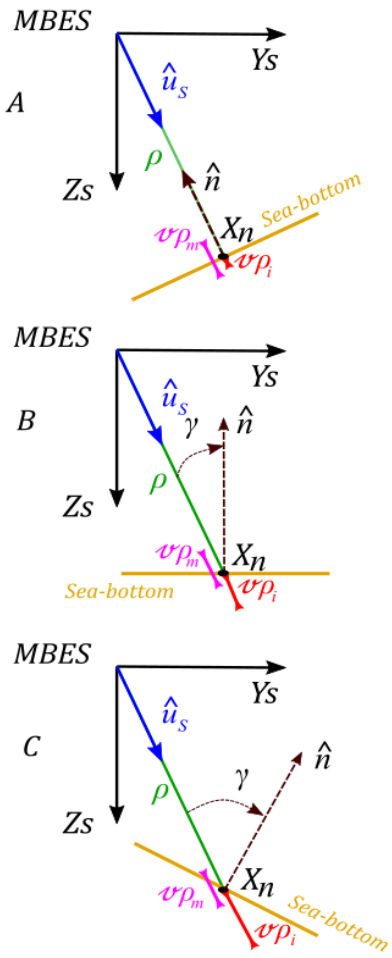

Figure 1.10 - The uncertainties related to the sounding errors ($\upsilon_{\delta\rho_m}$ and $\upsilon_{\delta\rho_i}$) can be observed in different seafloor contexts.

In the first geometry example (Figure 1.10.A), the incidence angle is equal to zero (where $\hat{n} = -\hat{u}_S$). Therefore, the morphological uncertainty ($\upsilon_{\delta\rho_i}$) has also a near-zero value since the morphological error is strongly related to the incidence angle γ. In a flat seafloor context (Figure 1.10.B), the value of $\upsilon_{\delta\rho_i}$ is greater than in Figure 1.10.A since the incidence angle is greater to 0. In Figure 1.10.C, the uncertainty related to the seafloor morphology increases when comparing with Figure 1.10.A and Figure 1.10.B. Indeed, such increase is directly related to the increase of the incidence angle. The morphological uncertainty has its maximum values in the

grazing angle areas where ($\hat{u}_S \perp \hat{n}$). Regarding the value of $v_{\delta\rho_m}$, it remains the same in the three examples since it considers the bathymetric measurements and its related uncertainty. Therefore, the uncertainty value associated to the soundings increases with the grazing angle which is consistent with Tidd (2005) observations. Furthermore, the study states that the swath of the MBES is limited by the grazing angles. Therefore, "a seafloor which results in acute incident angles throughout the swath can be reasonably expected to provide reduced quality data" (Tidd, 2005).

The influence of the seafloor morphology on the uncertainty located in the near nadir area for the simulated and real datasets are consistent with each other. Nonetheless, the range of the influence calculated for the outer beams of the simulated datasets are not in the same order as the one for the real datasets, especially the outmost beam value (i.e. 27% for flat seafloor and 40% for dune seafloor). These values can be directly associated to the grazing angle between these acoustic beams and the seafloor surface, as illustrated in Figure 1.10.C. In these simulated datasets, the outermost beams are characterized by more acute grazing angles, which may be avoided in a real data acquisition.

As synthetized in Figure 1.10, the model proposed in (1.15) is intimately related to the estimation of the normal associate to each sounded point. The estimated normal can be affected by the noise that can be present in the bathymetric data. Even if the normal computation with the robust PCA limit the noise influence, caution must be taken when interpreting the influence of seafloor morphology on the estimated uncertainty considering the proposed model (1.15). There would then be a combination of the morphology influence on the uncertainty value with the noise effect. In areas affected by noisy data, the influence of the seafloor morphology on the uncertainty exceeds 15%. However, in the real dataset shown in Figure 1.9, the noise is limited to outer beams of the swath being even difficult to observe in this figure. Furthermore, the anticipated use of the proposed model (1.15) concerns the post-processing phase. As a result, at that stage, most of the noisy points should be already filtered. Further experiments considering the proposed model (1.15) may also estimate the normal associated to each sounding from the DBM. Such estimation should evaluate not only the sensitivity related to the estimation of the normal from the bathymetric point cloud or from the DBM, but also the computational speed advantage related to the normal estimation.

As argued above, the anticipated use of the proposed model (1.15) should be in the post-processing phase, specifically in the data analysis stage. This information can be very helpful in the study of the sedimentary structures present on the seafloor surface (e.g. Debese et al., 2016; Di Stefano and Mayer, 2018). The characterization of these structures generally involves locating their salient features. For example, in the case of underwater dunes, we would try to locate the crest line. At that stage, the uncertainty estimated with (1.3) is available. It essentially characterizes the uncertainty related to the acquisition system. What the proposed model

brings here is the ability to improve the interpretation of the uncertainty according to the position of the sounding on the dune. As such, not only would the crest line be characterized, but also the uncertainty variation along the crest line would be available. This complementary information could be useful when studying the spatiotemporal variation of the detected structures and saliences. The knowledge of the morphological uncertainty could help discriminate real migration from location discrepancy related to the data uncertainty.

1.8 Conclusion

An estimation of the influence of seafloor morphology on the bathymetric data has been proposed in this paper. It relies on the classical georeferencing model, the bathymetric survey measurements, and their related uncertainties. The proposed model adds a new term, called the morphological uncertainty, to the classical uncertainty estimation model. It represents the contribution of the seafloor morphology to the uncertainty value. This representation relies on the incidence angle of the acoustic beams.

In addition to the proposed model, the second contribution of this work is the analysis of the influence of the seafloor morphology on the uncertainty of the bathymetric data. The relative differences between the uncertainties estimated by the classical model (1.3) and the proposed model (1.15) highlighted the impact of the morphological parameter. This difference was computed for simulated datasets, which were used to validate the model, and a real dataset. The latter, acquired by the Helen Irene Battle vessel of the CHS over a dune seafloor, shows an influence of the seafloor morphology on the uncertainty value up to 15% in almost all of the surfaces, with a few noisy points, presenting an influence greater than 15%. Such a contribution was mostly due to the incidence angle of the beam which varies significantly given the changing seafloor morphology induced by the dunes. The uncertainty increases with the grazing angle beams, such grazing being associated with beams in the swath outer part or with the presence of a particular bottom morphology located anywhere on the swath. Finally, the paper addressed the normal computation in the proposed model, which makes its involvement necessary in the post-processing phase. However, if this model is applied to noisy data, some care would be required when interpreting the uncertainty results, since the noise and morphological effect may be combined.

1.9 References

Amante, C. J. and Eakins, B. W. Accuracy of interpolated bathymetry in digital elevation models. *Journal of Coastal Research,* **2016**, SI 76. Pp. 123-133 DOI: 10.2112/SI76-011

AML Oceanographic. **2020**. Base-X Product Description, viewed 07th December 2021, http://www.mdsys.co.kr/down/AML/Base_X.pdf .

AML Oceanographic. Micro-X Product Description, viewed 07th December **2021**, https://stema-systems.nl/wp-content/uploads/2015/08/Micro-X_Brochure.pdf .

Applanix. POS MV OceanMaster, 2 pages **2019**, viewed 07th December 2021, https://www.applanix.com/downloads/products/specs/posmv/POS-MV-OceanMaster.pdf .

Beaudoin, J., Calder, B., Hiebert, J. and Imahori, G. Estimation of sounding uncertainty from measurements of water mass variability. *International Hydrographic Review,* **2009.** November 2009. Pp. 20-38.

Bjorn, J. and Einar, B. Time referencing in Offshore Survey Systems. FFI/RAPPORT-2006/01666. *Forsv Arets Forskninginstitutt* (Norwegian Defence Research Establishment) **2006**. 122 pages.

Byrne, J., S. and Schmidt, V. E. Uncertainty modeling for AUV acquired bathymetry. *U. S. Hydrographic Conference (US HYDRO)* **2015**. Gaylord Hotel, National Harbor, Matyland, USA. 25 pages.

Calder, B. R. and Mayer, L. A. Automatic processing of high-rate, high-density multibeam echosounder data. *Geochemistry Geophysics Geosystems* **2003**. Vol. 4, number 6, 22 pages. DOI: 10.1029/2002GC000486

Canadian Hydrographic Service. Traitement et analyse de données bathymétriques de CUBE. Pêches et Océans Canada **2012**. 7 pages.

Cassol, W. N. Définition d'un modèle d'incertitude-type composée pour les Systèmes LiDAR Mobiles. Master thesis. *Université Laval* **2018**, Québec, Canada, 111 pages.

Debese, N. Bathymétrie. Sondeurs, traitements des données, modèles numériques de terrain. Cours et exercices corrigés. *TECHNOSUP, éditions ellipses* **2013**. 404 pages.

Debese, N., Jacq, J.J. and Garlan, T. Extraction of sandy bedforms features through geodesic morphometry. *Geomorphology* **2016***, 267*. Pp. 82-97. doi:10.1016/j.geomorph.2016.05.013.

Di Stefano, M.; Mayer, L.A. An automatic procedure for the quantitative characterization of submarine bedforms. *Geosciences* **2018***, 8, 28*, doi:10.3390/geosciences8010028.

van Dijk, T.A.G.P.; van Dalfsen, J.A.; Van Lancker, V.; van Overmeeren, R.A.; van Heteren, S.; Doornenbal, P.J. 13—Benthic Habitat Variations over Tidal Ridges, North Sea, the Netherlands. In *Seafloor Geomorphology as Benthic Habita* **2012***t*; Elsevier: Amsterdam, The Netherlands; pp. 241–249, ISBN 9780123851406. https://doi.org/10.1016/B978-0-12-385140-6.00013-X

Dupont, V. Élaboration D'une Méthode D'extraction de Plans par Croissance de Régions Dans un Nuage de Points Bathymétriques Servant à Alimenter des Estimateurs D'erreur Hydrographique. Master Thesis, Université Laval, Québec, QC, Canada, **2020**; 120 pages.

Godin, A. The calibration of shallow water multibeam echo-sounding systems. *Department of Geodesy and Geomatics Engineering. University of New Brunswick* **1998**. Pp. 76-120.

Goulden, T. Prediction of error due to terrain slope in LiDAR observations. Technical Repport n° 265. *Department of Geodesy and Geomatics Engineering* **2009***. University of New Brunswick*. 150 pages.

Goulden, T. and Hopkinson, C. The forward propagation of integrated system component error within airborne LiDAR data. *Photogrammetry Engineering & Remote Sensing* **2010**, 76, n°5, pp. 589-601.

Hare, R. Depth and position error budgets for multibeam sounding. *International Hydrographic Review* **1995***,* Monaco, LXXII(2), pp. 37-69.

Hare, R., Eakins, B. and Amante, C. Modelling bathymetric uncertainty. *International Hydrographic Review* **2011**. November 2011. Pp. 31-42.

Hughes Clarke, J. E. 2018. The impact of acoustic imaging geometry on the fidelity of seabed bathymetric models. *Geosciences* **2018**, 8, 109.

International Hydrographic Organization. Standards for Hydrographic Surveys. *IHO publication n°44* **2020**. 6th edition, 49 pages.

Joint Committee for Guides in Metrology. Evaluation of measurement data – Guide to the expression of uncertainty in measurement. First edition, September **2008**. 134 pages.

Kongsberg. EM 2040 Multibeam Echosounder, **2021** 2 pages, viewed 07th December 2021, https://www.kongsberg.com/contentassets/e8fa4f09f25f4b1e86eda52cc1355dc7/em-2040---mkii-data-sheet.pdf

Lecours, V.; Dolan, M.F.J.; Micallef, A.; Lucieer, V.L. A review of marine geomorphometry, the quantitative study of the seafloor. *Hydrol. Earth Syst. Sci* **2016***. 20*. Pp. 3207–3244, DOI: 10.5194/hess-20-3207-2016.

Lurton, X. Theoretical modelling of acoustical measurement accuracy for swath bathymetric sonars. *International Hydrographic Review* **2003**, pp 17-30.

Naankeu Wati, G., Geldof, J. B. and Seube, N. **2016**. Error Budget Analysis for surface and underwater survey system. *International Hydrographic Review*, pp 21-46.

Schaer, P., Skaloud, J., Landtwing, S. and Legat, K. Accuracy estimation for laser point cloud including scanning geometry. 5th International symposium on mobile mapping technology **2007**, Padova, Italy, May 29–31, 8 p.

Seube, N. and Keyetieu, R. Multibeam Echo Sounders-IMU Automatic Boresight Calibration on Natural Surfaces. *Marine Geodesy* **2017**, 40:2-3, pp. 172-186, DOI: 10.1080/01490419.2017.1310156

Spectra Geospatial. SP90m GNSS receiver **2020**, 3 pages, viewed 13th June 2021.

Thibaud, R.; Del Mondo, G.; Garlan, T.; Mascret, A.; Carpentier, C. A Spatio-Temporal Graph Model for Marine Dune Dynamics Analysis and Representation. *Trans. GIS* **2013***,* 17, 742–762, DOI:10.1111/tgis.12006.

Tidd, R. A. The impact of varying seafloor topographies, and object geometris on resolution for multibeam echosounders and multi-angle swath bathymetry systems. *Proceedings of OCEANS **2005** MTS/IEEE*, Washington DC, pp. 2224-2227 Vol. 3, DOI: 10.1109/OCEANS.2005.1640096.

Chapitre 2 A Segmentation Approach to Identify Underwater Dunes from Digital Bathymetric Models

2.1 Résumé

L'identification des dunes sous-marines a un rôle central pour assurer la sécurité de la navigation. En effet, la présence de ces structures sédimentaires dynamiques sur le fond marin représente un danger pour la navigation, notamment dans les chenaux de navigation, et doit être mise en évidence pour éviter des collisions avec les navires. Cet article propose une nouvelle méthode dédiée à la segmentation des dunes dans le contexte fluviomarin. Son originalité repose sur l'utilisation d'un modèle conceptuel dans lequel les dunes sont caractérisées par trois saillances, à savoir, la ligne de crête et les deux pieds de dunes qui sont associées aux côtés en pente douce et en pente raide de la dune. La méthode de segmentation proposée implémente le modèle conceptuel en considérant le MNB (Modèle Numérique Bathymétrique) comme la représentation de la surface du fond marin à partir de laquelle les dunes doivent être segmentées. Une analyse morphométrique du fond est effectuée pour identifier les saillances des dunes. Elle est suivie d'une approche orientée-objet visant à éliminer l'approche basée uniquement sur les cellules individuelles de la surface du fond, formant ainsi des objets décrivant mieux les dunes présentes sur le fond. Pour valider la méthode de segmentation, plus de 850 dunes ont été segmentées dans le contexte fluviomarin du Fleuve Saint-Laurent. Un taux de performance de 92% de dunes bien segmentées a été atteint.

2.2 Abstract

The recognition of underwater dunes has a central role to ensure safe navigation. Indeed, the presence of these dynamic landforms on the seafloor represents a hazard for navigation, especially in navigation channels, and should be at least highlighted to avoid collision with vessels. This paper proposes a novel method dedicated to the segmentation of these landforms in the fluvio-marine context. Its originality relies on the use of a conceptual model in which dunes are characterized by three salient features, namely the crest line, the stoss trough, and the lee trough. The proposed segmentation implements the conceptual model by considering the DBM (digital bathymetric model) as the seafloor surface from which the dunes shall be segmented. A geomorphometric analysis of the seabed is conducted to identify the salient features of the dunes. It is followed by an OBIA (object-based image analysis) approach aiming to eliminate the pixel-based analysis of the seabed surface, forming objects to better describe the dunes present in the seafloor. To validate the segmentation method, more than 850 dunes were segmented in the fluvio-marine context of the Northern Traverse of the Saint-Lawrence River. A performance rate of nearly 92% of well segmented dunes (i.e., true positive) was achieved.

2.3 Introduction

Bathymetric data acquired by multibeam echosounder systems (MBES) can be used for multiple applications, the primary purpose being to produce nautical charts. These datasets with high-resolution and accuracy can be used to study the sea bottom morphology, to inspect underwater engineering structures, and for the maintenance in navigation channels by dredging operations (Debese et al., 2016). In this context, the recognition of the underwater sedimentary structures and their dynamics from a DBM (digital bathymetric model) is crucial to ensure safe navigation. Specifically, underwater dunes are large and mobile structures on the sea bottom. They represent a danger for navigation safety since shipping routes necessarily cross dune fields and sand banks, especially nearshore to access harbours and in navigation channels (Ogor, 2018).

Underwater dune identification and segmentation from a DBM is still a manual process. As mentioned by Ogor (2018), this task has many disadvantages, such as being time consuming, subjective, inaccurate, tedious, and less suited to handling large data flow. Indeed, underwater dunes, as many landforms, are fuzzy objects, and their perception may vary from different users depending on their background or experience. Few methods have been proposed to segment underwater dunes from a DBM. Di Stefano and Mayer (2018) proposed a method consisting of two steps. The first carries out the calculation of the terrain parameters. These parameters are calculated by the geomorphons method proposed by Jasiewicz and Stepinski (2012). The second step is the identification of the underwater dunes themselves and their characterization. In this second step, different geomorphon classes are aggregated in order to form the dune entity after a few processing operations. The authors proposed in Debese et al (2016) the segmentation of the underwater dunes through geodesic morphometry. This work addresses the segmentation of the dunes from a bathymetric TIN (triangulated irregular network) surface. This method extracts the salient features of the dunes, such as crest and valley lines. To deal with the presence of ripples, a significant difficulty when segmenting dunes, this work proposed an anisotropic filter to preserve the underwater dunes and eliminate the ripples. Ogor (2018) also proposed a method to segment and classify underwater dunes from the sea bottom surface. This work considers triangular meshes instead of a DBM regular grid. Differential geometry is used to identify crest lines. These are then used as seed regions to segment the underwater dunes. Masetti et al. (2018) proposed the BRESS method, which considers multiple inputs (DBM from MBES survey and backscatter mosaic) as well as the implementation of segmentation methods. In this method, the seafloor is initially segmented using geomorphons (therein called bathymorphons). Then the initial segments of the DBM are analyzed with their respective backscatter intensity to generate the final segments by merging or splitting the previous segments.

Almost all of these previous works consider underwater dunes in marine environments and not in fluvio-marine environments. Such environments are highly dynamic where dunes are organized in different patterns. Dunes are not isolated and well defined but form fields of underwater dunes, where these sedimentary structures are

adjacent to or superimposed on each other. Furthermore, such places are often important navigation channels, requiring frequent dredging operations to ensure navigation safety. As a result, surveyed dunes can be incomplete. Thus, methods proposed in the previous studies are inadequate for dune mapping in the fluvio-marine context. In this paper, we propose that a new solution for segmenting the dunes adapted to fluvio-marine environments is required. To meet this goal, we propose a cognitive approach in which the underwater dune object is defined through a conceptual model. The aim is to eliminate the subjectivity of dune identification according to the data acquisition scale and the lack of a formal dune definition.

The proposed model is applied to the Northern Traverse, a navigation channel in the Saint-Lawrence River (Québec, Canada). Most methods proposed in the literature considered the sea bottom modeled by a TIN. The raw datasets consisting of soundings recorded by the MBES were gridded as a surface and then exported as point clouds with a specific density of 1point/m2. Only the regular point clouds were available. These datasets were acquired in the context of the channel navigation maintenance (dredging). Backscatter information was not available.

This paper is organized in four sections. The first section proposes a state-of-the-art geomorphometry analysis and OBIA (object-based image analysis). The second section is dedicated to the definition of underwater dunes as sedimentary structures on the seabed surface. This definition, based on the literature, aims to introduce the salient features used in the proposed segmentation method. The third section presents the dune segmentation method itself. In this section, the dune landform is formalized through a conceptual model, and the operational model that implements it to segment the dune from a DBM is described. The fourth section provides the results and performances provided by the proposed segmentation method considering different sectors of the Northern Traverse study site in the Saint-Lawrence River. The last section presents the conclusions and the prospects for future research addressing the segmentation of underwater dunes from DBM.

2.4 Advanced Geomorphometry Analysis

The segmentation of underwater landforms from the seabed can be conducted using different methods given the context of the analysis and the data itself. In the marine context, as mentioned in Lecours et al. (2016), object features can be segmented from the seabed using pixel-based analysis. However, object-oriented methods such as object-based image analysis (OBIA) have become increasingly popular in marine studies to segment and classify landforms. Indeed, these methods generally associate geomorphometric analysis and OBIA approaches. These methods rely on the landform definition, which can be expressed as landform ontologies. In this section, we aim to review the different methods that can be employed to segment landforms from a sea bottom surface.

2.4.1 Geomorphometry

Landforms can be defined as geomorphometric objects. These objects generally have a third dimension (volumetric) and can be identified and segmented from a DEM (digital elevation model). The identification of landforms is intimately related to the resolution of the DEM and the analysis scale as well as the definition of the landform itself. The geomorphometry can be defined as the science of the quantitative characterization and analysis of the surfaces. It can be divided into general and specific geomorphometry. The first represents the calculation of terrain attributes, such as slope, orientation, curvature, and terrain variability. It generally uses neighborhood analysis in the DBM context. The latter focuses on the calculation of terrain features or objects and is relatively rare in the marine environment. Specific geomorphometry generally relies on the combined properties of several terrain attributes (Wood, 1996; Lucieer et al., 2018). In the bathymetric context, both general and specific geomorphometry are crucial in the interpretation, description, and classification of the sea bottom geomorphology.

The geomorphometric analysis proposed by Wood (1996) is based on differential geometry principles. This method calculates the geomorphometric parameters of a DEM from features extracted using quadratic approximation on a local window. Extracted features are peak, ridge, pass, plane, channel, and pit. Dragut and Blaschke (2006) proposed an OBIA approach to classify landform elements based on a geomorphometric analysis. In this method, the modeled surface is segmented considering a multi-scale approach. Regions are delineated considering areas with homogenous slope gradient and slope curvature characteristics. Geometric calculations are based on geomorphometric descriptors of the DEM, such as elevation, profile curvature, plan curvature, and slope gradient. Therefore, the surface can be classified using a structured hierarchy that groups the different geomorphometric classes into similar region classes. The resulting regions are classified into nine different landform element classes (i.e., peak, shoulder, steep slope, flat or gentle slope, side slope, nose slope, head slope, negative contact, and toe slope) considering fuzzy logic rules.

In the underwater context, Debese et al. (2016) proposed a method for underwater dune segmentation through geodesic morphometry using a TIN representing the seafloor. This method calculates the curvature of the surface in the differential scale space to identify the crest lines defining the dunes. Ogor (2018) also used differential geometry in order to extract the geomorphometry from a triangular mesh representing the seafloor. In fact, to extract the crestlines of the dunes from the modeled seabed, this work considered the estimation of the principal curvatures based on a local fitting approximation.

When conducting the analysis of a regular gridded DBM, the method developed by Jasiewicz and Stepinski (2012), introducing the concept of geomorphologic phenotypes (geomorphons), can be of interest for landform segmentation. This method is based on pattern recognition principles instead of differential geometry. As

highlighted by Di Stefano and Mayer (2018), geomorphons do not involve the derivation of the surface parameters. This method also eliminates the use of a fixed window for the terrain analysis, using an 8-neighborhood adapted to the terrain topography. The method describes the terrain based on the morphological terrain types including standard elements of landscape, such as ridge, peak, valley, pit, slope, etc. The identification of such standard elements of landscape can be used to identify the landforms primitives, in a cognitive approach. Indeed, this is the method used by Di Stefano and Mayer (2018) to segment the underwater dunes from DBM. Geomorphons have also been used in the seafloor segmentation method proposed in Masetti et al. (2018). In this work, the ten possible geomorphon (bathymorphon) classes were grouped into six possible "geoform" classes in order to simplify the classes proposed in Di Stefano and Mayer (2018). Each class represents a "bathymorphologic" element of the seafloor (e.g., flat, ridge, shoulder, slope, footslope, and valley).

2.4.2 OBIA

Pixel-based analysis of an image may be used as long as the pixel size remains coarser or similar in size to the objects of interest. However, when objects of interest are made up of several image pixels, object-based analysis is preferred. Objects of interest can be defined as discrete regions of an image that are internally coherent (i.e., pixels are homogeneous according to a predefined criteria) and different from their surroundings (i.e., the pixels inside the region are different from the pixels outside the region according to the predefined criteria). A distinction has to be made between the primitives of the objects of interest and the objects of interest themselves. The latter are objects matching real-world objects, such as landforms. The former are usually components of the objects of interest. Compared to single pixels, objects of interest are characterized by their shape that can be described by geometric measures, such as their size, length, etc. Topological relations can also be defined for objects of interest as well as for thematic classification (Benz et al., 2004; Castilla and Hay, 2008; Blaschke, 2010).

Usually, an OBIA approach involves two steps: segmentation and classification. The results of the segmentation are regions, namely groups of connected pixels extracted according to a homogeneity criterion. These regions are either object candidates or primitives of object candidates. They need to be further processed in order to be considered as meaningful objects or primitives. Mathematical morphology operations, such as opening and closing, can be used in order to better delineate the boundary of the objects or their primitives (Soille and Pesaresi, 2002; López-Ornelas, 2009). Once the segmentation is completed, the segmented regions can be aggregated to generate the objects (Dragut and Blaschke, 2006; d'Oleire-Oltmanns et al., 2013). This aggregation can be done by neighbourhood operations since regions belonging to the same object should be close to each other. Then, the classification step of the OBIA considers the shape of the aggregated regions and geomorphometric descriptors of the pixels composing the objects to define different classes and classify the segmented objects.

Ismail et al. (2015) applied an OBIA approach to the DBM to segment geomorphic features on the sea bottom in the context of the classification of submarine canyons. The work involves different types of sonar data (MBES and sidescan sonar data) and their derivatives (e.g., slope, plan curvature, slope curvature, rugosity, etc.). The marine landscape mapping is divided into two steps. The first step consists of terrain analysis using data resampling and an automated procedure for multiple scale analysis. In fact, this multiple scale analysis incorporates the terrain indices produced at different scales to optimise the detection of details and features for the characterisation of the seabed. The authors used the estimation scale parameter (ESP) proposed by Dragut et al. (2010) to estimate the scale parameters. The second step addresses the actual landscape classification. This step consists of a multivariate statistical analysis carried out considering the different types of data and derivatives. Given the large number of input data, principal component analysis (PCA) is applied to select the most significant features. Then, K-means clustering is carried out in order to generate six marine landscapes (e.g., channel floor, flanks, wall, or cliff) that represent the geomorphological features present in submarine canyons. The number K of clusters is determined through an optimization process.

Diesing and Thorsnes (2018) proposed an OBIA method for mapping cold-water coral carbonate mounds. It consists of the classical OBIA steps, namely segmentation and classification of the DBM. The segmentation is conducted according to a multi-resolution approach. More specifically, different segmentations are carried out at given resolutions. Finer resolutions provide smaller regions, while coarser resolutions provide larger regions. The classification is based on user-specified combinations of the region features (e.g., shape, extent, maximum pixel value, object mean value).

As previously mentioned, Masetti et al. (2018) proposed a method to segment the seafloor using a multiple input analysis with the bathymetry from the MBES and the backscatter mosaic. In this method, the seafloor DBM is initially segmented into six “geoform” elements. The resulting regions are area kernels (connected regions of common bathymorphon classes). Then, the method evaluates “each area kernel within the context of the backscatter mosaic much as an experienced analyst would use the backscatter to understand the context of given morphological regions”. The seafloor final segments are homogeneous and non-overlapping with specifically associated attributes that can be used for the seafloor analysis. The BRESS proposed in Masetti et al. (2018) was used in Sowers et al. (2020) to segment the seafloor in the marine landscape.

An OBIA approach was also used in Di Stefano and Mayer (2018) towards the segmentation of underwater dunes from a DBM. In this work, the segmentation relies on the geomorphometric analysis of the DBM using the geomorphons algorithm (Jasiewicz and Stepinski, 2012) as previously mentioned. In their proposed method, the pixels classified by the geomorphon, such as summit, ridge, spur, and slope, are associated with the dune landform. Indeed, all these geomorphons characterize the elements of the dunes that are further discussed in

the paper. Then, these pixels are reclassified into a dune class and the remaining pixels are set to null. The dunes are further processed and can be analyzed based on the calculation of their features.

Many OBIA approaches results in classified regions rather than landform objects. Indeed, the resulting primitives provided by the segmentation of the surface are generally landform elements rather than the landform itself. These primitives need to be further analyzed and then aggregated to build up the landforms. In the context of the Northern Traverse in the Saint-Lawrence River, this aggregation may not work, since the underwater dunes are adjacent rather than large, isolated dunes. The aggregation may result in a region with the presence of the dunes (field of dunes) instead of the dune objects. Since landforms are fuzzy objects, their perception and understanding are related to human cognition. Therefore, the description of a landform may vary from one user to another, and different geographical contexts can be defined in different ways (Deng, 2007; Arvor et al., 2019). As a result, an ontological structure describing the landforms and their components is necessary before developing the segmentation approaches. In other words, the ontology will provide the segmentation with a description of the regions to look for on the surface and the approach with a way to aggregate the relevant regions. In Guilbert et al. (2016), an example of such an ontology is proposed. The authors provide a framework to represent landforms defined by their salient features. Hence, the problem of landform identification and segmentation from a surface is to formalize their saliences using terms that can be later translated into an implementation (Guilbert and Moulin, 2017). The next sections present the definition of the underwater dune on the seafloor. Then, a conceptual model formalizes this definition, and an operational model allows the implementation of the segmentation approach.

2.5 Description of the Underwater Dunes

Before addressing the segmentation of underwater dunes from a DBM, it is important to better understand these complex sedimentary structures. The process of dune formation in the seabed can be described as follows (adapted from Ferret 2011): the presence of an irregularity on the sea-bottom affects the current causing a perturbation in the sediment repository. This perturbation creates zones of erosion–deposition and consequently creates other irregularities on the seabed. These initial irregularities are ripples, and the growth of the dunes is the consequence of the accumulation of sediments in these irregularities. Indeed, dune morphology is similar to ripple morphology.

An underwater dune is built up progressively through time by the accumulation of sediments brought by the flow on the seafloor, forming an elongated eminence. This accumulation generates a gentle slope facing the current, the stoss side of the dune, culminating at the crest of the dune. Passing from this line, sediments fall on the lee side of the dune, which is characterized by a steeper slope. Hence, the dune extension is delimited by the bottom of its sides, which corresponds to zones with a change in sediment accumulation. This transition zone is referred

to as the trough or the footslope. Since a dune is characterized by two slopes, it is bounded by two troughs. The sedimentary structure begins with a trough and a stoss side leading up to a crest line and follows with sediment avalanches down to the lee side in the direction of the trough (Garlan, 2007; Nichols, 2009). Thibaud et al. (2013) corroborate that a "sand dune is characterized by a more or less linear crest and two sides, a gentle one (stoss side) and a steep one (lee side), limited by a footslope and inner sedimentary discordance". Henceforward, we shall consider the term "trough" as the boundary of the dune. Figure 2.1 illustrates a representation of this sedimentary structure.

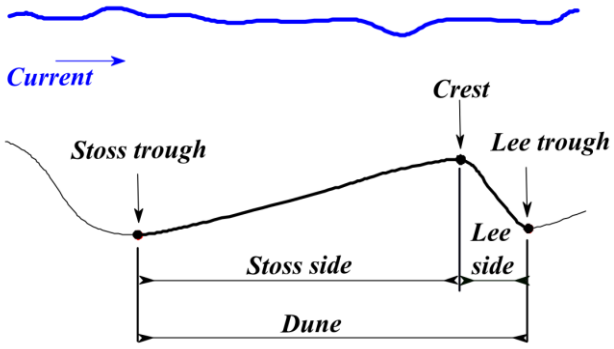

Figure 2.1 - Representation of a dune profile with the crest line, the lee and stoss troughs, and the lee and stoss sides.

The migration of dunes on the sea-bottom and their shape are correlated to their nature and to hydrodynamic factors. Dunes are related to relatively strong or large-scale sustained flows. They can be found in shallow marine environments, estuaries, deltas, and river channels (Boggs, 2006; Nichols, 2009; Thibaud et al., 2013). The correlation between the grain size, the velocity of the flow, and the sedimentary structure formed on the seabed can be observed in Figure 2.2.

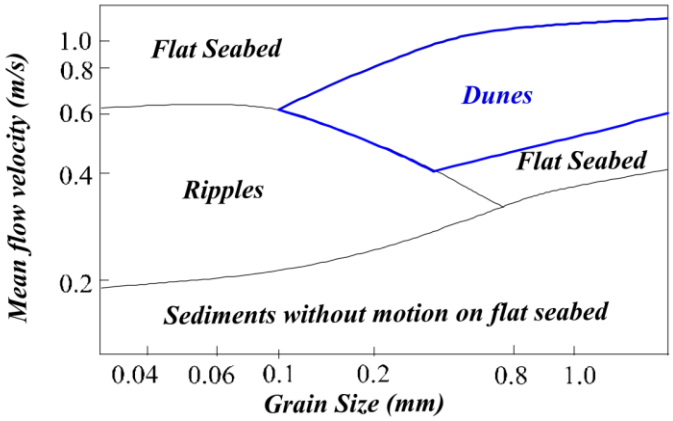

Figure 2.2 - Correlation between the flow velocity, grain size sediment, and the sedimentary structure formed, adapted from Nichols (2009).

Figure 2.2 shows that dunes are formed with a grain size ranging from fine sand to gravel (i.e., grain size greater than 0.1 mm up to more than 1.0 mm). Dunes are limited in finer sediments, such as silt or very fine sand. This limitation is related to the increase of sediment suspension in the flow. When the finer sediments are predominant, “the suspended load suppresses turbulence in the flow and flow separation does not occur” (Nichols, 2009). Due to the complex flow dynamics, smaller sedimentary structures, such as ripples, can superimpose on underwater dunes (Boggs, 2006; Debese et al, 2016).

The orientation of the crest lines of the dunes is usually perpendicular to the main direction of the current, although angular variations up to 20° can be observed (Garlan, 2007). As previously mentioned, dunes are larger sedimentary structures than ripples, according to the widely accepted classification of underwater dunes (Ashley, 1990). Dunes have a minimum wavelength of 0.6 m and height of 0.075 m. These measures can reach values greater than 100 m and 5 m for the wavelength and the height, respectively. The classification presented in Table 2.1 concerns sand structures generated by unidirectional currents, bidirectional currents, and the combination of both, and this classification estimates the dune height with the equation H=0.0677*L^0.8098, where L represents the wavelength of the dune.

Parameters	Small	Medium	Large	Very Large
Wavelength (m)	0.6 to 5	5 to 10	10 to 100	More than 100
Height (m)	0.075 to 0.4	0.4 to 0.75	0.75 to 5	More than 5

Table 2.1 - Dune classification, adapted from Ashley (1990).

Usually, the height and wavelength increase with flow velocity (Debese et al., 2016; Gutierrez et al., 2013). Instead of being estimated with the equation previously mentioned, the height of dunes can be measured as the shortest distance between a crest line and a line joining both troughs (van der Mark and Blom, 2007). Regarding the dune length, the wavelength is usually understood as the distance measured between two consecutive dunes at their crest lines. However, such a definition cannot be applied to isolated dunes. In such a context, the proposed wavelength definition is the horizontal distance between the lee and stoss trough of the same dune (Ferret, 2011). Dunes can also be isolated structures or included in a field of dunes on the sea bottom. Dunes with higher sinuosity and high degree of asymmetry (ratio between stoss and lee sides) are characterized by high migration rates, and more linear dunes have the slowest migration rates (Garlan, 2007; Garlan 2009; Debese et al., 2016).

2.6 Underwater dunes segmentation from a DBM

Using OBIA, image processing, and landform ontologies, we designed a method to segment underwater dunes from the sea bottom surface modeled by a DBM. In our approach, the salient features describing a dune, those

that can be easily perceived and agreed upon, need to be described. When such salient features are available, a complete spatial description of the dunes is not required. Indeed, they act as a skeleton on which the body of the landform is built. Therefore, our approach is formalized through a conceptual model, which relies on the description of the salient features of the dunes independently from the data. This model is then converted into a data-dependent operational model and implemented. The conceptual and operational model are described in this section.

2.6.1 Underwater Dunes Conceptual Model

The formalization of the underwater dunes through a conceptual model considers that this landform can be identified on the seabed from three salient features, namely the crest line, the stoss trough, and the lee trough. The crest line is a linear feature located in the higher zone of the dune. This feature is the upper bound of both sloping sides of the landform. The stoss and lee troughs represent the boundary of the dune objects and are also represented as linear features. They bound the stoss and lee sides, respectively. These boundaries are regarded as fuzzy rather than crisp since their position is not marked as clearly as the crest lines. Indeed, they define an area of transition with a change in the sedimentary accumulation. In fact, they represent a transition zone between the dune and the other sea bottom landforms. Even if they are the transition zone that delineates the boundary of the dune object, they are represented as lines. Therefore, the lee and stoss troughs can be completely or partially detected from a DBM, depending on the steepness of the slope associated with the sloping side of the dune. Accordingly, the conceptual model should consider that the troughs delineating the dunes boundaries can be composed of 1 or several trough segments. These trough segments are linear features on the sea bottom. In the conceptual model, the trough segment can be part of one trough or none, since some trough segments can belong to another underwater landform. The crest line is related to one lee and one stoss trough. However, lee and stoss troughs can be related to more than one crest line, since one trough can be part of several consecutive dunes (i.e., in a field of dunes), as illustrated in Figure 2.3.

In addition to the salient features, the conceptual model considers two components of the dune, namely the lee and stoss sides. These components are the sloping sides bounded by the salient features. That is, the lee side is the surface between the crest line and the lee trough, and the stoss side is the surface between the crest line and the stoss trough. These components link the dune salient features and allow a spatially complete object to be formed. One crest line is related to one lee and one stoss side. The stoss and lee troughs are the lower bound of the stoss and lee sides, respectively. In the case of an isolate dune, the stoss and lee troughs meet at their ends, thus completing the perimeter of the dune. Figure 2.4 summarizes the underwater dunes conceptual model.

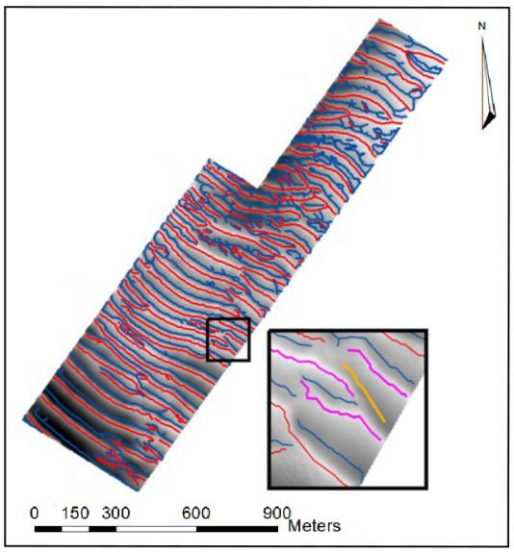

Figure 2.3 - Example of the crest lines (red) and troughs (blue) of a field of dunes identified from a DBM. In the magnified view (i.e., black frame), we can observe that one trough (yellow) can be related to more than one dune (identified with the magenta crest lines).

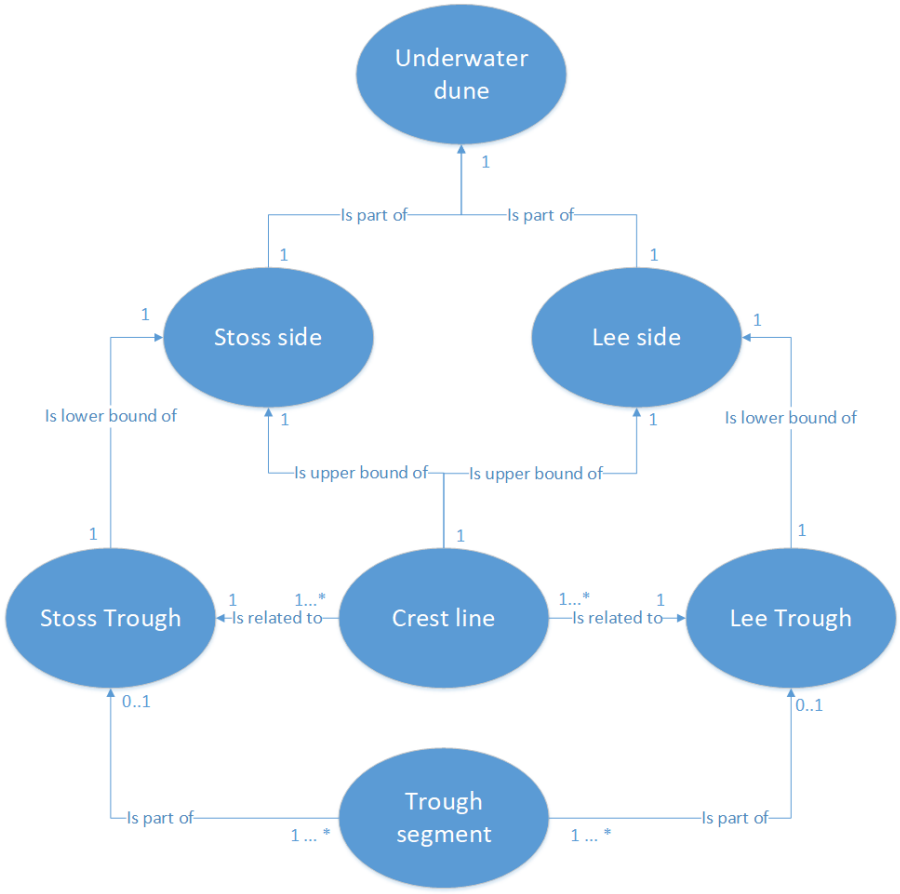

Figure 2.4 - Conceptual model of underwater dunes.

2.6.2 Operational Model

This section describes the operational model that allows the segmentation of underwater dunes from a DBM, considering the conceptual model described in the previous section. This model consists of two phases. The first phase addresses the salient features identification. As underlined in the conceptual model, these features are the crest line and the lee and stoss troughs as boundaries of the dune object. The second phase is the identification of the dune object itself from the salient features previously identified. The result is an image with segmented dune objects. Although our model seems to have some similarities with the approach proposed by Di Stefano and Mayer (2018) (including the fact that both models are organized in two phases), it is clearly different. Indeed, the proposed method identifies salient dune features (i.e., crest, troughs), while the approach proposed by Di Stefano and Mayer (2018) isolates regions potentially corresponding to dunes. Our method then analyzes the extracted salient features and combines them to form individual dunes. In contrast, Di Stefano and Mayer (2018) analyze the regions formed in the previous step and retain only those that are consistent with the three-dimensional dune features. As a result, our method extracts discrete objects while the approach proposed by Di Stefano and Mayer (2018) extract groups of adjacent pixels consistent with dune characteristics.

2.6.2.1 Phase I - Salient Features Identification

Phase I of the operational model addresses the identification of the sea-bottom salient features from a DBM. This phase consists of the following five processes:

1. Pixel-based classification of the sea bottom geomorphometry;
2. Identification of the crest lines;
3. Identification of the dune and non-dune regions;
4. Improvement of the crest lines of the dune regions;
5. Identification of the troughs.

All these processes are illustrated in Figure 2.5. Their rationale and contents are described in the following sections.

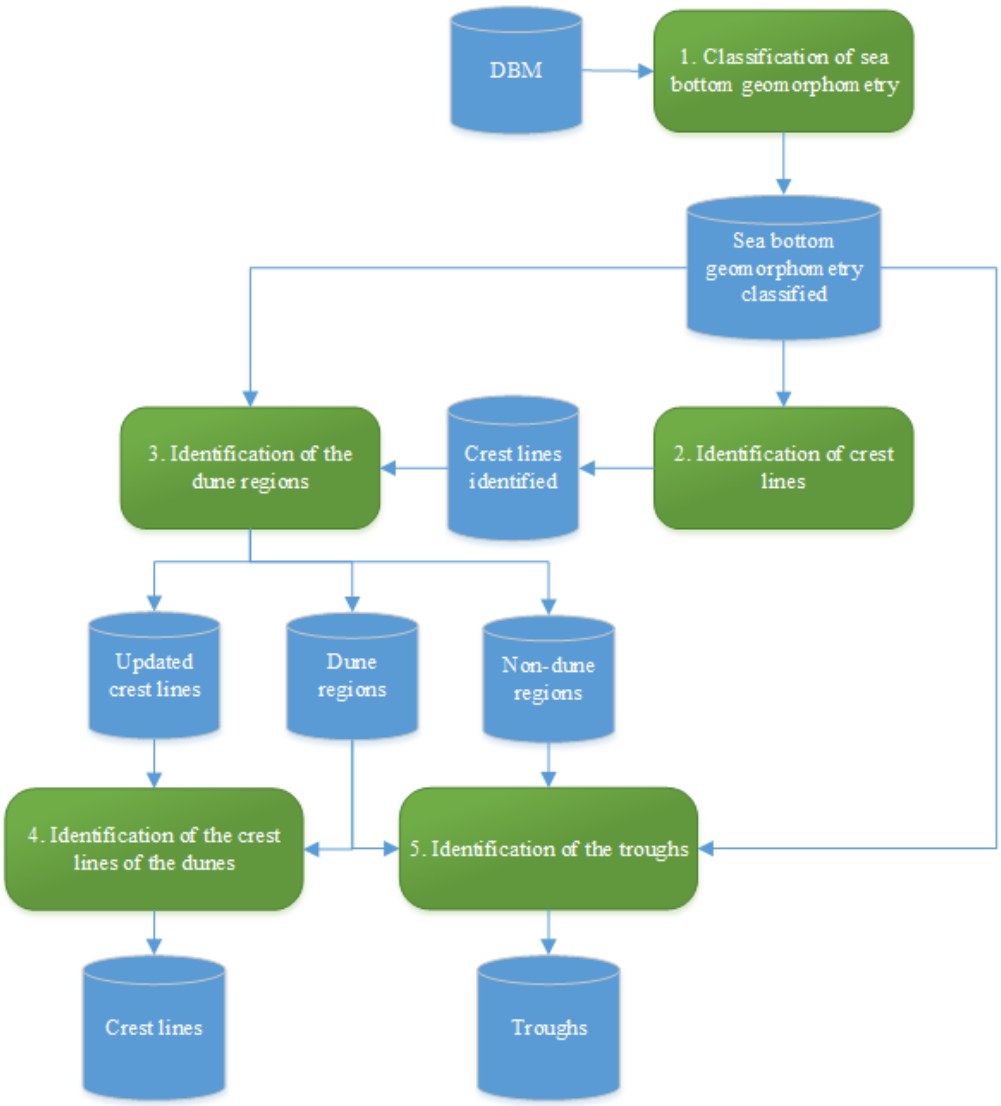

Figure 2.5 - Phase I of the dune segmentation approach.

1. Pixel-Based Classification of Sea Bottom Geomorphometry

The 1st process aims to identify the zones of the DBM that can be associated with underwater dunes in the sea bottom surface. For this purpose, a geomorphometric analysis of the sea bottom was performed. In our approach, this analysis was based on the geomorphons method (Jasiewicz and Stepinski, 2012). As previously mentioned, the geomorphons rely on the concept of geomorphologic phonotypes classification of the DBM. The result of this process is the classified geomorphometry of the DBM (i.e., each pixel has a geomorphometric class). In their approach, Di Stefano and Mayer (2018) extracted the entire dune landform by grouping and processing pixels classified as summit, ridge, spur, and slope. The dunes of the Northern Traverse of the Saint-Lawrence river cannot be segmented by grouping these different geomorphon classes. In this fluvio-marine

context, these sedimentary structures are not isolated dunes well defined on the seabed. Indeed, the studied zone consists of fields of dunes and superimposed structures in a highly dynamic context. Nonetheless, geomorphons are still useful in our approach to identify the salient features composing the underwater dunes.

2. Identification of Crest Lines

Since our approach is based on the salient features of the dunes defined by the proposed conceptual model, the 2nd process aims to identify the crest lines of the DBM. The crest lines of the DBM are represented as line segments located in crest regions. In the proposed operational model, these crest regions correspond to two geomorphons classes, namely summit and crest. As a result, neighboring pixels of the DBM belonging to either one of these two classes are grouped in a region. Then, the regions are filtered according to their extents to preserve only the most reliable and consistent ones with a dune crest. Furthermore, mathematical morphology operations (i.e., opening) are applied to remove non-significant regions. At that stage, the preeminent crest regions are identified. To convert the crest regions (i.e., surfaces) into crest lines (i.e., open contours), skeletonization is applied. The output is a binary image in which the intensity value of crest line pixels is set to 1, while the intensity value of the other pixels is set to 0.

3. Identification of the Dune and Non-Dune Regions

This process aims to identify the dune regions, which circumscribe the crest lines and consequently delineate their boundaries. In our approach, we considered that the boundaries of non-dune regions correspond to the troughs of the dunes when these non-dune regions are adjacent to the dunes. In fact, when two dunes are adjacent, this non-dune region should be linear, defining the trough line, which is the boundary between both dunes. As in the second process, non-dune regions are identified using five geomorphon classes (i.e., footslope, valley, depression, hollow, and flat). Neighboring pixels of the DBM belonging to either one of these five classes are aggregated forming a region. These regions are filtered according to their surface. The output of these steps is a binary image in which the intensity value of non-dune region pixels is set to 0, while the intensity value of the other pixels is set to 1. A binary image representing the dune regions is obtained directly by taking the complement (0 becomes 1 and 1 becomes 0) of the non-dunes binary image. A mathematical morphology operation (i.e., opening) is applied on the binary image of the dune regions in order to remove the non-significant zones. A filtering process is applied to preserve only the crest lines (i.e., cf. step 2) located inside dune regions. The non-dune regions binary image is updated as the image complement of the dune regions binary image. Thus, this process results in three binary images: non-dune regions; dune regions; and updated crest lines.

4. Improvement of the Crest Lines of the Dune Regions

Considering the dunes regions and the crest lines, the 4th process aims to identify and extract the crest lines of the dunes. To achieve this goal, the dune regions are filtered to preserve only the most consistent with the

surface area of underwater dunes. Since the crest lines are extracted using a skeletonization process (cf. 2nd process), some artefacts may appear at the ends of these extracted lines, like loops. This occurs when a pixel inside a crest region has not been classified as a summit or crest. To solve this issue, a filling process is applied to the crest lines, and the skeletonization process is applied again. The result of this process is a binary image in which the intensity value of the crest lines of the dunes regions is set to 1, while the intensity value of other pixels is set to 0.

5. Identification of the Troughs

This process aims to identify the troughs of the dune regions. These troughs will be associated with a crest line to compose a dune object in the second phase of the operational model. This process considers the non-dunes regions (cf. step 3) and the dune regions (cf. step 2) as well as the sea bottom classified geomorphometry (cf. step 1). The non-dune regions are filtered to remove non-significant objects. To delineate the troughs, an analysis of the geomorphometry of each non-dune region is conducted. Two scenarios are considered for non-dune region boundaries adjacent to the dune regions. The first considers the non-dune region as relatively flat. As such, its boundary is regarded as the trough of the adjacent dune regions. The second considers the non-dune as presenting some valley shape. In such a context, the region needs to be skeletonized. The resulting skeleton is regarded as the trough of the adjacent dune regions. The result of this process is a binary image in which the intensity value of the dune troughs is set to 1 while the intensity value of the other pixels is set to 0.

2.6.2.2 Phase II - Dune Identification

Phase II of the dune segmentation approach is the identification of the dune object itself from the salient features identified in phase I (crest lines and troughs). In this phase, the binary images with the crest lines and the troughs are considered. Phase II consists of three processes: the calculation of the crest lines attributes; the identification of the troughs associated with each crest line; and the creation of dune objects based on the identification of their crest line and troughs. These processes are illustrated in Figure 2.6 and described in the following sections.

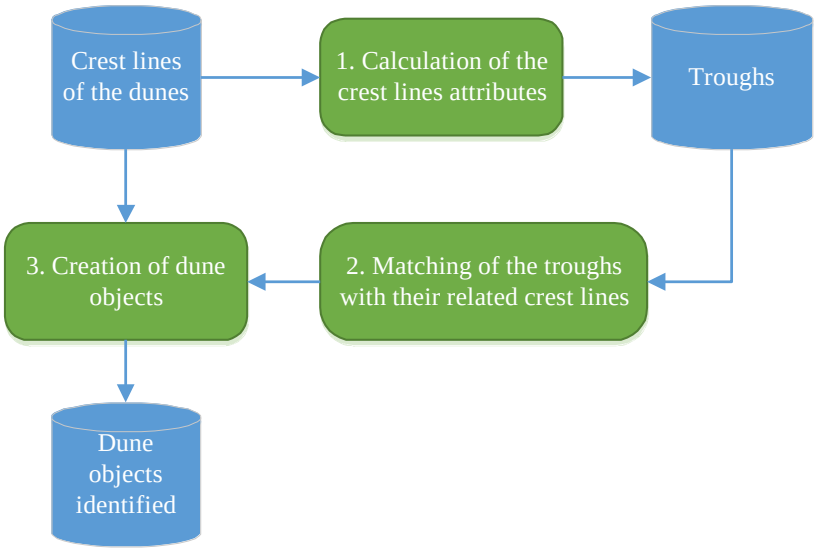

Figure 2.6 - Phase II of the dune segmentation approach.

1. Calculation of the Crest Line Attributes

First, the crest lines, identified in phase I, are labeled. Since each crest line is located inside a dune region, its label is used subsequently to label the dune region. Then, each start and end point of the crest lines are identified and used to compute the orientation angle of the lines. These attributes are involved in the identification of the troughs of each crest line. The results of this process are an image of the labeled crest lines as well as a database gathering their attributes.

2. Matching of the Troughs with Their Related Crest Lines

The 2nd process aims to match the troughs with their corresponding crest line. This matching yields the creation of a dune object. As detailed in the conceptual model, each dune has two troughs (lee and stoss troughs), and a trough consists of n trough segments. A mathematical morphology operation (i.e., dilation) is applied to the troughs to enhance their visibility and ensure the matching of the crest line and the troughs to delineate the dune object. Then, the nearest troughs to a crest line are searched for in order to find its related troughs. This search is conducted in the orthogonal direction to the crest line orientation and in a predefined range distance. This distance prevents the search for a trough that does not belong to the crest line. The matching of the trough boundaries to the crest line is done for each crest line labeled in the 1st process. This process results in a database consisting of the position of the pixels belonging to the troughs of each dune identified by its crest line.

3. Creation of Dune Objects

The 3rd process aims to create the dune object from the crest lines and their matched troughs. An aggregation of the pixels located between the crest line and the trough boundaries is carried out. This process may leave some holes in the surfaces created by the aggregation. To fill these holes, mathematical morphology operations

(i.e., closing) are applied. The result of this process is an image of the segmented dune objects. Each dune has the same label as its crest line.

2.7 Segmentation of the Dunes of the Northern Traverse of the Saint-Lawrence River

2.7.1 DBM description

The Northern Traverse is located in the transition zone between the river estuary and the middle estuary of the Saint-Lawrence River. This navigation channel has a width of approximately 305 m and a draft of 12.5 m, which makes it possible to navigate vessels with a draft of 15 m up to Québec City with the tide effect (Comité de Concertation Navigation de Saint Laurent Vision, 2004). The sectors considered in the segmentation approach can be observed in Figure 2.7.

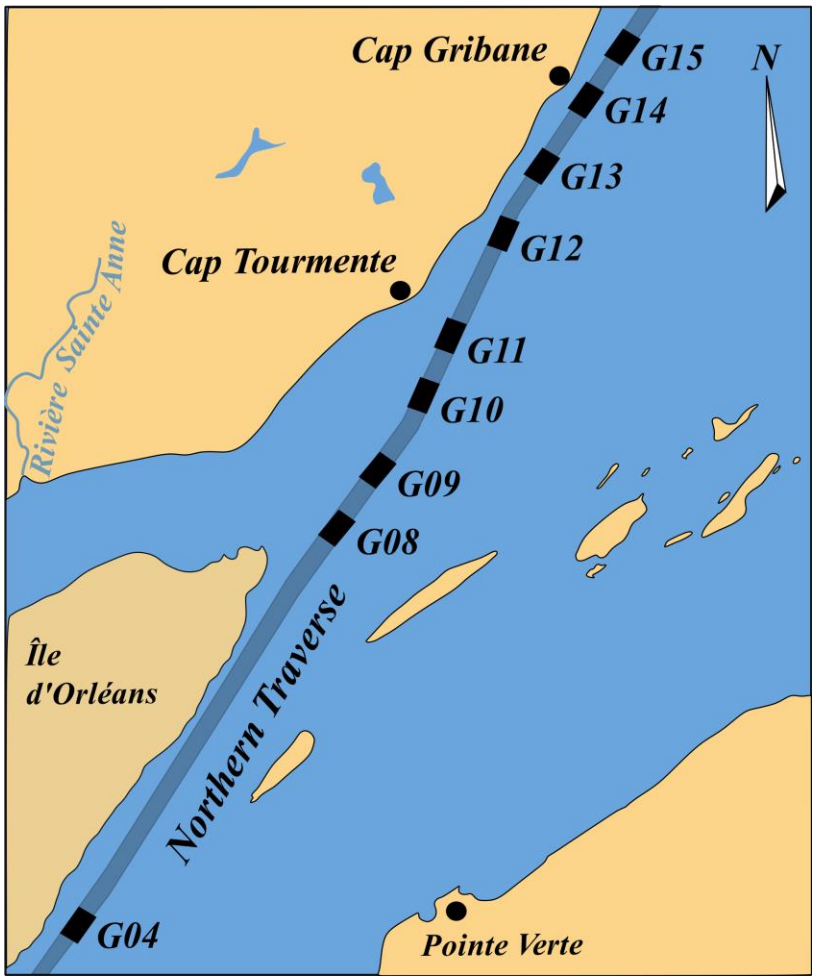

Figure 2.7 – Location within the Northern Traverse of the Saint Lawrence river of the studied sectors (e.g., G04, G08, …, G15).

As previously mentioned, the seafloor was modeled from the data provided by the Canadian Hydrographic Service (CHS) and Ocean Group, which consists of regularly spaced points of the seabed. Thus, regular a gridded DBM could be generated for the different sectors. In our study, the DBM resolution was 1 m for all considered sectors. Figure 2.7 shows nine sectors. However, in our study, we considered 14 DBMs computed over these nine sectors. Consequently, some sectors have more than one DBM (namely sectors G09, G10, G11, and G14). Even if the DBMs are in the same sector, the sedimentary structures on the surface are different due to the high dynamism of the Saint-Lawrence river in the studied zone. Additionally, since the datasets were surveyed in the context of maintenance of the navigation channel, DBMs in the same sector were computed with data acquired at different dates, with a time lapse of a few months to a few years. Specifically, the surveys aimed to detect and dredge the sedimentary structures that could represent a risk for safe navigation. Figure 2.8 illustrates a few examples of the Northern Traverse DBMs considered in which the different dune configurations on the seabed can be observed.

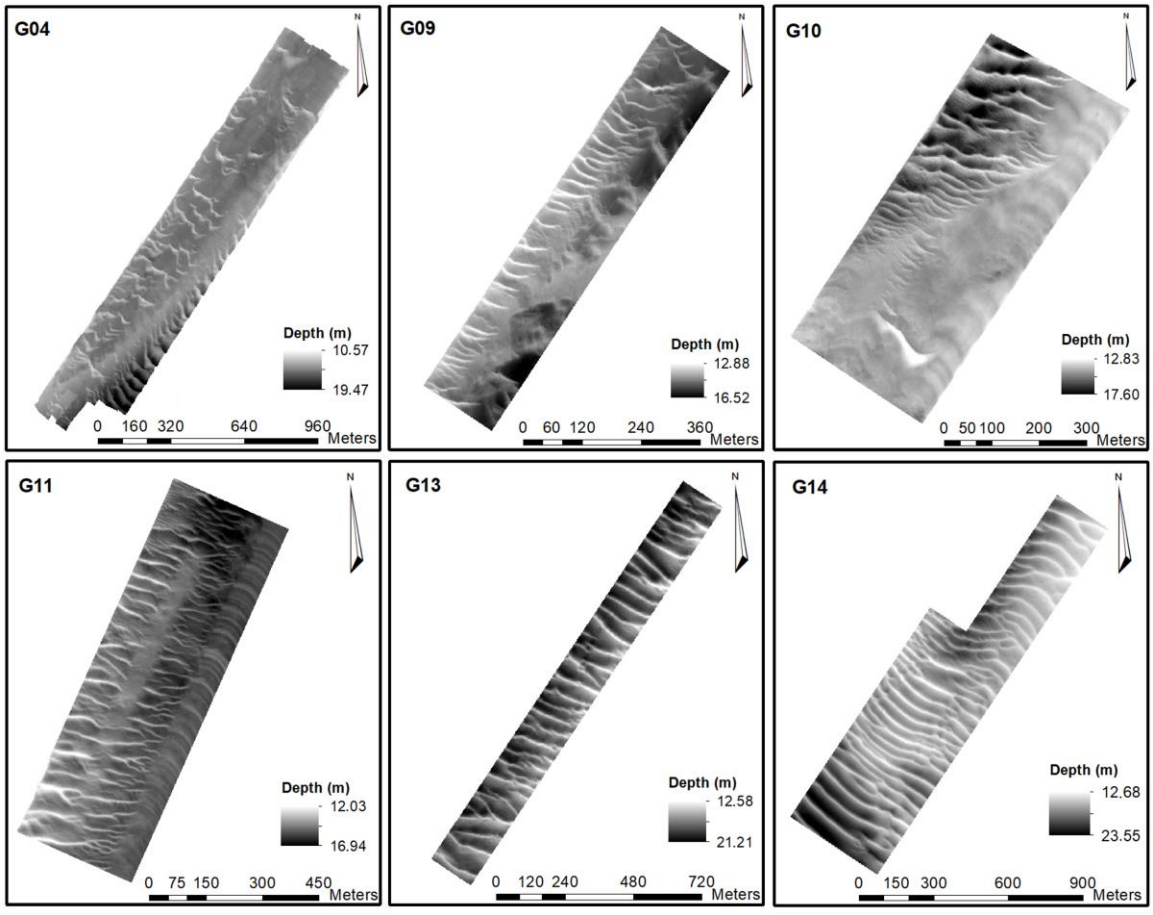

Figure 2.8 - DBM of the sectors G04, G09, G10, G11, G13, and G14 of the Northern Traverse.

The different DBMs presented in Figure 2.8 illustrates different configurations of the sedimentary structures present in the seabed of the Northern Traverse, with a depth ranging between 10.50 m and 23.50 m, namely isolated barchan or 3D dunes in G04; sinuous dunes isolated or in a field of dunes in G09, G10, and G11; as well as straight dunes in a field of dunes in G13 and G14. This dune diversity is due to different factors, such as the flow (current) velocity and the grain size. The nine sectors of the Northern Traverse were considered to evaluate the robustness of the proposed segmentation approach by segmenting a large number of sedimentary structures in many different configurations.

2.7.2 Segmentation results

The developed segmentation approach from DBM is based on the conceptual model of underwater dunes previously defined. Salient features are first identified by employing the geomorphons (Jasiewicz and Stepinski, 2012). This method uses four parameters to classify the geomorphometry of the sea bottom: the outer search radius, the inner search radius, the flatness threshold, and the flatness distance. The values of the parameters considered in the generation of the geomorphon classes can be observed in Table 2.2.

Parameter	Values
Outer search radius	[5, 10, 15, 20, 25, 30]
Inner search radius	[1, 2, 3, 4, 5]
Flatness threshold	[0.5, 1, 1.5, 2, 2.5, 3]
Flatness distance	[0, 0.5, 1, 2, 3, 4, 5]

Table 2.2 - Values of the parameters used in the generation of geomorphon classes.

The values of the geomorphon parameters presented in Table 2.2 come from an adaptation of the sensitivity study conducted by Dupont (2020). In this research, the author used the geomorphon algorithm to segment the seafloor using three datasets. The first dataset was a flat sea bottom. The second dataset involved slopes and flat areas. The third dataset was acquired in a rocky underwater canyon context. A comparative analysis was conducted in order to determine the relevant values for the geomorphon parameters. It was done using only a subset of all the sectors (surfaces illustrated in Figure 2.8). A visual comparison involving the dunes identified from the DBM and the results of the geomorphon, as made by Di Stefano and Mayer (2018), yielded the following parameters: 15 (outer search radius), 4 and 5 (inner search radius), 1 and 1.5 (flatness threshold), and 2 (flatness distance). Please note that two values were used for the inner search radius and the flatness threshold for the sea bottom modeled surfaces. The geomorphon classifications can be observed in Figure 2.9.

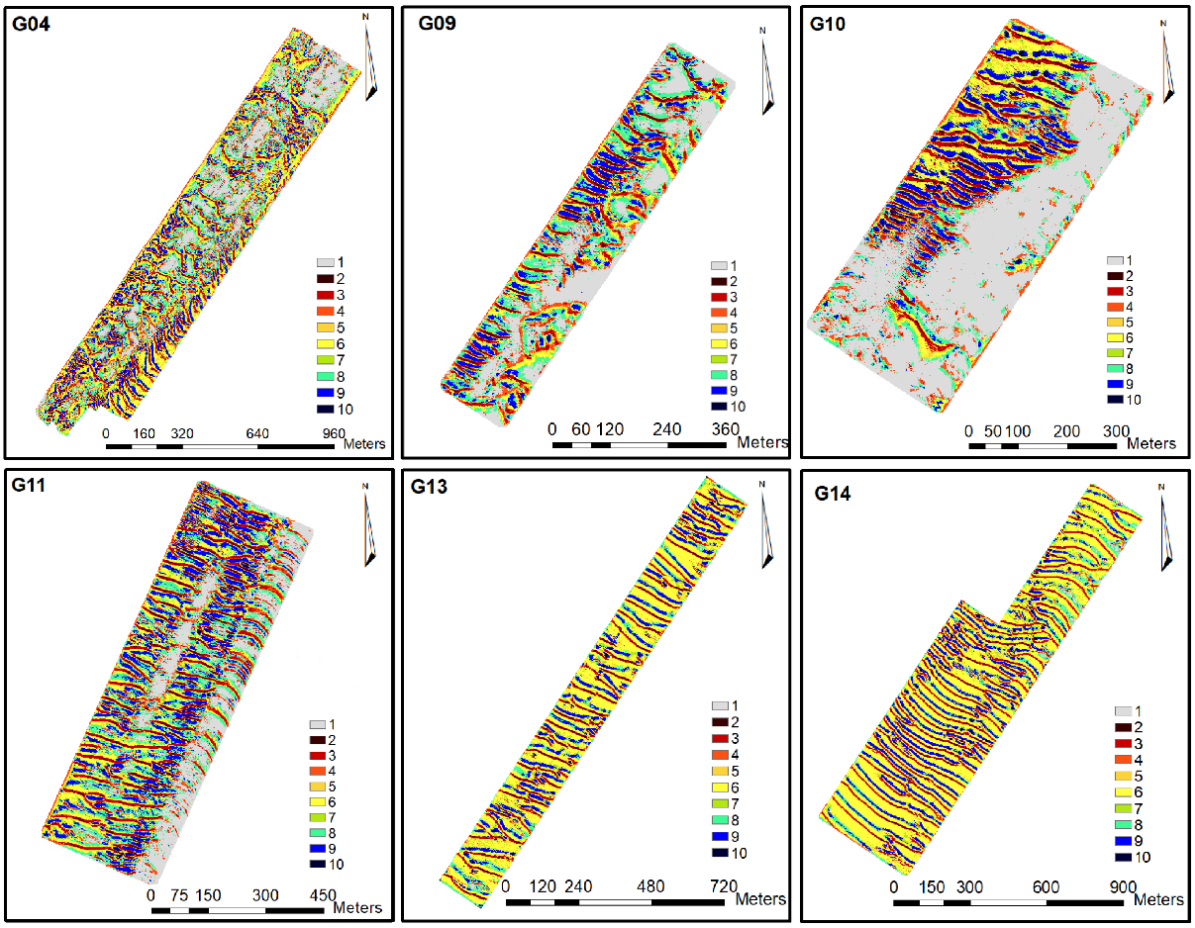

Figure 2.9 - Geomorphon surface of the DBM illustrated in Figure 2.8, where 1 represents flat, 2 summit, 3 ridge, 4 shoulder, 5 spur, 6 slope, 7 hollow, 8 footslope, 9 valley, 10 depression.

Processes 2 to 5 from phase I are applied considering the geomorphon surfaces generated. Figure 2.10 illustrates the results of phase I, which are the crest lines and troughs of the dunes identified.

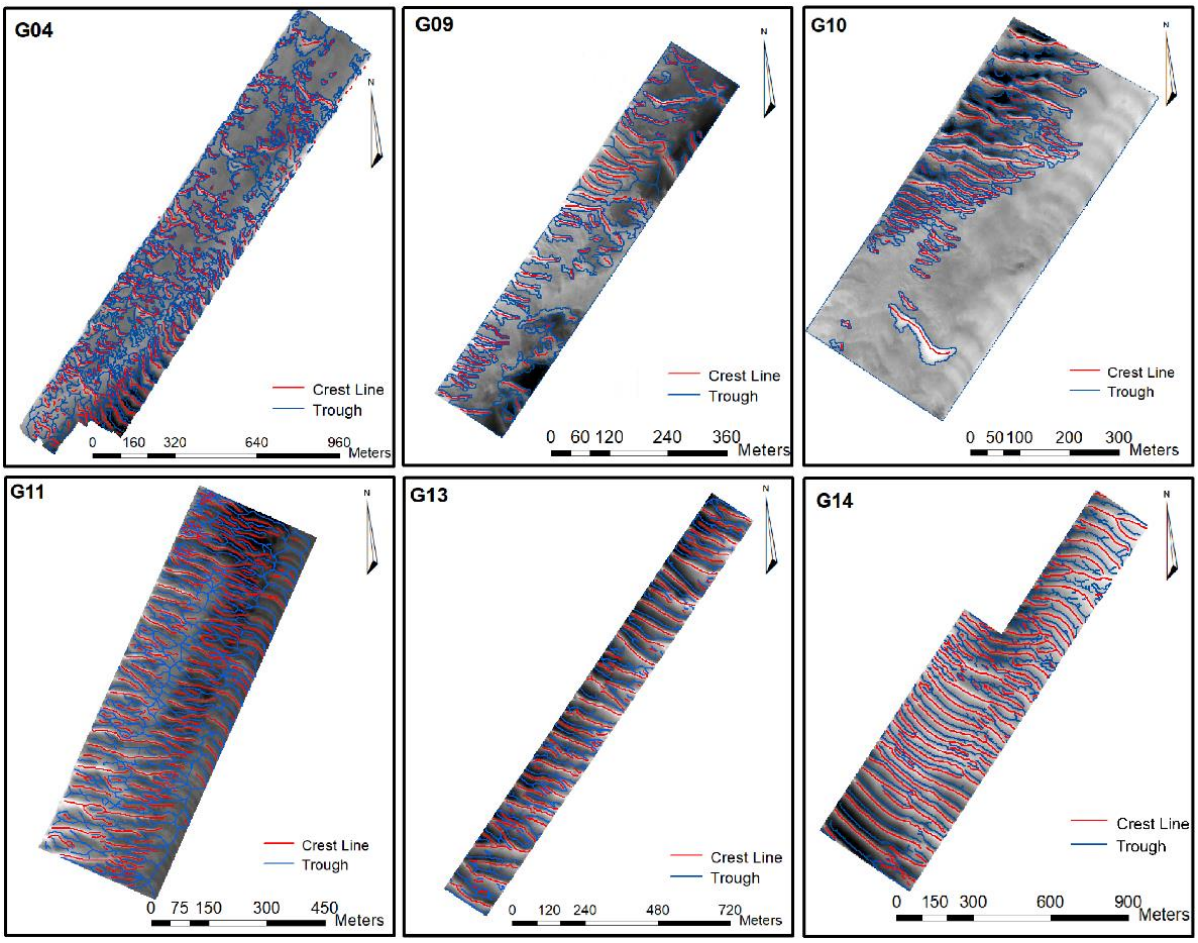

Figure 2.10 - The salient features of the underwater dunes identified for sectors G04, G09, G10, G11, G13, and G14 of the Northern Traverse. The salient features (crest lines in red and troughs in blue) are superimposed on the DBM.

Once the salient features have been identified, the three processes of phase II are applied. From the 14 considered DBMs, a total of 882 underwater dunes were segmented. Figure 2.11 presents the number of segmented dunes for each DBM of the Northern Traverse.

Figure 2.12 illustrates the dune objects segmented from the DBM shown in Figure 2.8.

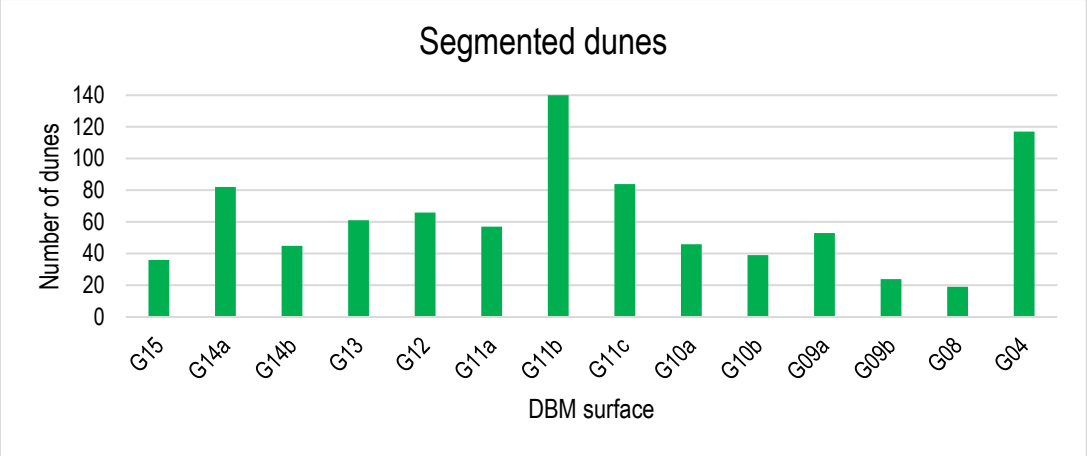

Figure 2.11 - Number of segmented dunes by DBM surface.

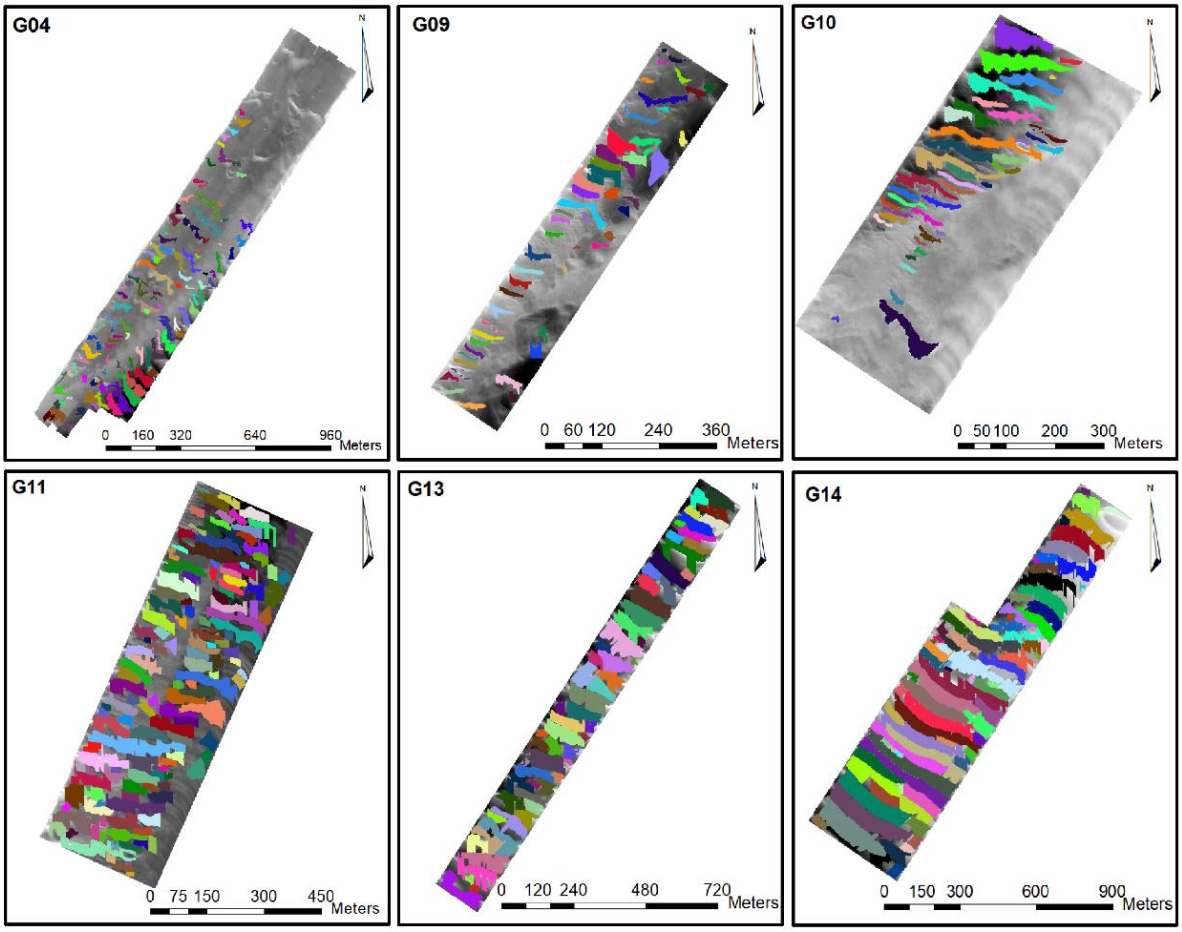

Figure 2.12 - Segmented dunes of the sectors G04, G09, G10, G11, G13, and G14 of the Northern Traverse. The different dune objects are represented by colored polygons. The dune objects are superimposed on the DBM.

Figure 2.13 presents a 3D view of G04, G10, G13, and G14 surfaces to better visualize the segmented dunes.

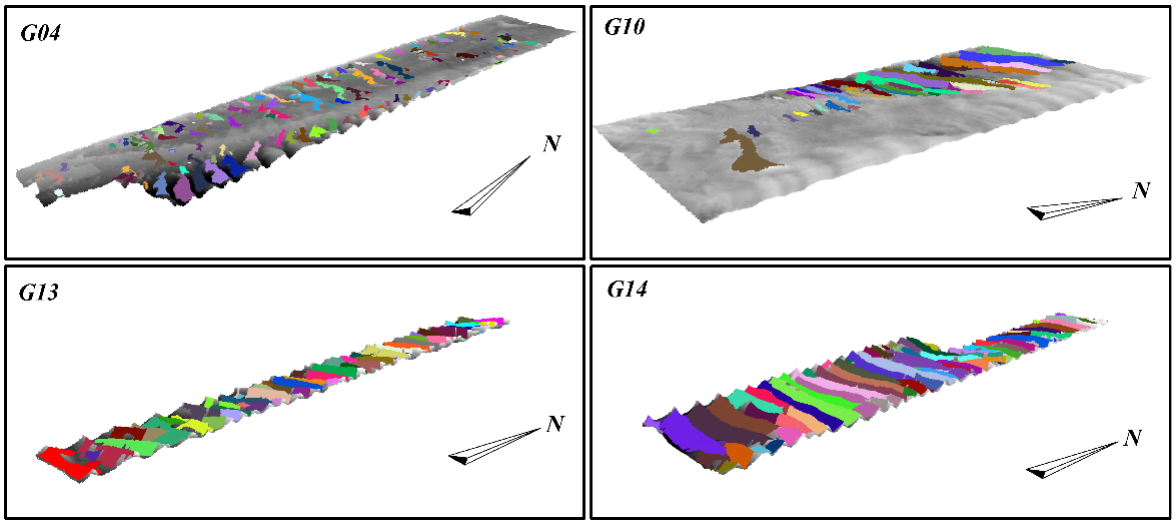

Figure 2.13 - Three-dimensional visualisation of the surfaces G04, G10, G13, and G14 with segmented dunes (colored). Please note the vertical exaggeration of 5.

The results of the dune segmentation approach are analyzed in the next section.

2.7.3 Segmentation result analysis and discussion

In order to analyse the results presented in the previous section and assess the performance of the proposed segmentation method, a ground truth was built for each DBM by manually selecting the dunes on the surface. Three performance measures were computed by comparing the dunes in the ground truth and the dunes in the segmented DBM, namely true positive, false positive, and false negative rate. A true positive is considered when a minimum of 50% of the segmented area of the dune coincides with its area in the ground truth. A false positive is considered when the area of the segmented dune coincides with less than 50% in the ground truth or when this dune does not have a related dune in the ground truth. A false negative is when the proposed method fails to segment a dune existing in the ground truth (adapted from Nguyen et al., 2020). Figure 2.14 summarises the three performance measures for each DBM.

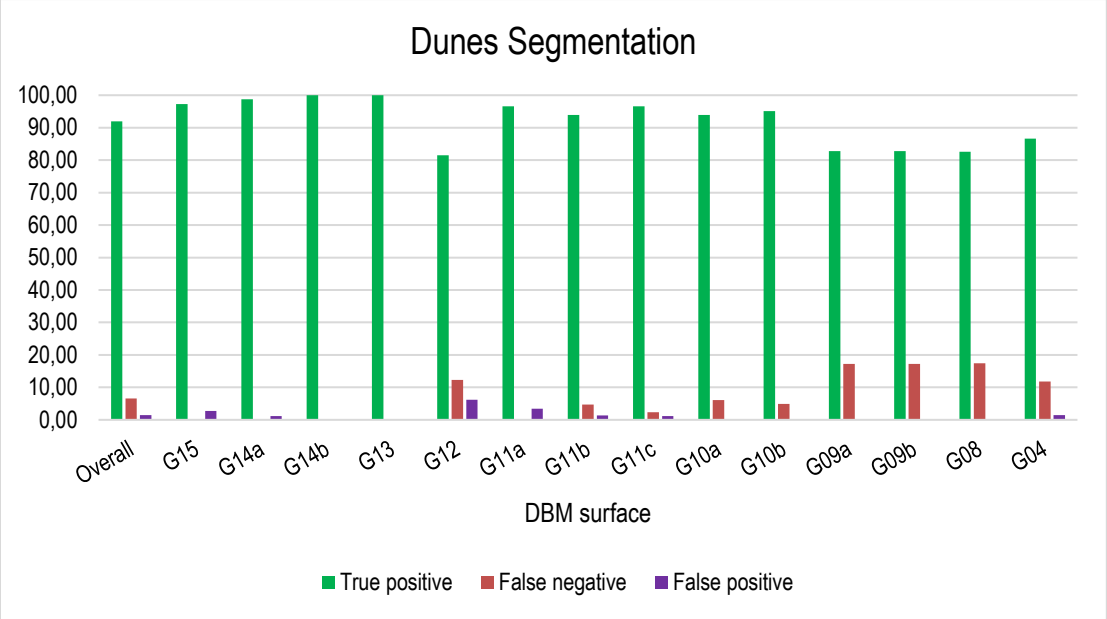

Figure 2.14 - Performance measures of the proposed method, namely true positive, false negative, and false positive rates. Please note that we present the overall performance considering all the surfaces.

The overall performance of the proposed dune segmentation method, averaging the results over all DBMs, is 91.9% of true positive, 6.6% of false negative, and 1.5% of false positive. This means that out of the 882 segmented dunes, 868 were true positive, 14 were false positive, and 62 were false negative. Among the 14 DBMs, nine had a true positive rate higher than 93%, with two even reaching 100% (i.e., G13 and G14b). The true positive rate of G14a and G15 was greater than 97%, with only one false positive detection each. The segmented dunes from surfaces G14a and G13 can be observed in Figures 2.12 and 2.13. Among the false positives, 35% were small structures present in the seafloor detected as dunes, and 65% were structures that had been partially dredged. These dunes were altered by machinery and do not have clearly delineated salient features required for the dune segmentation. An example of dredged dunes in different surfaces can be observed in Figure 2.15.

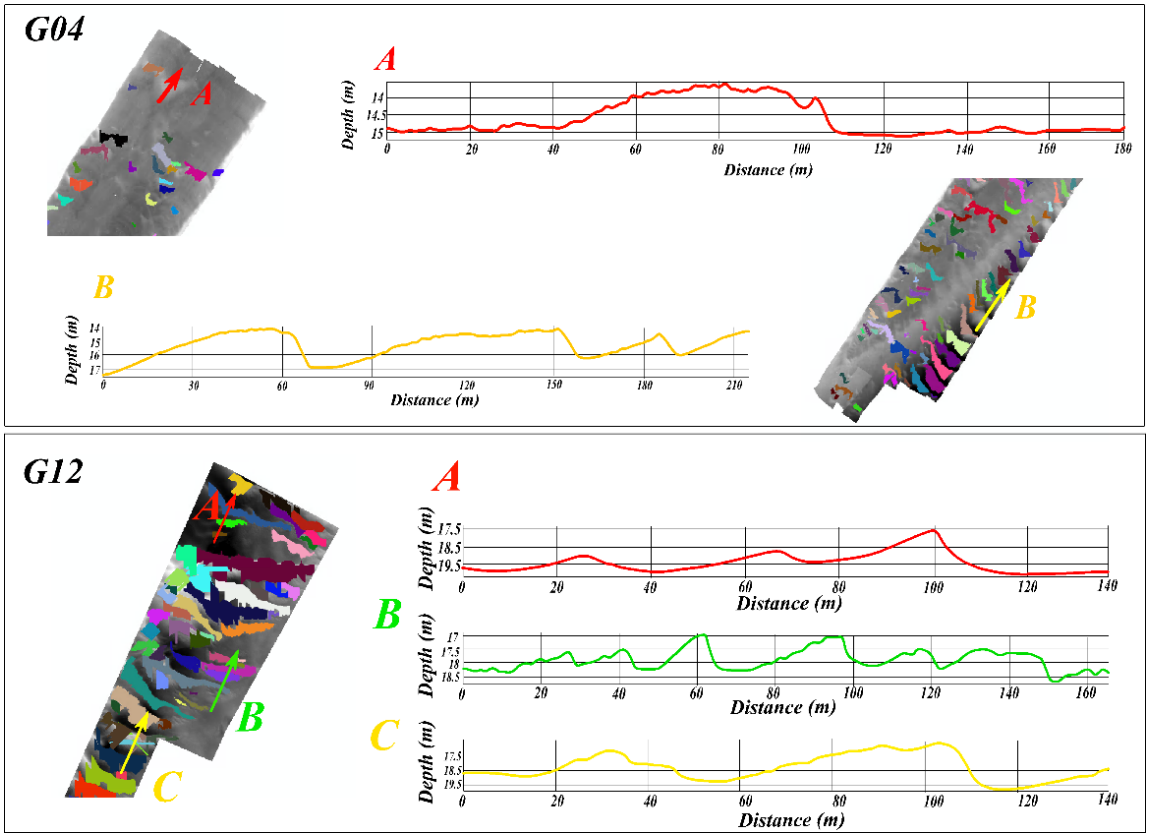

Figure 2.15 - False positive dredged dunes segmented from surfaces G04 and G12. The arrows illustrate the profiles and their directions on the DBM.

Relying on profiles A and B of G04, we can infer the dunes were not identified because their crests were dredged and therefore were not detected. In B, only the portion of the dune that was not dredged was detected. The highest false positive rate was observed in G12, with 6.2%. In this surface, among the 81 identified sedimentary structures, 5 false positives were associated with the central dune in profile C of G12 presented in Figure 2.15. This specific dune does not have a well delineated crest line, and therefore 5 small structures, possibly ridges, were detected instead in this partially dredged dune. Profile A of G12 shows dunes correctly segmented from G12 DBM. In other surfaces, false positives were also related to the absence of a well delineated crest line. Regarding the false negative, after analyzing the statistics of this performance measure, we conclude that its occurrence was related to the presence of small dunes on the DBM. In fact, the segmentation of these dunes was not possible with our method since the geomorphometric classification does not identify the crest lines of these sedimentary structures. The false negatives in the results are mostly associated with the resolution of the DBM. These smaller structures responsible for the false negative should be detected with a finer resolution of the DBM. Figure 2.16 illustrates four examples of false negative on surfaces G09a and G10a.

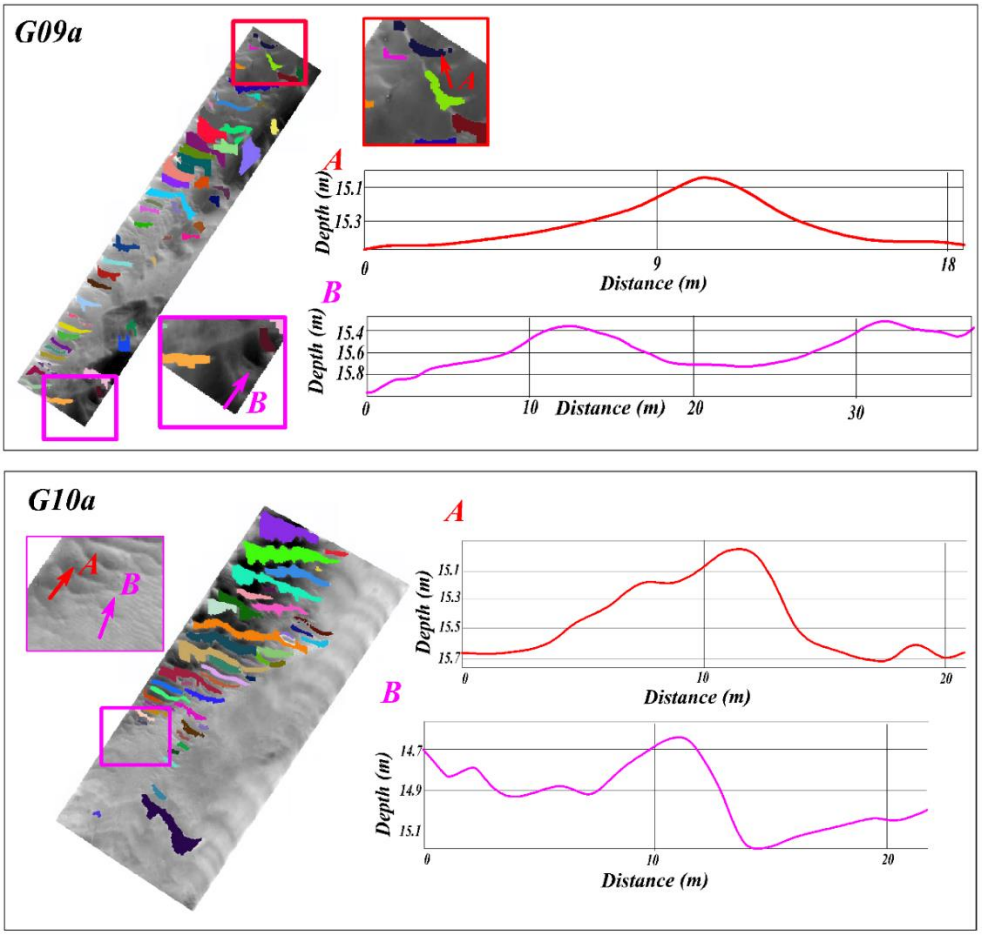

Figure 2.16 - False negative of surfaces G09a and G10a. The arrows illustrate the profiles and their directions on the DBM.

Profiles A and B of surface G09a and B of surface G10a show two small dunes with a height below 40 cm, characterizing small dunes. Either the geomorphometric classification did not detect the crest line or the crest was removed by the filtering process. The false negative illustrated in profile A of surface G10a (Figure 2.16) was also removed by filtering for not having a significant surface to be considered as an underwater dune. After analyzing the false negative, we conclude that the small dunes (height inferior to 40 cm, Table 2.1) were identified manually, but the segmentation method was not able to identify them. Indeed, in these small structures, the salient features were not properly identified by the geomorphometric analysis. Consequently, these small dunes were not segmented. In the proposed method, the identification of the salient features is dependent of the scale of the analysis, as highlighted by Di Stefano and Mayer (2018). Indeed, the identification of the salient features of the dunes is related to the resolution of the DBM. The resolution of the bathymetric surface is related to the bathymetric data uncertainty and quality as proposed by the Canadian Hydrographic Service (2012). However, in this research, the DBMs of the Northern Traverse were generated using a point cloud with regularly spaced points. Therefore, based on the density of the point cloud, the 1 m resolution was chosen. Then, the

identification of small dunes with a wavelength between 0.6 m and 5 m and a height between 0.075 m and 0.4 m becomes impractical, since the DBMs considered in the Northern Traverse have a pixel resolution of 1 m.

2.8 Conclusions

A novel method dedicated to underwater dune segmentation was proposed in this paper. This method is based on the underwater dunes formalized concept through the conceptual model. The segmentation method relies on a geomorphometric analysis of the seabed and mathematical morphology operations to delineate the salient features of the dunes. Then, an OBIA approach was used to match the salient features, thus generating the dune objects. To validate the segmentation method, more than 850 dunes were segmented on the Northern Traverse of the Saint-Lawrence river. The segmented dune objects displayed significant diversity regarding their characteristics, namely straight dunes; tridimensional dunes; barchan dunes; dunes belonging to a field of dunes (adjacent structures); and isolated dunes.

The originality of our segmentation method lies in the dune conceptual model at the basis of this approach. Thanks to this model, identifying the dunes requires only the identification of the dune salient features (crest line, stoss trough, and lee trough) rather than all the dune components. These features delineate the dune object itself. Therefore, formalizing the conceptual and operational models provides an efficient way to segment underwater dunes from the DBM. Indeed, these models can be reused with different datasets with minor adjustments. As an example, the geomorphometric parameters involved in the identification of the salient features can be adapted for different contexts and scales of analysis. In addition, the geomorphon algorithm is not the only one that could be used to conduct the geomorphometric analysis of the DBM (i.e., phase 1 of the proposed method).

The paper focused on underwater dunes situated in a fluvio-marine context. Further experiments will be dedicated to assessing the performance of our method in other contexts (e.g., marine dunes). Additionally, further work should be invested in assessing the impact of DBM with finer and coarser resolutions on the segmentation performances, especially on its capacity to detect small dunes. In addition, relying on the segmentation method, future work will be dedicated to dune classification. Since the conceptual model formalizes the dune by its salient features, these features are not only used to identify them but also should be used to characterize and classify them. The classification should consider the classes well established in the literature (e.g., as in Ashley, 1990) and extend these categories based on the dune geometry (e.g., asymmetry index, orientation) and expert knowledge (e.g., risk for safe navigation). Future work related to the classification should also consider the backscatter data in order to specify the categories of dunes using the dune geometry and expert knowledge. In fact, if this information is available with the dataset, the segmentation method could

be improved by using a multiple input, similarly to what has been proposed in Masetti et al. (2018) with the BRESS algorithm.

2.9 References

Arvor, D.; Belgiu, M.; Falomir, Z.; Mougenot, I.; Durieux, L. Ontologies to interpret remote sensing images: Why do we need them? *Giscience Remote Sens*. **2019**, 56, 911–939, doi:10.1080/15481603.2019.1587890.

Ashley, G.M. Classification of large-scale subaqueous bedforms: A new look to an old problem. *J. Sediment. Petrol*. **1990**, 60, 160–172.

Benz, U.C.; Hofmann, P.; Willhauck, G.; Lingenfelder, I.; Heynen, M. Multi-resolution, object oriented fuzzy analysis of remote sensing data for GIS-ready information. *ISPRS J. Photogramm. Remote Sens*. **2004**, 58, 239–258, doi:10.1016/j.isprsjprs.2003.10.002.

Blaschke, T. Object based image analysis for remote sensing. *ISPRS J. Photogramm. Remote Sens*. **2010**, 65, 2–16, doi:10.1016/j.isprsjprs.2009.06.004.

Boggs, S. Principles of Sedimentology and Stratigraphy, 4th ed.; Chapter 4 Sedimentary structures; Chapter 9 Marginal Marine Environments; *Pearson Prentice Hall: Upper Saddle River*, NJ, USA, **2006**; pp. 74–116, 289–333, ISBN 0-13-154728-3.

Canadian Hydrographic Service (CHS). Traitement et Analyse de Données Bathymétriques de CUBE; *Pêches et Océans Canada*, Canada, **2012**; 7 pages.

Castilla, G.; Hay, G.J. Image objects and geographic objects. *In Object-Based Image Analysis, Lecture Notes in Geoinformation and Cartography*; Blaschke, T., Lang, S., Hay, G.J., Eds.; Springer: Berlin/Heidelberg, Germany, **2008**; Chapter 1.5, 20 pages; doi:10.1007/978-3-540-77058-9_5.

Comité de Concertation Navigation de Saint Laurent Vision 2000. Stratégie de Navigation Durable Pour le Saint-Laurent; Ministère des Transports du Québec et Pêches et Océans Canada: Québec, QC, Canada **2004**; 114 pages.

Debese, N.; Jacq, J.J.; Garlan, T. Extraction of sandy bedforms features through geodesic morphometry. *Geomorphology* **2016**, 267, 82–97, doi:10.1016/j.geomorph.2016.05.013.

Deng, Y. New trends in digital terrain analysis: Landform definition, representation, and classification. *Prog. Phys. Geogr.* **2007**, 31, 405–419.

Di Stefano, M.; Mayer, L.A. An automatic procedure for the quantitative characterization of submarine bedforms. *Geosciences* **2018**, 8, 28, doi:10.3390/geosciences8010028.

Diesing, M.; Thorsnes, T. Mapping of cold-water coral carbonate mounds based on geomorphometric features: An object-based approach. *Geosciences* **2018**, 8, 38, doi:10.3390/geosciences8020034.

Dragut, L.; Blaschke, T. Automated classification of landform elements using object-bases image analysis. *Geomorphology* **2006**, 81, 330–344, doi:10.1016/j.geomorph.2006.04.013.

Dragut, L.; Tiede, D.; Levick, S.R. ESP: A tool to estimate scale parameter for multiresolution image segmentation of remotely sensed data. *Int. J. Geogr. Inf. Sci*. **2010**, 24, 859–871, doi:10.1080/13658810903174803.

Dupont, V. Élaboration D'une Méthode D'extraction de Plans par Croissance de Régions Dans un Nuage de Points Bathymétriques Servant à Alimenter des Estimateurs D'erreur Hydrographique. Master Thesis, Université Laval, Québec, QC, Cananda, **2020**; 120 pages.

Ferret, Y. Morphodynamique de Dunes Sous-Marines en Contexte de Plate-Forme Mégatidale (Manche Orientale). Approche Multi-Échelles Spatio-Temporelles. Interfaces Continentales, Environnement. Ph.D. Thesis, Université de Rouen, Mont-Saint-Aignan, France, **2011**.

Garlan, T. Study on Marine Sandwave Dynamics. *Int. Hydrogr. Rev*. **2007**, 8, 26–37.

Garlan, T. GIS and Mapping of Moving Marine Sand Dunes. Presented at the 24th International Cartography Conference, (ICC 2009), Santiago, Chile, 15–21 November **2009**.

Guilbert, E.; Moulin, B. Towards a Common Framework for the Identification of Landforms on Terrain Models. *ISPRS Int. J. Geo-Inf*. **2017**, 6, 12.

Guilbert, E.; Moulin, B.; Cortés Murcia, A. A conceptual model for the representation of landforms using ontology design patterns. ISPRS Annals of the Photogrammetry, Remote Sensing and Spatial Information Sciences, Volume III-2. *In Proceedings of the XXIII ISPRS Congress*, Prague, Czech Republic, 12–19 July **2016**; 8 pages.

Gutierrez, R.R.; Abad, J.D.; Parsons, D.R.; Best, J.L. Discrimination of bed form scales using robust spline filters and wavelet transforms: Methods and application to synthetic signals and bed forms of the Rio Paraná, Argentina. *J. Geophys. Res. Earth Surf*. **2013**, 118, 1400–1419, doi:10.1002/jgrf.20102.

Ismail, K.; Huvenne, V.A.I.; Masson, D.G. Objective automated classification technique for marine landscape mapping in submarine canyons. *Mar. Geol*. **2015**, 362, 17–32, doi:10.1016/j.margeo.2015.01.006.

Jasiewicz, J.; Stepinski, T.F. Geomorphons—a pattern reconigtion approach to classification and mapping of landforms. *Geomorphology* **2012**, 182, 147–156, doi:10.1016/j.geomorph.2012.11.005.

Lecours, V.; Dolan, M.F.J.; Micallef, A.; Lucieer, V.L. A review of marine geomorphometry, the quantitative study of the seafloor. *Hydrol. Earth Syst. Sci*. **2016**, 20, 3207–3244, doi:10.5194/hess-20-3207-2016.

López-Ornelas, E. High resolution images: Segmenting, extracting information and GIS integration. *World Acad. Sci. Eng. Technol.* **2009**, 54, 172–177.

Lucieer, V.; Lecours, V.; Dolan, M.F.J. Charting the course for future developments in marine geomorphometry: An introduction to the special issue. *Geosciences* **2018**, 8, 477, doi:10.3390/geosciences8120477.

van der Mark, C.F.; Blom, A. A New & Widely Applicable Bedform Tracking Tool; University of Twente: Enschede, The Netherlands, **2007**; 44 pages.

Masetti, G.; Mayer, L.A.; Ward, L.G. A Bathymetry- and Reflectivity-Based Approach for Seafloor Segmentation. *Geosciences* **2018**, 8, 14, doi:10.3390/geosciences8010014.

Nguyen, T.H.; Daniel, S.; Guériot, D.; Sintès, C.; Le Caillec, J.M. Super-resolution-based snake model—an unsupervised method for large-scale building extraction using airborne LiDAR data and optical image. *Remote Sens.* **2020**, 12, 1702, doi:10.3390/rs12111702.

Nichols, G. Sedimentology and Stratigraphy, 2th ed.; Chapter 4 Processes of transport and sedimentary structures; Wiley-Blackwell, A John Wiley & Sons,Ltd., Publication: West Sussex, UK, **2009**; pp. 44–68.

Ogor, J. Design of Algorithms for the Automatic Characterization of Marine Dune Morphology and Dynamics. Ocean, Atmosphere. Ph.D. Thesis, ENSTA-Bretagne, Brest, France, **2018**.

d'Oleire-Oltmanns, S.; Eisank, C.; Dragut, L.; Blaschke, T. An object-based workflow to extract landforms at multiple scale from two distinct data types. *IEEE Geosci. Remote Sens. Lett*. **2013**, 10, 947–951.

Soille, P.; Pesaresi, M. Advances in mathematical morphology applied to geosciences and remote sensing. *IEEE Trans. Geosci.* Remote Sens. **2002**, 40, 2042–2055.

Sowers, D.C.; Masetti, G.; Mayer, L.A.; Johnson, P.; Gardner, J.V.; Armstrong, A.A. Standardized Geomorphic Classification of the Seafloor within the United States Atlantic Canyons and Continental Margin. *Front. Mar. Sci*. **2020**, 7, 9, doi:10.3389/fmars.2020.00009.

Thibaud, R.; Del Mondo, G.; Garlan, T.; Mascret, A.; Carpentier, C. A Spatio-Temporal Graph Model for Marine Dune Dynamics Analysis and Representation. *Trans. GIS* **2013**, 17, 742–762, doi:10.1111/tgis.12006.

Wood, J. The Geomorphological Characterization of Digital Elevation Models. Ph.D. Thesis, University of Leicester, Leicester, UK, **1996**.

Chapitre 3 An Approach for the Automatic Characterization of Underwater Dunes in Fluviomarine Context

3.1 Résumé

L'identification des formes de relief sous-marins joue un rôle important dans l'étude de la morphologie du fond marin. Dans ce contexte, la segmentation et la caractérisation des dunes sous-marines permettent de mieux comprendre la dynamique associée au fond marin, puisque la formation de ces structures est directement liée aux conditions environnementales, telles que courant, marée, granulométrie, etc. De plus, cette identification et caractérisation permettent de sécuriser la navigation, notamment dans les vois navigables nécessitant un entretien régulier. Cet article propose une nouvelle méthode pour caractériser automatiquement les dunes sous-marines. Son originalité repose sur l'extraction de descripteurs morphologiques liés non seulement à la dune, mais aussi aux champs où elles sont localisées. Également, cette approche considère la surface de la dune dans sa globalité plutôt qu'une série de profils ou des cellules regroupées en région comme cela est généralement fait dans les méthodes proposées dans la littérature. Considérant la surface du fond modélisée par un MNB (Modèle Numérique Bathymétrique), les saillances des dunes (i.e. ligne de crête et pieds des dunes) sont tout d'abord identifiées au moyen d'une analyse morphométrique. Les dunes sont ensuite formées en mettant en correspondance les lignes de crête avec leurs pieds de dune respectifs. Ensuite, une série de descripteurs morphologiques sont calculés, en considérant les saillances des dunes, la surface de chacune de ces structures ainsi que leur distribution spatiale dans le champ où elles sont localisées. La validation de la méthode proposée a été effectuée sur plus de 1200 dunes dans le contexte fluviomarin de la Traverse Nord du Saint-Laurent.

3.2 Abstract

The identification of underwater landforms represents an important role in the study of the seafloor morphology. In this context, the segmentation and characterization of underwater dunes allow a better understanding of the dynamism of the seafloor, since the formation of these structures are directly related to environmental conditions, such as current, tide, grain size, etc. In addition, it helps ensuring safe navigation, especially in the context of navigation channels requiring periodic maintenance. This paper proposes a novel method to automatically characterize the underwater dunes. Its originality relies on the extraction of morphological descriptors related not only to the dune itself, but also to the fields where the dunes are located. Furthermore, the proposed approach involves the entire surface of the dunes, rather than profiles or group of pixels as generally found in previous works. Considering the surface modelled by a DBM (Digital Bathymetric Model), the salient features of the dunes (i.e. crest line, stoss trough, and lee trough) are first identified using a geomorphometric analysis of

the DBM. The individual dunes are built by matching the crest lines with their respective troughs according to an object-oriented approach. Then, a series of morphological descriptors, selected through a literature review, are computed by taking advantage of the dune salient features, surface representation and spatial distribution in the fields where they are located. The validation of the proposed method has been conducted using more than 1200 dunes in the fluviomarine context of the Northern Traverse of the Saint-Lawrence River.

3.3 Introduction

The occurrence of sedimentary structures on the seafloor surface is related to the interaction between relatively strong or large-scale sustained flows and the sediments present on the water column. Different structures can be associated with distinct hydrodynamical factors, such as the flow velocity, the grain size of sediment transported by the flow, the meteorological conditions, tidal regime, etc. An underwater dune is a sedimentary structure present on the seafloor of shallow marine environments, estuaries, deltas, and river channels. These sedimentary structures can have a high migration rate on the seafloor based on the environmental dynamism (Le Bot, 2001; Cheng et al., 2004; Best, 2005; Boggs, 2006; Nichols, 2009; Andreotti et al., 2012; Lefebvre et al., 2016). Therefore, the segmentation and characterization of the underwater dunes have multiple purposes. In the context of navigation, the identification of these structures is particularly useful to ensure safe navigation. In addition, it improves efficiency and effectiveness of maintenance activities, such as dredging (Debese et al., 2016; Lecours et al., 2016; Debese et al., 2018). The identification of these sedimentary structures provides realistic seafloor representation to hydrodynamic simulation models involved in flood risk assessment in coastal areas. The recognition of dunes on the seafloor can also be used in the study of the sand banks erosion (Yan et al., 2021) and in the changes of the morphosedimentary dynamics of the seafloor (Cheng et al., 2022). They also contribute to the temporal monitoring of marine habitats (van Dijk et al., 2012).

High-resolution surveys using multibeam echosounders (MBES) allow the production of seafloor digital surfaces, such as digital bathymetric models (DBMs), from which the dunes can be identified. Dune identification and characterization by different experts, such as geomorphologists and hydrographers, is still mostly performed visually from DBMs (Parsons et al., 2005). However, this task is time-consuming, subjective, and less suited to large volumes of data. Hence, different computer-aided approaches have been proposed to segment underwater dunes from DBMs to alleviate the subjectivity and burden of this task. Generally, these approaches consider a geomorphometric analysis of the seafloor in order to identify the dunes or their salient features. For example, the authors of (Di Stefano and Mayer, 2018) proposed a method which identifies and segments the dunes in three steps. The first step performs a geomorphon classification (Jasiewicz and Stepinski, 2012) of the seafloor, extracting the crest line of the dunes. The second step identifies the dune itself, aggregating specific geomorphon classes. Then, the third step identifies the lee and stoss sides of the dunes. This step also computes dune metrics from equidistant vertical profiles along the dune. Cassol et al. (2021) state that a dune can be identified

from its salient features, i.e., its crest line and its troughs. Hence, they proposed an approach where crest lines and troughs are first detected as lines from the DBM using mathematical morphology and image processing after an initial geomorphometric analysis of the seafloor. The DBM is segmented into dunes in a second step considering an object-based approach, matching each crest line with its respective troughs. The result is the dune objects segmented in a raster file.

Even if dunes can be automatically segmented, their characterization is mostly accomplished manually. As a result, it is often subjective and inaccurate. Such characterization can also be performed through the computation of morphological descriptors using the profiles of the dunes. An example is the computation of the angles of the sloping sides of the dunes. They are calculated based on the profile of the dune between the line connecting the crest line and the troughs of the dune (Di Stefano and Mayer, 2018; Lebrec et al., 2022). Since we consider the dune as an object identified on the seafloor by its salient features, it can be characterized by different morphological descriptors related to its full surface rather series of sampled profiles. In addition, the identification of dunes present within the same field helps to correlate their characteristics and, by the same token, to characterize the field. In this paper, we propose an automatic method to (1) extract morphological descriptors towards a comprehensive characterization of the underwater dunes and (2) compute morphological descriptors of dune fields, moving towards a comprehensive characterization of underwater dunes and the fields where they are located. To our knowledge, such a method is currently missing in the literature. Ultimately, the availability of such morphological descriptors will allow a better understanding of the dunes and their development, which represent crucial knowledge for hydrospatial data users (Hains et al., 2021).

The paper is organized into four sections. The first section is a state of the art on the dune formation process, its definition as a sedimentary structure, and the dune morphological descriptors described in the literature. The second section presents the proposed method dedicated to the automatic extraction of morphological descriptors related to dune objects and dunes fields. The third section presents the experimental results related to the application of the method in the Northern Traverse of the Saint Lawrence River. This study zone was chosen since this navigation channel is a well-surveyed area given the presence of dunes fields on the seafloor. The fourth section discusses the experimental results and the method learning outcomes on the studied area, before concluding and providing perspectives for future research addressing the study and analysis of underwater dunes.

3.4 Underwater Dunes

In this section, we present the underwater dune formation process as well as the morphological descriptors related to this sedimentary structure.

3.4.1 Formation of the Underwater Dunes

Underwater dunes (henceforward dunes) are the result of sediment transportation through time by a flow. In fact, there is a correlation between the grain size of the sediments and the flow velocity in the resulting sedimentary structure formed on the seafloor (Figure 3.1). The dune migration and shape are correlated to its nature and to hydrodynamic factors (Amos et al., 1984; Bartholdy et al., 2005; Landeghem et al., 2009; Nichols, 2009; Thibaud et al., 2013).

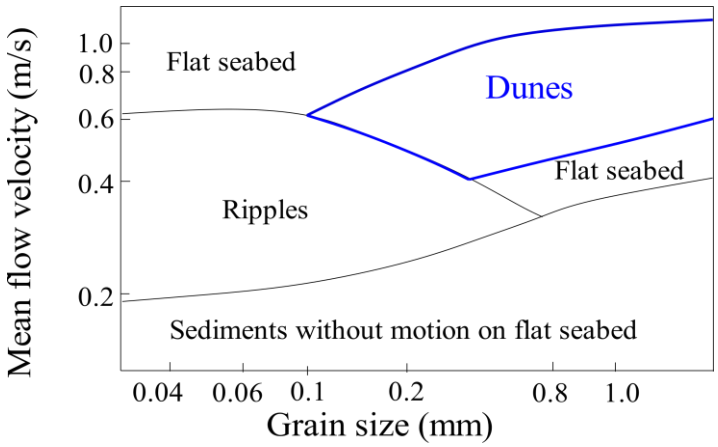

Figure 3.1 - Correlation between the flow velocity, grain size sediment, and the sedimentary structure formed (adapted from Nichols, 2009).

Figure 3.1 shows that dunes are formed with grain size ranging from gravel to fine sand (i.e., grain size greater than 0.1 mm up to more than 1.0 mm). Dunes are limited in finer sediments, such as silt or very fine sand (Nichols, 2009). According to the dunes classification proposed by Ashley (1990), dunes have a height ranging from 0.075 m up to 5 m and spacing from 0.6 m to more than 100 m. The height and spacing of dunes usually increase with the flow velocity (Gutierrez et al., 2013; Debese et al., 2016). These and other morphological descriptors shall be further described in the paper. Dunes have a gentle slope facing the current and a steep slope in its direction. A crest line separates these two slope sides, which are bounded by its troughs. The gentle slope is defined as the stoss side and is bounded by the crest line and the stoss trough. The steep slope of the dune is defined as the lee side and is bounded by the crest line and the lee trough. The lee side of the dune indicates the migration direction of this structure. The stoss and lee sides of the dunes are adjacent to each other (Le Bot, 2001; Ferret, 2011; Thibaud et al., 2013; Cassol et al., 2021). Figure 3.2 illustrates a representation of this sedimentary structure and its related features.

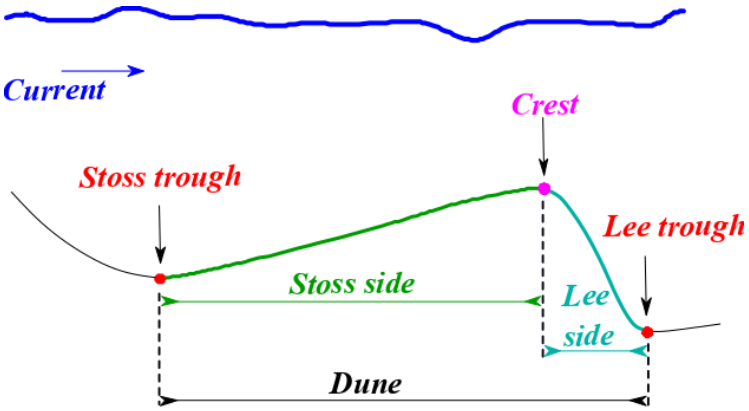

Figure 3.2 - Dune profile with the crest line, the lee and stoss troughs, and lee and stoss sides.

Due to the complex flow dynamics, smaller sedimentary structures, such as ripples, can superimpose on underwater dunes (Ashley, 1990; Boggs, 2006). As highlighted by Le Bot (2001), the presence of superimposed structures on the dunes varies according to the grain size sediment and the dimensions of the dune. The superimposed structures can be from a few centimeters high up to a few meters, yielding asymmetric structures. These structures are formed on the dune stoss trough, and they migrate to the crest line of the dune, avalanching on the lee side (Ferret, 2011). In the proposed research, the available data and related 1 m resolution DBM do not have a resolution fine enough to analyze smaller structures that can superimpose on dunes, such as ripples. Thus, they will not be considered in the rest of the paper. Dunes can be found on the seafloor as isolated structures or adjacent to each other. The troughs of an isolated dune bound this structure with the stoss and lee troughs, which are associated with only one crest line. In the context of adjacent dunes, the troughs can be associated with more than one crest line. Indeed, the lee trough of a dune is the stoss trough of the following dune in the field. Figure 3.3 illustrates the difference between an isolated dune and adjacent dunes.

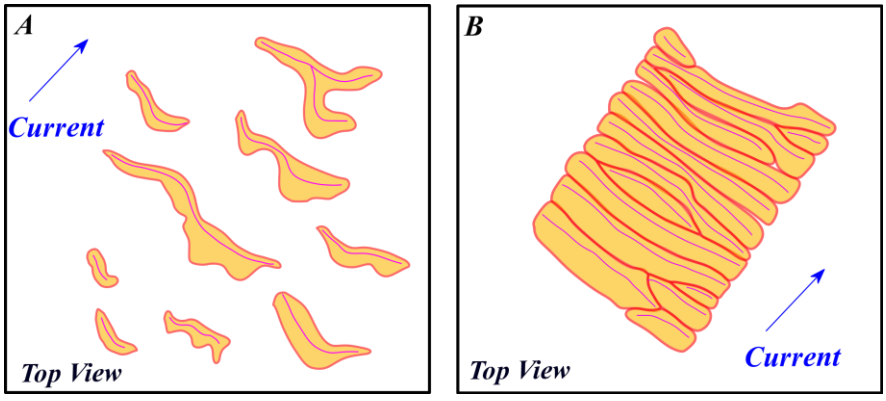

Figure 3.3 - Isolated dunes (A) and adjacent dunes (B) on the seafloor. The red lines represent the troughs and the magenta lines represent the crest line of the dunes.

3.4.2 Morphological Descriptors of the Dunes

Dunes can be characterized once they have been identified and segmented from the DBM. This characterization is based on different morphological descriptors. In this section, we aim to review and describe the morphological descriptors that can be calculated for each dune object as well as the method used for such calculation. Different morphological descriptors of the dunes can be measured considering the salient features used to compute them on the DBM. These morphological descriptors can be estimated in different ways as discussed by van der Mark and Blom (2007), Gutierrez et al. (2013) and Thibaud et al. (2013). Indeed, different definitions are applied, depending on the research field and expert knowledge of the analysis. Thus, a formalization of how to estimate these morphological descriptors for the dunes and which features should be considered is required.

Starting with the crest line, its length can be estimated considering its starting and ending points. Furthermore, these points are used to assess the dune orientation angle. This angle can be estimated in two different ways. The first is the dune migration direction relative to the north, as proposed by (Knaapen, 2005), illustrated in Figure 3.4A. The second is the direction of the line passing through the starting and ending point of the crest line of the dune, illustrated in Figure 3.4B. This second orientation angle is usually perpendicular to the main direction of the current, although angular variations up to 20° can be observed (Garlan, 2007 and 2009; Ogor, 208). The depth corresponds to the distance between the crest line and the water surface. This measure can be estimated based on the depth values of the crest line that can be found on its corresponding pixels in the DBM. In addition, the height of the dunes can be measured as the shortest distance between a crest line and a line joining both troughs (van der Mark and Blom, 2007). Figure 3.4 illustrates the descriptors associated with the crest line.

The spacing of the dune on a field and its width can also be computed. The spacing can be estimated as the distance between the crest lines of two consecutive dunes, characterizing the distance between these structures in a field. The width of the dune can be measured as the distance between the stoss and lee trough of the dune (van der Mark and Blom, 2007) or as the horizontal distance between its lee and stoss troughs (Berné, 1991; Le Bot, 2001; Ogor, 2018). Figure 3.5 illustrates the spacing and the width of the dunes.

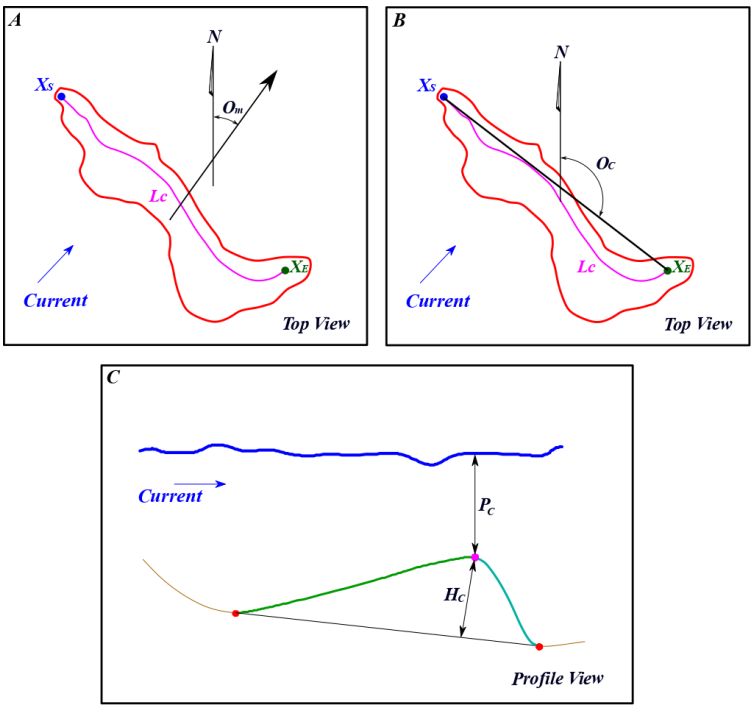

Figure 3.4 - Descriptors estimated for the crest line of the dunes. The crest line is displayed in magenta and the troughs in red. X_S and X_E represents, respectively, the starting and ending points of the crest line. In (A,B), L_C represent the length of the crest line. The migration direction of the dune relative to the north (O_m) is presented in (A). The orientation angle (O_C) of the crest line of the dune, usually perpendicular to the current, is presented in (B). The height (H_C) and depth (P_C) of the dune are illustrated in (C).

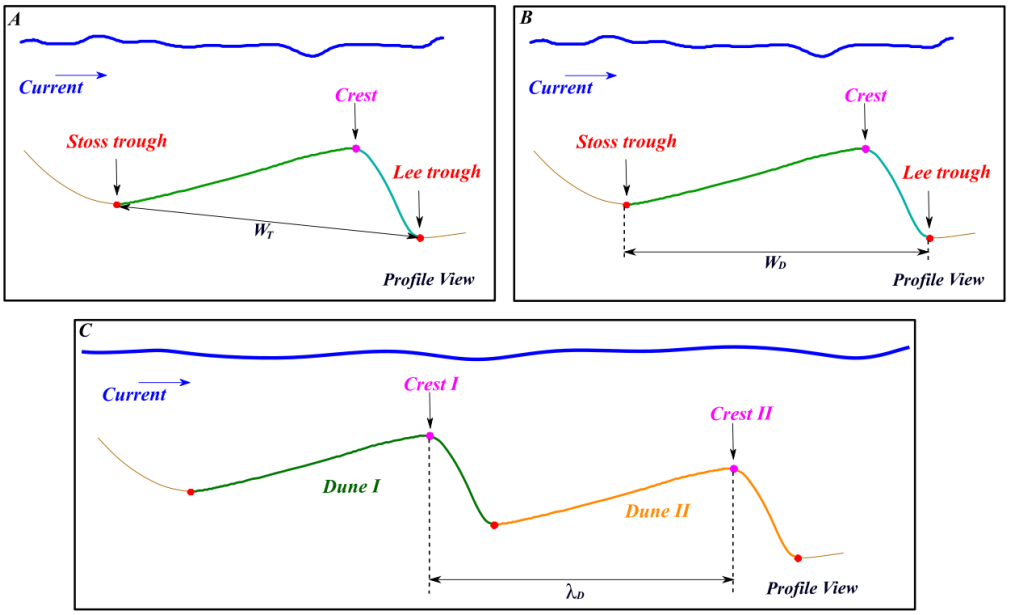

Figure 3.5 - Width and spacing of the dunes. In (A), the width is represented by the distance between the dune stoss and lee troughs (W_T). In (B), the width is represented by the horizontal distance between the dune lee

and stoss troughs (W_D). In (C), the width is represented by the spacing measured between two consecutive dunes at their crest lines (λ_D).

We can also estimate different descriptors for the stoss and lee sides of the dune, as their width and sloping angles (Lebrec et al., 2022). These descriptors are illustrated in Figure 3.6.

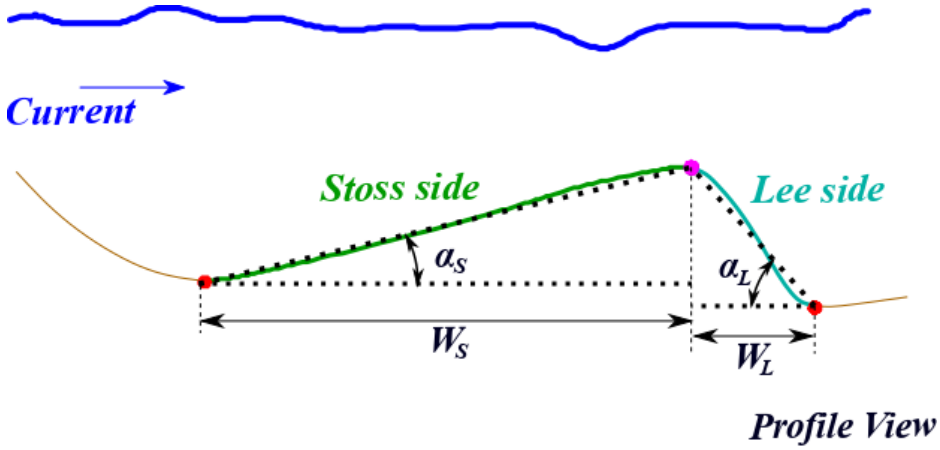

Figure 3.6 - Measurements for dune stoss and lee sides. W_S, W_L, α_S, and α_L represent, respectively, the width of the stoss side, the width of the lee side, the angle of the stoss side, and the angle of the lee side (adapted from Lebrec et al., 2022).

Dunes can also be characterized by different index values, which are calculated based on the dune measurements previously described. The dune symmetry index (3.1) is defined as the ratio between the stoss and lee side widths (Berné, 1991; Ferret, 2011; Lebrec et al., 2022).

$$Sy_d = {}^{W_S}/_{W_L} \qquad (3.1)$$

The symmetry index value usually ranges between 1 and 6. Other definitions of this index may be found in the literature as mentioned by Ogor (2018). The steepness index (3.2) can be defined as the ratio between the height of the crest line and the width of the dune (Ogor, 2018).

$$St_d = {}^{H_C}/_{W_D} \qquad (3.2)$$

The measurements and indices reviewed above are usually defined using a dune profile. Therefore, these sectional views reduce the characterization of the dune to a 2D interpretation, whereas the dunes are 3D structures. Consequently, such measurements and indices vary along the dune structure. Different descriptors exist to describe the morphology of the dunes, such as the already defined length of the crest line. The dune

sinuosity index (3.3) can be estimated based on the ratio between the length of the crest line (L_c) and the geodetic distance (D_C) between the crest line extremities (Berné, 1991; Ogor, 2018; Lebrec et al., 2022).

$$Si_d = {}^{L_c}/_{D_C} \qquad (3.3)$$

The measurements considered in the sinuosity index (3.3) can be observe in Figure 3.7.

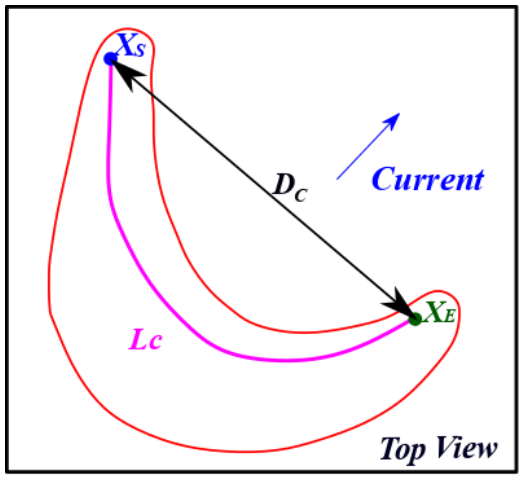

Figure 3.7 - Measurements considered in the computation of the sinuosity index. L_c represents the length of the crest line and X_S, X_E the starting and ending point of the crest line, respectively. D_c represents the geodetic distance between the crest line extremities (adapted from Ogor, 2018).

3.5 Underwater Dunes Characterization from a DBM

This section aims to describe the proposed automatic method to extract the morphological descriptors of the dunes from the seafloor. Our method is divided into two main processes: dune segmentation and dune characterization. This method considers the seafloor surface modelled by a regular gridded DBM. The processes and phases of our method are illustrated in Figure 3.8.

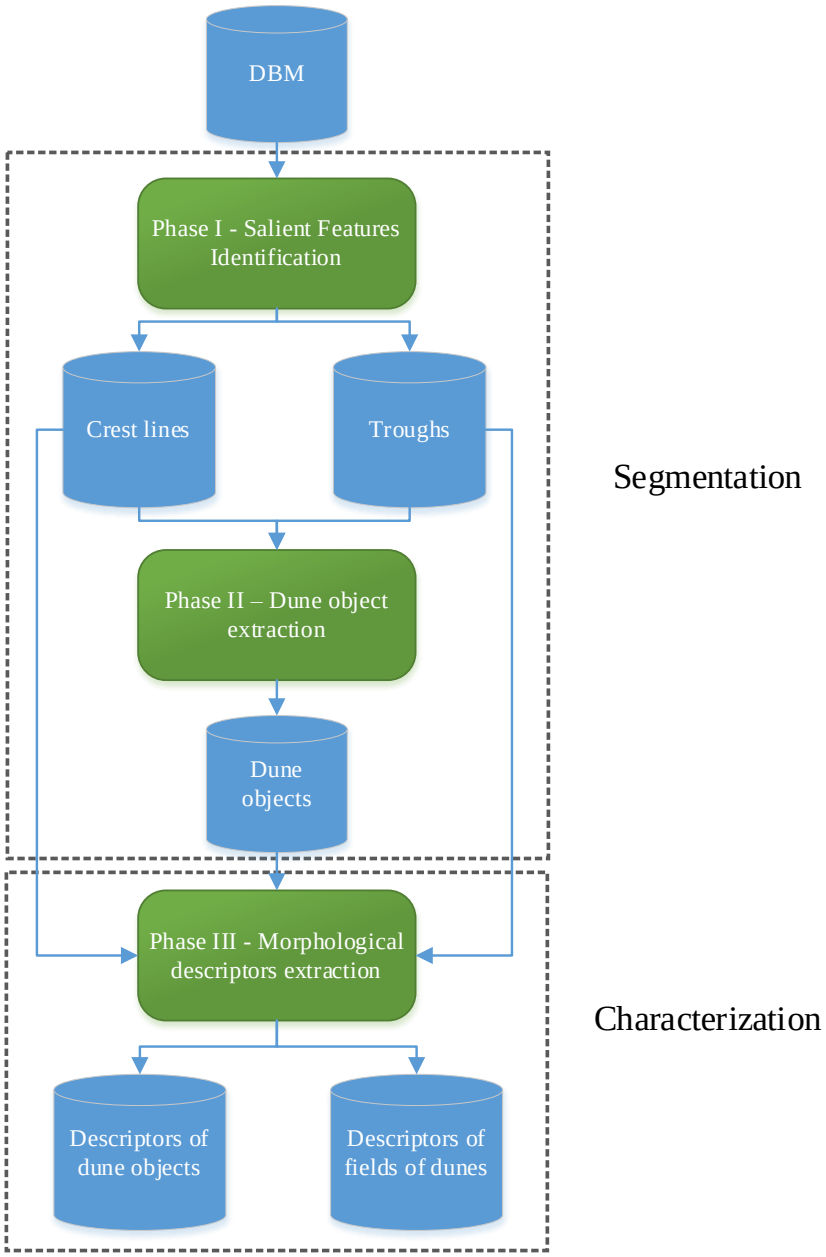

Figure 3.8 - Proposed method for automatic extraction of dune morphological descriptors and field of dunes morphological descriptors.

The first process (i.e., the segmentation approach) considered in the proposed method is described by Cassol et al. (2021) with the dune landform formalized by a conceptual model. This model considers that a dune can be identified on the seafloor by three salient features, namely, the crest line, stoss trough, and lee trough. The crest line is the linear feature located in the higher zone of the dune. This feature is the upper bound of both sloping sides of the dune (i.e., stoss and lee sides). The stoss and lee troughs represent the boundary of the dune objects, also represented by linear features. These troughs bound the stoss and lee sides, respectively. In

the conceptual model, the stoss and lee sides are considered as two components of the dune object. Phase I of the method identifies the three salient features of the dunes from the DBM. In this phase, a morphometric analysis of the seafloor is carried out using the geomorphon algorithm (Jasiewicz and Stepinski, 2012). Salient features are identified after an analysis of the geomorphometric surface and the DBM. Figure 3.9 illustrates the dune object identified using Phase I processing while considering the dune salient features and components.

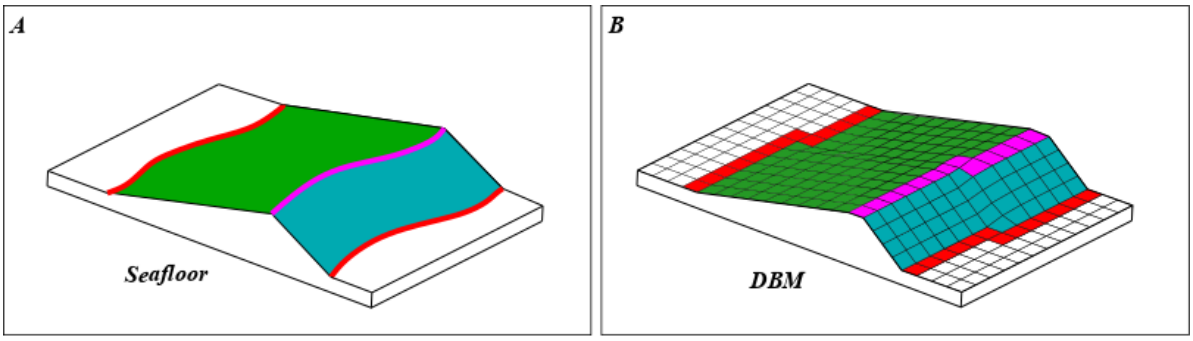

Figure 3.9 - The dune object identified using its salient features and components. In (A), the dune object on the seafloor is schematized. In (B), the dune object is schematized as identified on the DBM grid. The crest line is in magenta, the trough lines are in red, the stoss sides are displayed in green, and the lee sides are displayed in blue.

Phase II of the method consists of the extraction of the dune object itself considering the salient features identified in Phase I. In this second phase, the troughs are matched with their corresponding crest lines. This matching is carried out by searching the nearest troughs of the crest lines. This search is conducted in the orthogonal direction of the crest line orientation with a predefined range distance limit. Then, the dune object is created by aggregating the pixels located in the area between the crest line and the troughs. In this phase, mathematical morphology and image processing are used to extract the dune object. The result of Phase II is the dune object identified by the same label as its crest line. Figure 3.10 illustrates an overview of the segmentation approach from the DBM.

Once the dunes have been segmented from the DBM, the second process of the proposed method consists in calculating the morphological descriptors defined in the previous section. Phase III divides these descriptors in two categories. The first one consists of the descriptors of the dune objects, which use the salient features. Here, the following descriptors are used: dune orientation; depth; width; height; stoss and lee angles; stoss and lee widths; asymmetry; sinuosity; and steepness. The second category consists of descriptors that describe how dunes are distributed in the dune field. For that purpose, we propose the following descriptors: the mean spacing between two consecutive dunes; the standard deviation of the dunes spacing; and the dune density of the field.

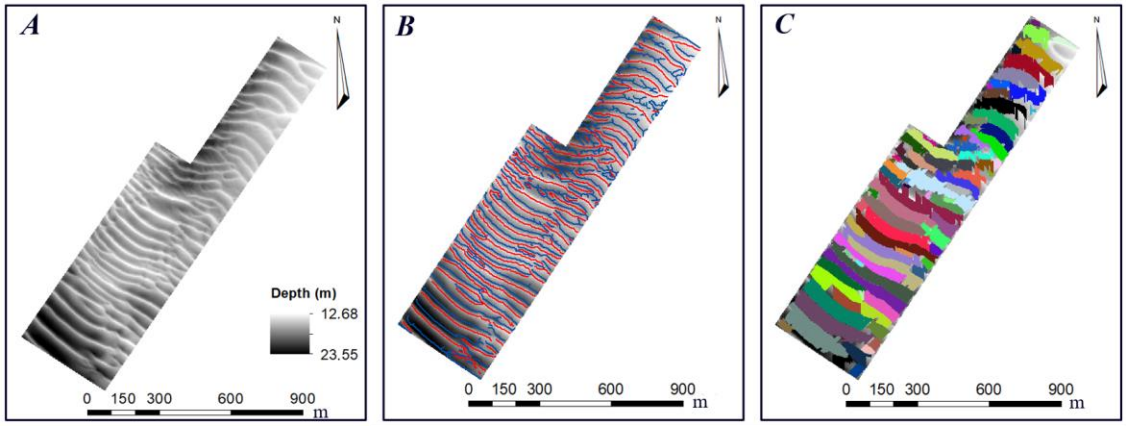

Figure 3.10 - Data and results for the dune segmentation approach proposed by Cassol et al. (2021) for the sector G14 of the Northern Traverse. (A,B) illustrate, respectively, the DBM and the salient features of the dunes identified in Phase I; the crest lines are displayed in red and the troughs in blue. In (C), the dune objects segmented in Phase II are presented. Please note that each segmented dune illustrated in (C) are represented with a different color.

The following paragraphs explains the extraction, from the DBM, of the main measures used to calculate the morphological descriptors of the dunes. The approach takes advantage of Phase II results, namely the matching of each crest line pixel with its corresponding pixel on the stoss trough and the lee trough, as further illustrated in Figure 3.11. Please note the use of the median value instead of the mean value for some descriptors, in order to avoid outliers.

- The *dune orientation* is computed using the segment joining the starting and ending pixel of the crest line. We considered the direction facing the lee side of the dune. The segment orientation angle is measured from the north (Om) as proposed by Knaapen (2005). This orientation is chosen so that the information can later be correlated to the current orientation.

- The *depth* (P_C) of a dune is computed using the depth of each pixel of the crest line, as illustrated in Figure 3.11A. The minimum value among these pixels (i.e., closest to the water surface) is considered as the dune depth, since this information is valuable to detect dunes representing a risk for safe navigation.

- The *width* (W_D) is defined as the horizontal distance between the dune lee and stoss troughs. To compute this measure, we considered the stoss and lee trough pixels matched with each crest line pixel. Therefore, a width value is computed for each pixel composing the crest line, as illustrated in Figure 3.11B. The median value among all crest line pixels is considered as the dune width.

- The *height* of a dune (H_C) also considers the matching between the pixels of the crest line and the troughs. A height value is computed for each crest line pixel as the distance between the crest line pixel and the line joining the stoss and lee troughs (see Figure 3.4C). The median value among all the crest line pixels is considered as the height of the dune.

- The *stoss and lee angles* (α_S and α_L), as well as *stoss and lee widths* (W_S and W_L), are computed in a similar fashion as the measures related to the crest line. The median values computed are considered as the stoss and lee angles, as well as stoss and lee widths of the dune.

- The *sinuosity index* (Si_d) is computed considering (3.3). The geodetic distance (D_C) is calculated as illustrated in Figure 3.7. Please note that the length of the crest line (L_c) is not computed as the number of pixels composing the crest line. Instead, the geometric distance between the centers of the pixels is used to increase accuracy given the variability of the crest line sinuosity.

- The *steepness* and *symmetry* indexes are computed for each dune object considering the values previously estimated for the width (W_D, W_S, and W_L) and height (H_C), as defined in (3.1) and (3.2).

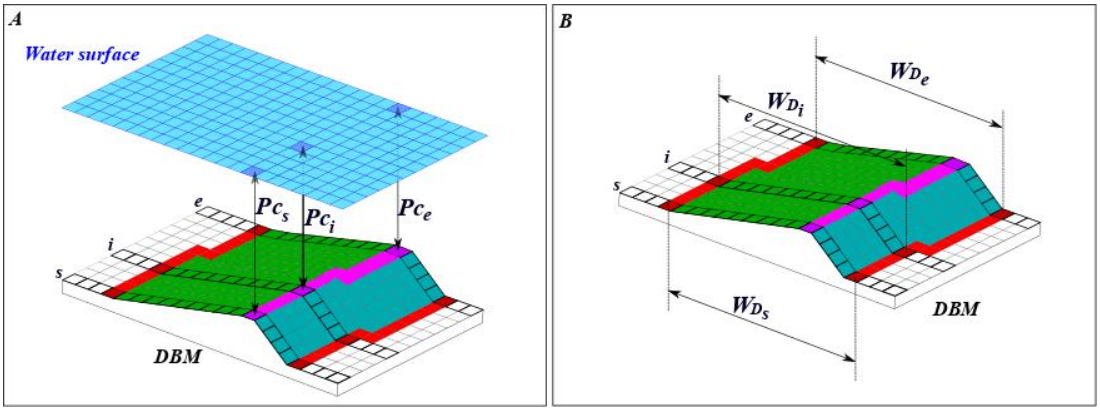

Figure 3.11 - (A) schematized the extraction of the depth associated with each pixel of the crest line. (B) illustrates the estimation of the width for each cell of the crest line of the dune. The crest lines are in magenta, the trough lines are in red, the stoss sides are displayed in green, and the lee sides are displayed in blue. As previously mentioned, we can observe that for each crest line pixel, our extraction method matched a stoss trough pixel and a lee trough pixel in the morphological descriptors computation.

Phase III of the proposed method also extracts the morphological descriptors of the dunes field, as explained in the following paragraphs.

- The *spacing* between two consecutive dunes in a field is computed considering the distances between the crest lines of each dune. The computation of the spacing requires a direction. Therefore, the median

value of the dune orientation of the objects located on the field is considered here. The spacing is computed for each pixel of the crest lines, as illustrated in Figure 3.12. Then, the mean value is considered as the spacing (λ_S) of the dunes of a field.

- The *standard deviation of the spacing* ($\sigma_{\lambda S}$) is computed considering all the spacing values of the dunes on a field. This descriptor is useful to characterize the dunes dispersion on the seafloor surface.

- The *dunes density* (f_D) is computed using the ratio between the surface of the field covered by dunes (A_{CD}) and the total surface of the field (A_{field}), as described in (3.4). f_D is a third-order descriptor mentioned by Ashley (1990), therein also called fullbeddedness or fraction of the seafloor covered by dunes.

$$f_D = {A_{CD}}/{A_{field}} \qquad (3.4)$$

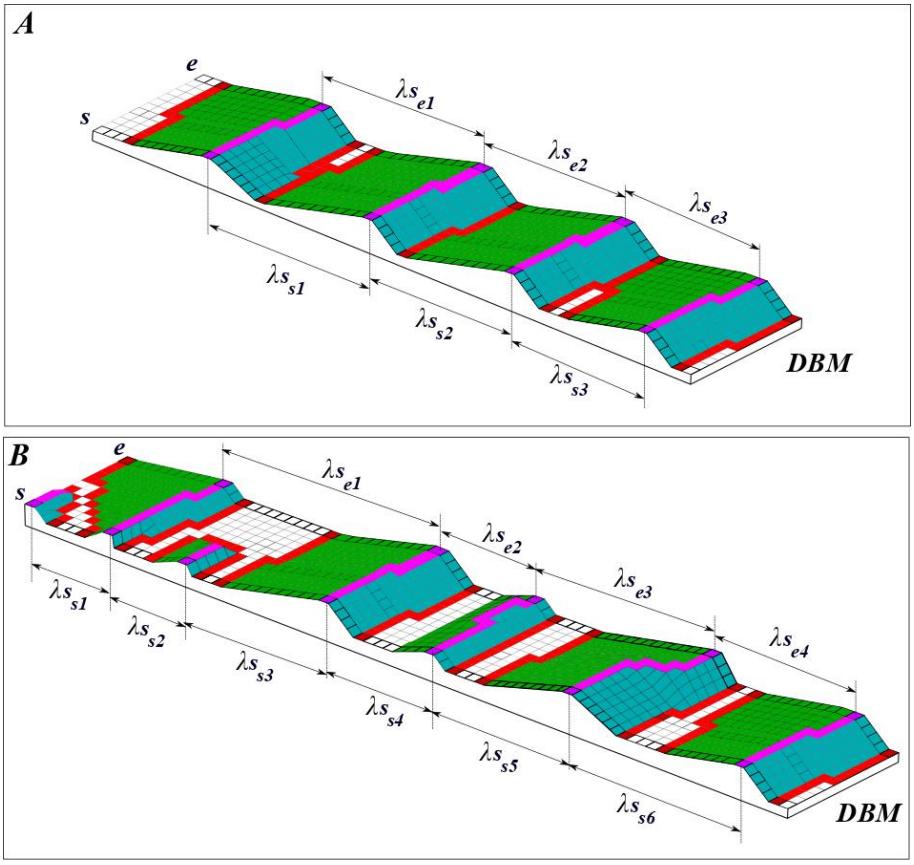

Figure 3.12 - Spacing between the crest lines of two consecutive dune objects. The crest lines are in magenta, the trough lines are in red, the stoss sides are displayed in green, and the lee sides are displayed in blue. λ_S represents the spacing between dunes while s and e represents, respectively, the starting and ending point of

the crest lines. (A) presents adjacent dunes in a field and (B) presents isolated dunes on a field. The dunes in (A) are more equally spaced than in (B), considering the spacing (λ_S) between these objects calculated for each pixel of the crest lines.

In Figure 3.12, two different dune fields are displayed, i.e., a field where the dunes are adjacent to each other (cf. Figure 3.12A) and a field with isolated dunes (cf. Figure 3.12B). Therefore, the spacing between the dunes (λ_S) is more variable in Figure 3.12B than in Figure 3.12A. Consequently, the standard deviation ($\sigma_{\lambda S}$) is expected to be higher for isolated dunes (Figure 3.12B) than adjacent dunes (Figure 3.12A). In addition, the fraction of the seafloor covered by dunes (f_D) shall be higher in the field with adjacent dunes (Figure 3.12A) than in the field with isolated dunes (Figure 3.12B).

3.6 Characterization of the Dunes of the Northern Traverse of the Saint Lawrence River

3.6.1 The Northern Traverse of the Saint Lawrence River

The Saint Lawrence River estuary is a high-dynamic environment, of a length of 400 km, with a width of 15 km at upstream (i.e., north of Orléans Island) and 70 km downstream. The dimensions are such that the hydrodynamic conditions prevailing downstream are typically marine and those upstream are typically estuarine. Different physical agents are responsible for the sediment dynamics in the Saint Lawrence, such as tide, waves, and ice (Drapeau, 1992). The zone used to validate the proposed characterization method is the Northern Traverse of the Saint Lawrence River. This navigation channel is located in the transition zone between the river estuary and the middle estuary of the Saint Lawrence River with a width of approximately 305 m and a draft of 12.5 m (Comité de concertation navigation de Saint Laurent Vision, 2004). This navigation channel was chosen for being a well-surveyed and controlled zone. Therefore, it provides some ground truth to further analyze the morphological descriptors computed with the proposed method in the different sectors of the Northern Traverse. The Canadian Hydrographic Service (CHS) and Ocean Group acquired the data used in this paper in the context of the maintenance of the navigation channel. The surveys mainly aimed to detect and dredge the sedimentary structures that could represent a risk for safe navigation. The available data consists of a regular gridded DBM with a resolution of 1 m.

The Northern Traverse is divided into different sectors. In this paper, nine sectors of the navigation channel are considered with 17 DBMs. Consequently, some sectors have more than one DBM (namely sectors G04, G09, G10, G11, and G14). The DBMs considered in the same sector were acquired at different dates, with a time lapse ranging over a few days to a few years. Even if the DBMs are in the same sector, the sedimentary structures on the surface are different due to the high dynamism of the Saint Lawrence River in the studied zone.

In total, 1234 dunes were segmented from the 17 considered surfaces, using the approach proposed by Cassol et al. (2021). This segmentation approach has proven to be efficient with a performance rate of 92% of well-segmented dunes (i.e., true positive). Figure 3.13 illustrates the location of the different sectors of the Northern Traverse considered in this analysis. It also presents examples of DBMs and segmented dunes for different sectors.

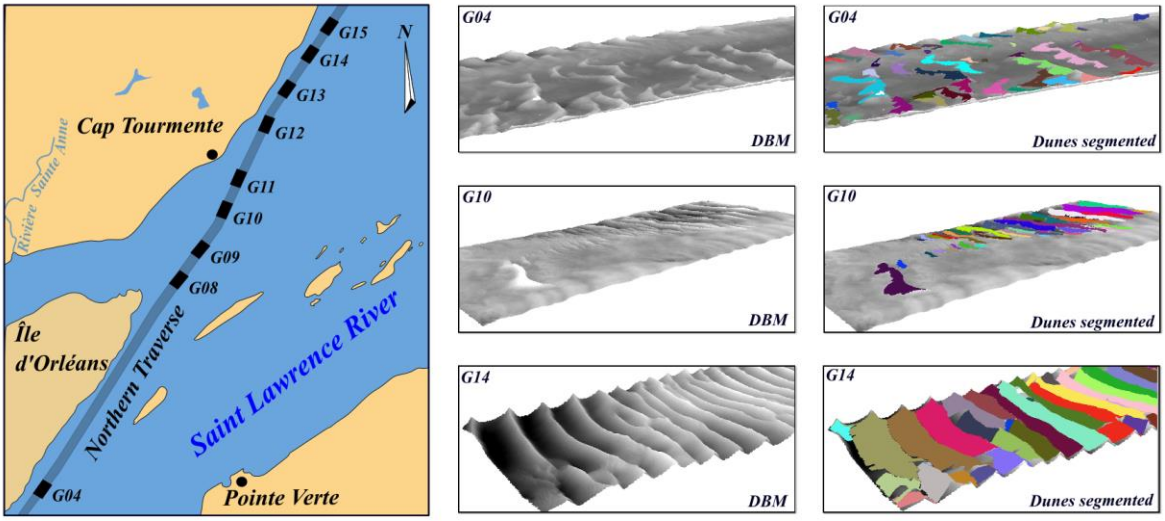

Figure 3.13 - Considered sectors of the Northern Traverse of the Saint Lawrence River as well as 3D representations of some DBMs and segmented dunes (colored objects superimposing the DBM surfaces). To better observe the dunes on the seafloor, a vertical exaggeration of 5 is used in the 3D representations.

Different configurations of the dunes can be observed in the sectors illustrated in Figure 3.13. In Sector G04, we can observe more sinuous isolated dunes, with a depth ranging approximately from 13.5 m to 18 m. A few isolated dunes can be observed in sectors G09 and G10, with a depth ranging from approximately 13 m to 16.5 m. In sector G14, adjacent dunes can be observed with a depth ranging from approximately 13 m to 23 m.

3.6.2 Morphological Descriptors of the Dunes of the Northern Traverse

Once the dunes are segmented (i.e., Phases I and II), the morphological descriptors can be extracted (Phase III), as described in the previous section. In Figure 3.14, we present the results of the morphological descriptors computation for the 1234 dunes segmented from the 17 DBMs over the nine sectors of the Northern Traverse. Given the large number of dunes, results are displayed as histograms.

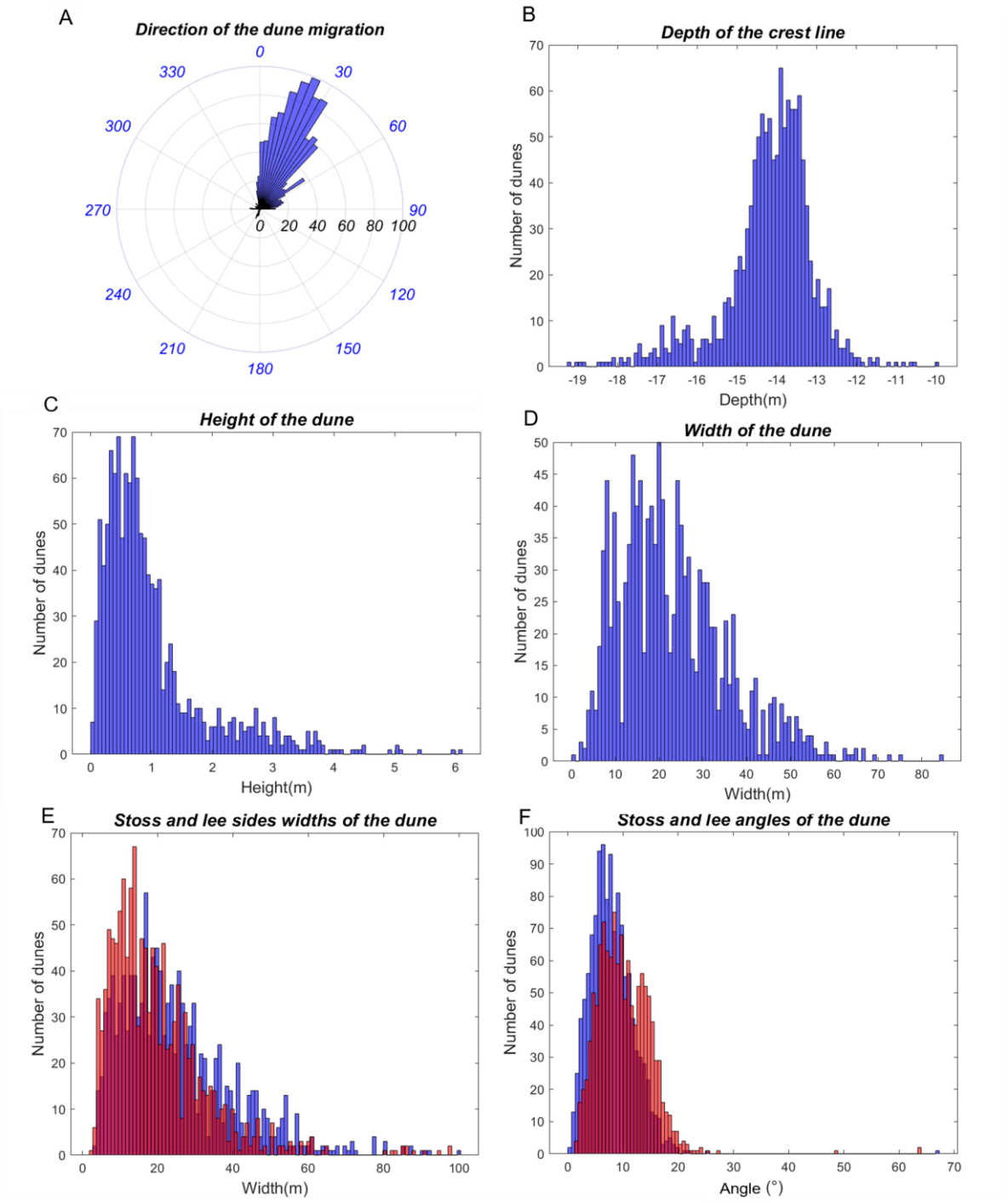

Figure 3.14 - Histograms of the morphological descriptor values. Please note that in (A-D) the descriptors of the dunes are in blue. In (E,F), the stoss descriptors are in blue and the lee descriptors are in red. The additional color (i.e., orange) results from the superposition of the red and blue colors.

The median dune orientation value is approximately 29°, which is in the same direction as the dune migration, as shown in Figure 3.14A. The depth of the dune objects of the Northern Traverse ranges from 9.95 m to 19.25

m, with a median depth value of 14.02 m, as observed in Figure 3.14B. The height of the dune objects (Figure 3.14C) ranges from 3.7 cm to 6.10 m with a median height of 0.74 m, and the width (Figure 3.14D) varies from 6 m up to 84.85 m with a median width of 21.21 m. The stoss side has a median value of 21 m while the lee side has a median value of 17 m, as observed in Figure 3.14E. The median value of the stoss angle is 7.68° and the median value of the lee angle is 9.78°, as observed in Figure 3.14F. Figure 3.15 presents the histograms with the symmetry, angular symmetry, sinuosity, and steepness indexes of the dune objects.

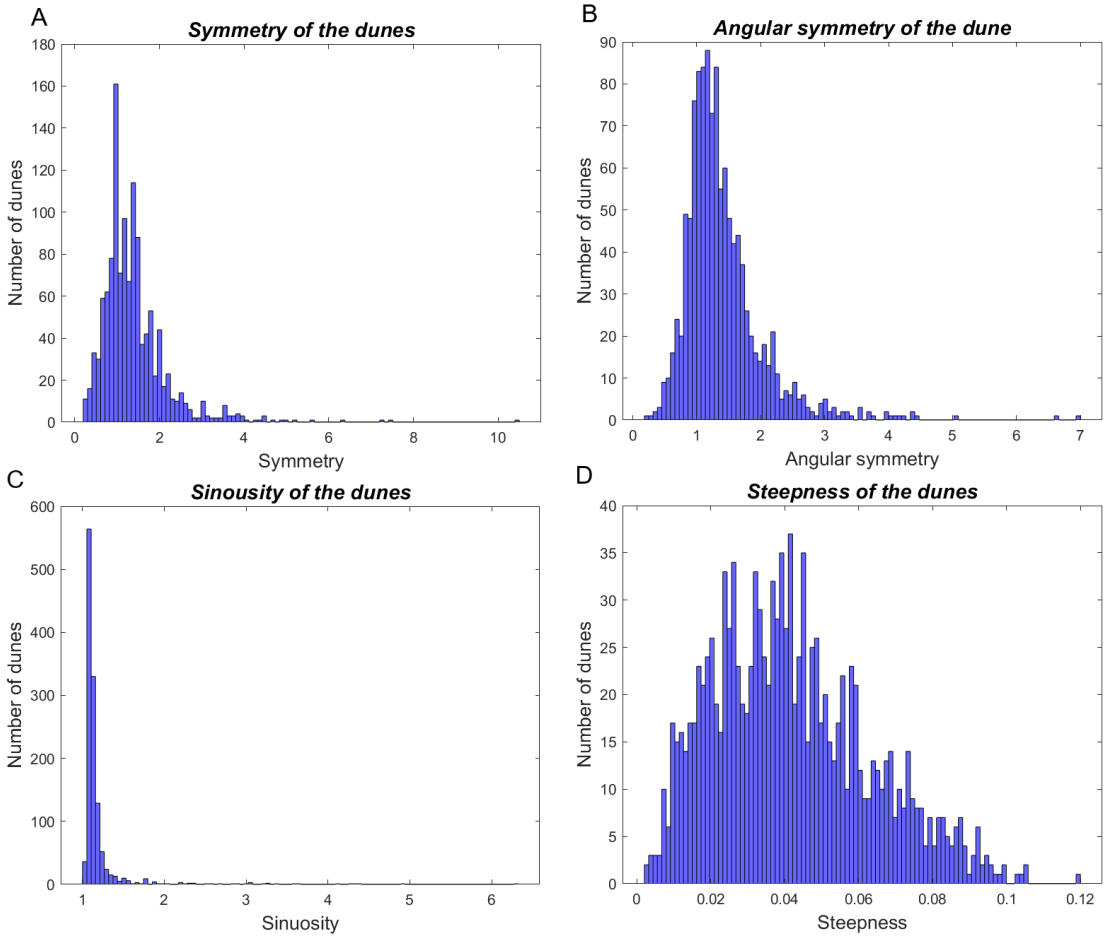

Figure 3.15 - Histograms of the symmetry indexes. (A): the symmetry index calculated with the width of the stoss and lee sides of the dunes. (B): the angular symmetry index calculated with the angles of the stoss and lee sides. (C): the sinuosity. (D): the steepness values of the dunes.

In addition to the symmetry index (3.1), the angular symmetry index is calculated using (3.5).

$$Sy_d = {}^{\alpha_L}/_{\alpha_S} \qquad (3.5)$$

The reason for calculating both symmetry indexes is related to the segmentation approach. In fact, the segmentation may partially detect the stoss and lee troughs. Consequently, the stoss and lee sides may be partially extracted as well. Such incomplete identification impact significantly the estimation of the width descriptors of the dunes (i.e., WD, WS, and WL). On the contrary, in such context, the angular descriptors of each side of the dune can be reliably estimated. The angular symmetry index ranges from 0.20 to 14.2, with a median value of 1.27, as illustrated in Figure 3.15B. The value of the symmetry index based on the width ranges from 0.2 to 10.5, with a median value of 1.21 (Figure 3.15A). The reason for having values lower than 1 is due to the imperfect identification of the stoss and lee troughs in the segmentation approach, as previously mentioned. Therefore, in the proposed method, the angular symmetry index is used to characterize the dune objects. The sinuosity index, as illustrated in Figure 3.15C, ranges from 1.01 to 6.32, with a median value of 1.11. The steepness index ranges from 0.0025 to 0.1197, with a median value of 0.0398 (Figure 3.15D).

The morphological descriptors previously computed for each dune object may also be used to characterize the fields where they are located. Indeed, by considering each sector of the Northern Traverse as a field, we can group the dunes by sector and consider the median values of their morphological descriptors to characterize each field. Therefore, Table 3.1 presents the median values of the morphological descriptors of the dune objects according to the field to which they belong.

Sector	O_m (°)	P_C (m)	H_C (m)	W_D (m)	Si_d	Sy_a
G04	57.18	13.52	0.60	16.97	1.16	1.49
G08	33.69	13.71	0.43	20.81	1.11	1.43
G09	21.92	13.94	0.54	8.49	1.10	1.34
G10	20.22	14.25	0.48	12.00	1.10	1.10
G11	21.80	14.03	0.78	23.42	1.10	1.16
G12	23.33	16.47	0.84	21.00	1.11	1.52
G13	27.21	14.94	2.45	34.00	1.09	1.25
G14	36.19	14.42	2.64	36.00	1.09	1.24
G15	201.48	15.15	1.66	28.00	1.10	1.54

Table 3.1 - Morphological descriptors of the fields of the Northern Traverse sectors. Om is the median orientation, Pc the minimum depth of the crest line, *Hc* is the median height, *Wd* is the median width of the dunes, Si_d is the sinuosity of the dune, and Sy_a is the angular symmetry of the dunes.

As previously mentioned, the median migration direction of the 1234 segmented dunes is 29°. Table 3.1 shows that, while sectors ranging from G08 to G14 have a migration direction fluctuating around 29°, the migration of sectors G04 and G15 is 57° and 201°, respectively. For G04, the migration direction is still consistent with the

flow direction of the channel. However, for G15, this direction is in the opposite direction of the preceding sector (G14), which indicates the dominance of the tidal current over the flow direction of the Saint Lawrence River. The dunes located in the southern sectors (i.e., G04 … G10) are generally smaller in height and width, and are also shallower than the dunes of the northern sectors (G11 … G15). This is consistent with the visual analysis of the Northern Traverse nautical charts, as shall be further discussed in the paper. The descriptors directly associated with the fields (i.e., λ_S, $\sigma_{\lambda S}$, f_D) are also calculated for the nine sectors of the Northern Traverse, as presented in Table 3.2.

Sector	λ_S (m)	$\sigma_{\lambda S}$ (m)	f_D (%)
G04	70.95	66.66	29
G08	39.47	35.16	17
G09	48.35	48.80	18
G10	38.78	41.58	46
G11	38.47	28.42	61
G12	46.29	29.29	51
G13	47.13	28.35	76
G14	48.51	23.55	86
G15	52.72	26.41	62

Table 3.2 - Spacing between the dune objects (λ_S), standard deviation ($\sigma_{\lambda S}$), and fullbeddedness (f_D) for the nine dunes fields of the Northern Traverse.

Table 3.2 shows that the spacing associated with each field of the Northern Traverse ranges from, approximately, 39 m in sector G10 to 71 m in sector G04. The standard deviation of the spacing ranges from approximately 24 m in sector G14 to 67 m in sector G04. In addition, the coverage of dunes on the seafloor ranges from approximately 86% of the seafloor in sector G14 to 17% in sector G08.

3.7 Analysis and Discussion

This section aims to discuss and analyze the morphological descriptors extracted from the dune objects of the Northern Traverse with the proposed method. The analysis will focus on the fields of the Northern Traverse rather than on the individual dune objects. Indeed, as the results of the previous section have shown, whether it is the morphological descriptors of the dunes or those of the fields, all contribute to characterize the fields to which the dunes belong.

The Northern Traverse being a navigation channel, the depth of the dunes is an important morphological descriptor of these sedimentary structures. Figure 3.16 presents the median value of this descriptor for each

sector of the Northern Traverse. The sectors are ordered sequentially on the x-axis in accordance with their spatial arrangement in the North Traverse (i.e., G04 is the southernmost sector and G15 the northernmost sector). Moreover, consecutive sectors are equally spaced on the x-axis.

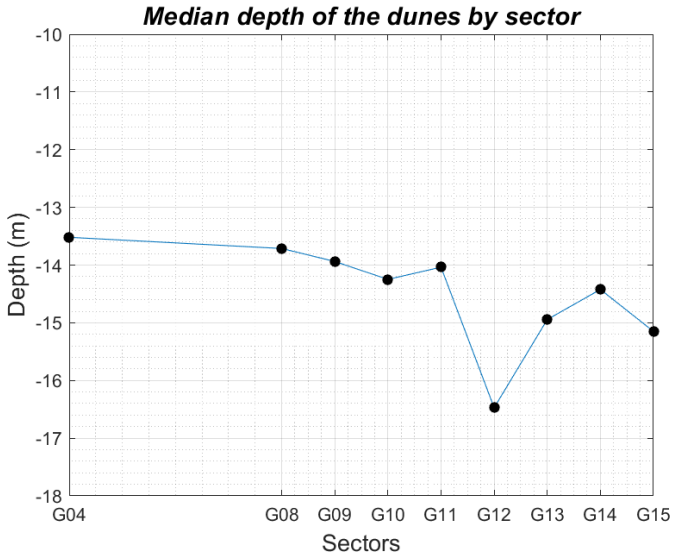

Figure 3.16 - Median-depth of the dunes per sector. Please note that consecutive sectors are equally spaced. Since sectors G05, G06, and G07 are not considered, sectors G04 and G08 are more distant than the other consecutive sectors.

As illustrated by Figure 3.16, the further downstream the sector (i.e., G04 to G15), the deeper the dunes. Therefore, this is consistent, since the navigation channel is located in the transition zone between the river (i.e., shallower) and the estuarine area (i.e., deeper). This finding is also explained by the dynamism of the navigation channel. As specified by experts of this channel, to ensure a minimal depth of 12.5 m, preventive dredging is carried out twice a year. The preventive dredging depth is different for each sector: 13.3 m for sector G04; 13.8 m for sectors G08, G09, and G10; 13.9 m for sectors G11, G12, and G13; and 14.7 m for sectors G14 and G15. In Figure 3.16, dunes in sector G12 are deeper than dunes located in the neighboring fields. This is consistent with the expert analysis, since the dunes located in this specific sector are naturally deeper without human intervention. Thus, the depth automatically extracted from the 1234 segmented dune objects of the Northern Traverse by the proposed method is consistent with the expert analysis of the sector and with the general description of the Northern Traverse given by (Comité de concertation navigation de Saint Laurent Vision, 2004).

Figure 3.17 illustrates the median values of the height and width of the dunes for the sectors of the Northern Traverse. The sectors are sequentially ordered and spaced on the x-axis, as displayed in Figure 3.16.

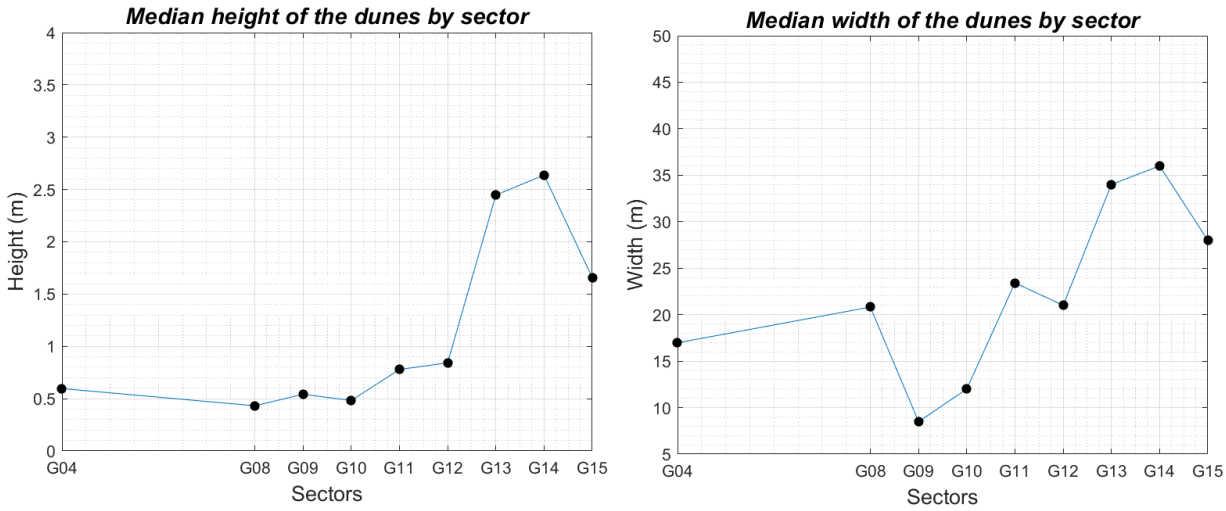

Figure 3.17 - Median height and width of the dunes per sector.

Figure 3.17 shows the height and width of the dunes are correlated. Indeed, the highest dunes are in the same sector as the widest dunes, and the narrowest dunes are in the same sector as the smallest dunes. The descriptors of the dunes fields (i.e., λ_S, $\sigma_{\lambda S}$, f_D) are illustrated in Figure 3.18.

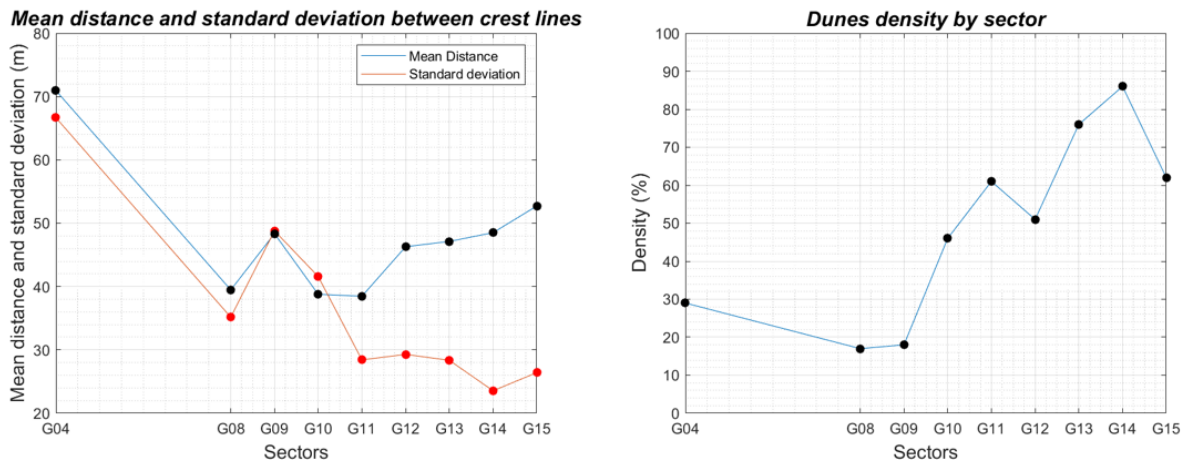

Figure 3.18 - In the left, the spacing (λ_S) between the dunes and the standard deviation ($\sigma_{\lambda S}$) per sector. In the right, the fraction of the seafloor covered by dunes (f_D) per sector.

The spacing between dunes (λ_S) and standard deviation ($\sigma_{\lambda S}$) share similar values in the southern sectors (i.e., G04–G10), as illustrated in Figure 3.18. However, in the northern sectors (i.e., G11–G15), the value of $\sigma_{\lambda S}$ is remarkably lower than the value of λ_S. Thereby, it shows that the dunes on the southern sectors are more spatially dispersed than the dunes on the northern sectors. This conclusion is supported by the fraction of the seafloor covered by dunes (f_D), as illustrated in Figure 3.18. The southern fields have less than 50% of their

surface covered by dunes. On the contrary, the northern fields have more than 50% of the seafloor covered by dunes. By analyzing these three descriptors (i.e., λ_S, $\sigma_{\lambda S}$, f_D), one can state that the dunes on the northern fields are adjacent to each other, while the southern sectors consist of isolated dunes. This is consistent with the expert knowledge expressed by the professionals responsible for the maintenance of the Northern Traverse. Therefore, this demonstrated that the morphological descriptors, automatically extracted by the proposed method, adequately characterize the dune fields of the navigation channel. Furthermore, such morphological descriptors may be useful to better understand the relationship between the dunes and their hydrodynamic factors. As an example, Figure 3.19 illustrates the relationship between dunes and the flow current.

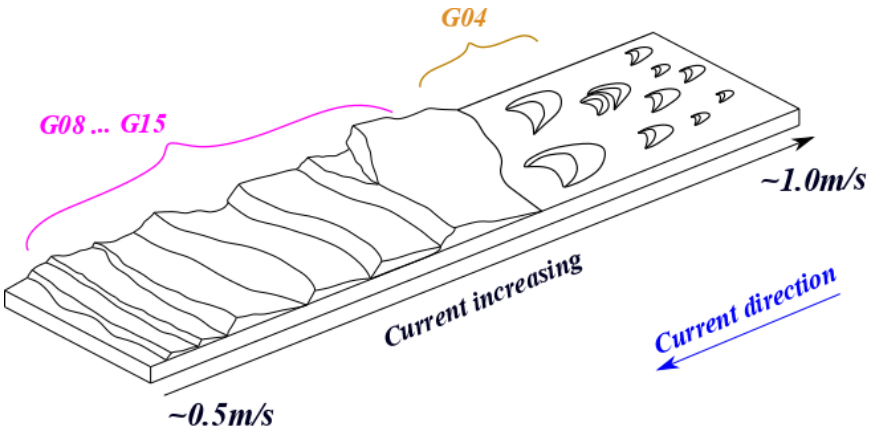

Figure 3.19 - Relationship between the dune fields and the flow current (adapted from Kenyon, 1970; Le Bot, 2001). The fields of the Northern Traverse were placed on the figure based on the size of the dunes.

Even if Figure 3.19 is an approximation in terms of current and dune sizes, it is possible to position the sectors of the Northern Traverse based on the dune field descriptor values (cf. Figures 3.17 and 3.18). It could be assumed that the flow current increases from sector G08 to sector G15 since dunes in sectors G08 to G12 are smaller than dunes in sectors G13, G14, and G15. The isolated dune objects of the southernmost sector (i.e., G04) may result in a stronger flow current than the sectors located to its north.

3.8 Conclusions

An automatic characterization method for dunes was proposed in this paper. This method is based on the morphological descriptors of, respectively, the dune objects and the field where they are located. The characterization relies on the dune objects extracted from the DBM by the segmentation approach proposed by Cassol et al. (2021). The proposed method automatically extracts morphological descriptors of the dune objects and the fields where they are located. These morphological descriptors are computed based on the surface of each dune object as well as its three salient features (i.e., crest line, stoss trough, and lee trough). To validate the proposed approach, more than 1200 dunes are characterized over nine fields of the Northern Traverse of

the Saint Lawrence River. The dunes and the fields considered in this paper present a significant diversity regarding their characteristics.

The first contribution of our paper is the automatic extraction of the morphological descriptors of the dune objects segmented from a DBM. This automatic extraction with the conceptual model of the dunes prevents the subjectivity of manual calculation. Our method is also more suited to large volumes of data being significantly less time consuming than characterizing dunes visually. The study of dunes located on a field and the characterization of the field itself are useful for the description of the seafloor, as discussed in previous section. The second contribution of the paper is the automatic characterization of the dune fields. Indeed, our method proposes the standard deviation of the spacing ($\sigma_{\lambda S}$) as a new descriptor of the fields, complementing those available in the literature (i.e., dune density and spacing of the dunes). In addition, this descriptor can be accurately assessed by taking advantage of the salient features of each dune object. As a result, the characterization of the fields is not only conducted by means of field descriptors, but also by means of individual dune descriptors. As demonstrated, the proposed method provides a reliable and efficient solution to segment and characterize the dune fields and objects from the seafloor surface.

Future work will be dedicated to assessing the performance of the method in contexts other than fluviomarine, namely marine and fluvial. In addition, its application using DBM at different resolution will also be investigated. Another research direction will concern the use of additional data, such as grain size for different dune fields, backscatter data (as considered by Masetti et al., 2018), current velocity, and tidal information. If these multiple datasets are available with the DBM of the seafloor, it may be possible to improve the characterization method. Indeed, the morphological descriptors of dune objects and fields may be correlated to the hydrodynamic and environmental factors. The correlation between the morphological descriptors discussed in this paper and dune shapes mentioned in the literature (e.g., linear, sinuous, barchan, etc.) may also be investigated further. Finally, the spatiotemporal migration of the underwater dunes may be considered in future research. Indeed, the descriptors computed with the proposed approach may be useful towards the identification of the same dune objects through different surveys.

3.9 References

Amos, C.L.; King, E.L. Bedforms of the Canadian eastern seaboard: A comparison with global occurrences. *Mar. Geol.* **1984**, *57*, 167–208.

Andreotti, B.; Claudin, P.; Devauchelle, O.; Duràn, O.; Fourrière, A. Bedforms in a turbulent stream: Ripples, chevrons and antidunes. *J. Fluid Mech.* **2012**, *690*, 94–128. https://doi.org/10.1017/jfm.2011.386

Ashley, G.M. Classification of large-scale subaqueous bedforms: A new look to an old problem. *J. Sediment. Petrol.* **1990**, *60*, 160–172.

Bartholdy, J.; Flemming, B.W.; Bartholomä, A.; Ernstsen, V.B. Flow and grain size control of depth-independent simple subaqueous dunes. *J. Geophys. Res.* **2005**, *110*, F04S16. https://doi.org/10.1029/2004JF000183.

Berné, S. Architecture et Dynamique des Dunes Tidales. Exemples de la Marge Atlantique Française. Ph.D. Thesis, Université des Sciences et Techniques de Lille Flandres-Artois, Westhoek, France, 1991.

Best, J.L. The fluid dynamics of river dunes: A review and some future research directions. *J. Geophys. Res.* **2005**, *110*, F04S02. https://doi.org/10.1029/2004JF000218.

Boggs, S. Sedimentary structures. In *Principles of Sedimentology and Stratigraphy*, 4th ed.; Pearson Prentice Hall: Upper Saddle River, NJ, USA, 2006; Chapter 4, pp. 74–116. ISBN 0-13-154728-3.

Cassol, W.N.; Daniel, S.; Guilbert, É. A Segmentation Approach to Identify Underwater Dunes from Digital Bathymetric Models. *Geoscience* **2021**, *11*, 361. https://doi.org/10.3390/geosciences11090361.

Cheng, H.Q.; Chen, W.; Li, J.F.; Jiang, Y.H.; Hu, X.; Zhang, X.L.; Zhou, F.N.; Hu, F.X.; Stive, M.J.F. Morphodynamic changes of the Yangtze Estuary under the impact of the Three Gorge Dam, of estuarine engineering interventions and of climate-induced sea level rise. *Earth Planet. Sci. Lett.* **2022**, *580*, 117385. https://doi.org/10.1016/j.epsl.2022.117385.

Cheng, H.Q.; Kostaschuk, R.; Shi, Z. Tidal currents, bed sediments, and bedforms at the South Branch and the South Channel of the Changjiang (Yangtze) Estuary, China: Implications for the ripple-dune transition. *Estuaries* **2004**, *27*, 861–866.

Comité de concertation navigation de Saint Laurent Vision 2000. *Stratégie de Navigation Durable Pour le Saint-Laurent*; Ministère des Transports du Québec et Pêches et Océans: Québec, QC, Canada, 2004; 114p.

Debese, N.; Jacq, J.J.; Garlan, T. Extraction of sandy bedforms features through geodesic morphometry. *Geomorphology* **2016**, *267*, 82–97. https://doi.org/10.1016/j.geomorph.2016.05.013.

Debese, N.; Jacq, J.-J.; Degrendele, K.; Roche, M. Toward Reliable Volumetric Monitoring of Sandbanks. In *Geomorphometry*; Elsevier Science: Boulder, CO, USA, 2018.

Di Stefano, M.; Mayer, L.A. An automatic procedure for the quantitative characterization of submarine bedforms. *Geosciences* **2018**, *8*, 28. https://doi.org/10.3390/geosciences8010028.

van Dijk, T.A.G.P.; van Dalfsen, J.A.; Van Lancker, V.; van Overmeeren, R.A.; van Heteren, S.; Doornenbal, P.J. 13—Benthic Habitat Variations over Tidal Ridges, North Sea, the Netherlands. In *Seafloor Geomorphology as Benthic Habitat*; Elsevier: Amsterdam, The Netherlands, 2012; pp. 241–249, ISBN 9780123851406. https://doi.org/10.1016/B978-0-12-385140-6.00013-X

Drapeau, G. Dynamique sédimentaire des littoraux de l'estuaire du Saint Laurent. *Géographie Phys. Quat.* **1992**, *46*, 233–242. https://doi.org/10.7202/032907ar.

Ferret, Y. *Morphodynamique de Dunes Sous-Marines en Contexte de Plate-Forme Mégatidale (Manche Orientale). Approche Multi-Échelles Spatio-Temporelles. Interfaces Continentales, Environnement*; Université de Rouen: Rouen, France, 2011.

Garlan, T. Study on Marine Sandwave Dynamics. *Int. Hydrogr. Rev.* **2007**, *8*, 26–37.

Garlan, T. GIS and Mapping of Moving Marine Sand Dunes. Presented at the 24th International Cartography Conference, Santiago, Chili, 15–21 November 2009.

Gutierrez, R.R.; Abad, J.D.; Parsons, D.R.; Best, J.L. Discrimination of bed form scales using robust spline filters and wavelet transforms: Methods and application to synthetic signals and bed forms of the Rio Paraná, Argentina. *J. Geophys. Res. Earth Surf.* **2013**, *118*, 1400–1419. https://doi.org/10.1002/jgrf.20102.

Hains, D., Bergmann, M., Cawthra, H. C., Cove, K., Echeverry, P., Maschke, J., Mihailov, M. E., Obura, V., Oei, P., Pang, P. Y., Ponce, R. and Roperez, J. Hydrospatial…A global movement. *International Hydrographic Review*, **2021**. Pp. 147-153.

Jasiewicz, J.; Stepinski, T.F. Geomorphons—A pattern reconigtion approach to classification and mapping of landforms. *Geomorphology* **2012**, *182*, 147–156. https://doi.org/10.1016/j.geomorph.2012.11.005.

Kenyon, N.H. Sand Ribbons of European tidal Seas. *Mar. Geol.* **1970**, *9*, 25–39.

Knaapen, M.A.F. Sandwave migration predictor based on shape information. *J. Geophys. Res.* **2005**, *110*. https://doi.org/10.1029/2004JF000195.

Landeghem, K.J.J.; Wheeler, A.J.; Mitchell, N.C.; Sutton, G. Variations in sediment wave dimensions across the tidally dominated Irish Sea, NW Europe. *Mar. Geol.* **2009**, 263, 108–119. https://doi.org/10.1016/j.margeo.2009.04.003.

Le Bot, S. Morphodynamique de Dunes Sous-Marines Sous Influence des Marées et des Tempêtes. Processus Hydro-Sédimentaires et Enregistrement. Exemple du Pas-de-Calais. Ph.D. Thesis, Université de Lille I, Villeneuve-d'Ascq, France, 2001.

Lebrec, U.; Riera, R.; Paumard, V.; O'Leary, M.J.; Lang, S.C. Automatic Mapping and Characterisation of Linear Depositional Bedforms: Theory and Application Using Bathymetry from the North West Shelf of Australia. *Remote Sens.* **2022**, *14*, 280. https://doi.org/10.3390/rs14020280.

Lecours, V.; Dolan, M.F.J.; Micallef, A.; Lucieer, V.L. A review of marine geomorphometry, the quantitative study of the seafloor. *Hydrol. Earth Syst. Sci.* **2016**, *20*, 3207–3244. https://doi.org/10.5194/hess-20-3207-2016.

Lefebvre, A.; Paarlberg, A.J.; Winter, C. Characterising natural bedform morphology and its influence on flow. *Geo-Mar. Lett.* **2016**, *36*, 379–393. https://doi.org/10.1007/s00367-016-0455-5.

van der Mark, C.F.; Blom, A. *A New & Widely Applicable Bedform Tracking Tool*; University of Twente, Faculty of Engineering Technology, Department of Water Engineering and Management: Enschede, The Netherlands, 2007; 44p.

Masetti, G.; Mayer, L.A.; Ward, L.G. A Bathymetry- and Reflectivity-Based Approach for Seafloor Segmentation. *Geosciences* **2018**, *8*, 14.

Nichols, G. Processes of transport and sedimentary structures. In *Sedimentology and Stratigraphy*, 2nd ed.; Wiley-Blackwell, A., Ed.; John Wiley & Sons Publication: West Sussex, UK, 2009; Chapter 4, pp. 44–68.

Ogor, J. Design of Algorithms for the Automatic Characterization of Marine Dune Morphology and Dynamics. Ocean, Atmosphere. Ph.D. Thesis, ENSTA-Bretagne, Brest, France, 2018.

Parsons, D.R.; Best, J.L.; Orfeo, O.; Hardy, R.J.; Kostaschuk, R.; Lane, S.N. Morphology and flow fields of three-dimensional dunes, Rio Paranà, Argentina: Results from simultaneous multibeam echo sounding and acoustic Doppler current profiling. *J. Geophys. Res.* **2005**, *110*, F04S03. https://doi.org/10.1029/2004JF000231.

Thibaud, R.; Del Mondo, G.; Garlan, T.; Mascret, A.; Carpentier, C. A Spatio-Temporal Graph Model for Marine Dune Dynamics Analysis and Representation. *Trans. GIS* **2013**, *17*, 742–762. https://doi.org/10.1111/tgis.12006.

Yan, G.; Cheng, H.Q.; Jiang, Z.Y.; Tengm, L.Z.; Tang, M.; Shi, T.; Jiang, Y.H.; Yang, G.Q.; Zhou, Q.P. Recognition of fluvial bank erosion along the main stream of the Yangtze River. *Engineering* **2021**. 19 pages. https://doi.org/10.1016/j.eng.2021.03.027.

3.10 Complément à l'article

3.10.1 Analyse complémentaire des résultats

Le développement d'une approche de caractérisation des dunes automatisée et systématique proposée dans ce chapitre repose sur le modèle conceptuel formalisant l'identification des dunes sur la surface du fond marin à partir de leurs saillances. Les valeurs obtenues pour les descripteurs des dunes et des champs de la Traverse Nord calculés à l'aide de notre approche se sont révélées cohérentes avec la connaissance dont disposent les experts œuvrant dans ce chenal de navigation. Également, ces résultats ont permis de constater une corrélation entre différents descripteurs (e.g. hauteur, largeur) ce qui avait déjà été mis en évidence et discuté dans la littérature (Ashley, 1990). Au-delà de ces constats, il n'est pas possible à l'heure actuelle d'en déduire davantage de connaissance à propos de la précision, de l'exactitude, de la capacité de généralisation des descripteurs proposés. En effet, pour une validation plus rigoureuse des résultats obtenus, il serait nécessaire de disposer de plus de données de vérité terrain associées au site d'étude. Aussi, ces structures sédimentaires évoluant dynamiquement en fonction de l'environnement dans lequel elles se trouvent, la validation devrait prendre en compte différents facteurs environnementaux comme la vitesse et la direction du courant, la granulométrie des sédiments, la turbidité de l'eau, la marée, etc. Ces facteurs permettraient d'avoir une compréhension plus réaliste des phénomènes intervenant sur le fond de l'eau au moment d'interpréter les statistiques et les graphiques produits à partir des descripteurs. En termes de pertinence, d'usage et d'utilisabilité des descripteurs produits, de telles analyses ne peuvent être menées que dans le cadre d'une collaboration multidisciplinaire. En effet, les dunes sous-marines ne seront pas perçues avec la même finalité pour un professionnel de la maintenance du chenal de navigation (i.e. localiser voire estimer l'évolution des dunes pour les draguer) que pour un géomorphologue (i.e. comprendre la formation et l'évolution de la structure sédimentaire en fonction de

l'environnement). Un tel travail collaboratif permettra donc de mettre en lumière lesquels des descripteurs ont une plus-value en fonction d'usages prédéfinis.

3.10.2 Efficacité calculatoire de l'approche

L'efficacité calculatoire de la méthode de segmentation et de caractérisation des dunes sous-marines a été sommairement évaluée afin d'établir un ordre de grandeur du temps de traitement requis pour chaque MNB. A titre d'exemple, le MNB du secteur G15 de la Traverse Nord de résolution 1m et de dimensions 707m par 907m, a nécessité un temps de traitement d'approximativement 12,5 secondes sachant que l'ordinateur utilisé avait les spécifications suivantes : 12 Go RAM; processeur Intel Core i7-3770 à 3,40 GHz. Le traitement considère comme intrants le MNB et la classification morphométrique à l'aide de l'algorithme des geomorphons. Les fichiers résultants sont une image avec les lignes de crête, une image avec les pieds des dunes, une image avec les objets dunes et un fichier .CSV avec les descripteurs morphologiques de chaque objet dune identifié. Les fonctions utilisées dans l'environnement Matlab peuvent être consultées à l'Annexe A.

Conclusion

Retour sur les objectifs de recherche

L'objectif général de ce projet de recherche était de concevoir et développer une méthode de segmentation des dunes sous-marines orientée-objet qui permette la caractérisation efficiente et objective des dunes en considérant la qualité des données acquises. Afin d'atteindre cet objectif général, trois objectifs spécifiques ont été définis.

Le premier objectif spécifique était la conception d'un modèle d'analyse de l'influence de la morphologie du fond marin sur la valeur de l'incertitude-type composée relative aux données bathymétriques. Le modèle proposé considère la propagation de l'incertitude des mesures à partir du modèle de géoréférencement direct des points de sonde. De plus, il ajoute un nouveau terme, l'incertitude morphologique, au modèle classique d'estimation de l'incertitude des données bathymétriques. Ce terme représente la contribution de la morphologie du fond marin à la valeur d'incertitude estimée pour les coordonnées des points sondés. L'estimation de l'incertitude morphologique est liée à l'angle d'incidence formé entre la normale de chaque point et le faisceau. Le modèle proposé a été validé au moyen de données simulées et réelles. À partir de cette validation, on constate que l'influence de la morphologie du fond sur l'incertitude des données peut être considérée négligeable (i.e. inférieure à 1%) lorsque les faisceaux ne sont pas rasants à la surface levée. Néanmoins, lorsque les faisceaux sont rasants à la surface du fond, que ce soit en fond plat ou en présence de dunes, la morphologie du fond a une influence significative sur la valeur d'incertitude estimée pour les données bathymétriques. Suite à la conception et à la validation du modèle d'analyse de l'influence de la morphologie du fond marin sur l'incertitude des données bathymétriques, cet objectif spécifique est considéré comme atteint.

Plusieurs éléments d'amélioration du modèle ont été identifiées lors de ce travail. L'un d'eux concerne la validation du modèle avec une gamme plus élargies de données réelles, acquises dans différents contextes, tels que le fond marin plat, en pente, avec la présence de structures sédimentaires (i.e. rides) ou d'affleurements rocheux. Cette diversité de fond permettrait d'observer la variation de l'influence de la morphologie du fond sur les données dans ces différents contextes dans la perspective d'améliorer l'interprétation des surfaces résultantes et des structures qui y sont présentes. Un autre élément d'amélioration concerne l'usage de mesures supplémentaires acquises par le système hydrographique. En effet, certaines de ces mesures sont prises en compte dans le géoréférencement des données bathymétriques et dans le calcul de leur incertitude par les logiciels de traitement des données hydrographiques spécialisés (e.g. Qimera), mais elles ne sont pas facilement accessibles aux utilisateurs des données. C'est le cas par exemple des mesures de vitesse angulaire. De nouvelles études pourraient donc être menées avec des jeux de données pour lesquels ces mesures sont

disponibles. Il serait alors possible de les inclure dans le modèle d'estimation de l'influence de la morphologie du fond marin sur l'incertitude des données bathymétriques.

Le calcul de la normale de chaque point sondé par le système bathymétrique joue un rôle fondamental dans l'estimation de l'influence du fond sur la valeur d'incertitude des données acquises. Tel que mentionné précédemment, le nouveau terme d'incertitude morphologique ajouté au modèle d'estimation d'incertitude est intimement lié à l'angle d'incidence calculé entre la normale du point sondé et le faisceau. Ainsi, la présence de bruit dans les données peut biaiser l'analyse de l'influence effective du fond sur l'incertitude. Le modèle proposé dans ce projet considère l'estimation de la normale par la méthode PCA robuste (Dupont, 2020). Malgré la robustesse de cette méthode, elle présente encore une sensibilité au bruit, étant donné que l'estimation de l'angle d'incidence est liée au voisinage des points sondés. Ainsi, des améliorations peuvent être apportées à cette étape d'estimation de la normale, soit en filtrant les points bruités, soit en investiguant les approches présentant moins de sensibilité au bruit que la PCA. Il serait également possible d'élargir le voisinage des points sondés en fonction de la morphologie du fond (ex. un fond plat ou un fond avec des dunes) afin de diminuer le poids des points bruités dans l'estimation de la normale. Une étude pourrait également être menée afin d'analyser la variation de la valeur de l'incertitude des données bathymétriques, notamment la contribution de la composante morphologique en fonction de l'ouverture angulaire de la fauchée.

Le deuxième objectif spécifique de ce projet de recherche était de concevoir et de développer une méthode orientée-objet de segmentation de la surface numérique représentant le fond marin pour l'identification des dunes sous-marines. La méthode proposée est basée sur la formalisation des objets dunes sous-marines à partir d'un modèle conceptuel. Ce modèle établit que les objets dunes peuvent être segmentés à partir de l'identification de leurs saillances. L'identification des saillances (ligne de crête et pieds de dunes) a été effectuée à partir d'une analyse morphométrique de la surface du fond marin et des opérations de traitement d'image, notamment des fonctions de morphologie mathématique. En utilisant une approche orientée-objet, les dunes ont été segmentées en mettant en correspondance la ligne de crête et les pieds de dunes de chaque objet identifié. Suite à la conception et au développement de la méthode orientée-objet, des expérimentations ont été menées afin d'en évaluer ses performances. Des données bathymétriques acquises dans la Traverse Nord du Saint-Laurent ont été utilisées à cet effet. Les résultats obtenus ont montré un taux de bonne segmentation de 92%. A l'issue de cette évaluation, il est considéré que le deuxième objectif spécifique a été atteint. On considère néanmoins que, compte tenu du rôle important que joue l'analyse morphométrique dans la démarche proposée, il serait pertinent de mettre en œuvre et d'évaluer des techniques autres que celle des Géomorphons, comme la morphométrie géodésique (Debese et al., 2016) ou la géométrie différentielle (Ogor, 2018). Il serait alors possible de mesurer l'indépendance de la solution vis-à-vis des Géomorphons et, le cas échéant, de bâtir une formalisation générale de la solution non liée aux techniques intervenant dans les traitements qui la composent.

Le troisième objectif spécifique concernait la conception et le développement d'une méthode de caractérisation des dunes sous-marines au moyen de descripteurs morphologiques impliquant les saillances des dunes. La méthode proposée s'appuie sur l'approche de segmentation des dunes impliquant l'identification de ses saillances. En considérant ces dernières et la surface de la dune segmentée, la méthode calcule différents descripteurs morphologiques, sélectionnés à partir de la littérature, pour les objets dunes et pour les champs où les dunes sont situées. Également, un nouveau descripteur morphologique des champs de dunes a été introduit. Celui-ci permet d'évaluer la dispersion des dunes dans le champ (i.e. l'écart-type de l'espacement des dunes). La méthode de calcul des descripteurs a été appliquées à 1234 dunes de la Traverse Nord du Saint Laurent. Les résultats obtenus ont été validés par différents professionnels experts responsables de la maintenance de ce chenal de navigation. La méthode proposée s'appliquant de manière systématique sans faire intervenir l'utilisateur au moment de définir les paramètres, il est possible d'affirmer qu'elle est robuste et objective. Ainsi, le troisième objectif spécifique est considéré atteint. Puisque les trois objectifs spécifiques établis ont été accomplis, l'objectif général de ce projet de recherche est également considéré comme atteint.

Afin d'élargir la validation des méthodes proposées dans ce projet et d'évaluer leur capacité de généralisation, des surfaces présentant différentes résolutions devront être expérimentées. Il sera alors possible de segmenter des dunes de tailles plus grandes ou plus petites que celles traitées dans cette recherche. Comme la qualité de l'estimation des descripteurs morphologiques des dunes est liée à la résolution du MNB, il sera également possible de réaliser des analyses et tirer des conclusions complémentaires concernant la caractérisation des dunes. Dans cette même perspective, l'approche proposée peut être étendue à d'autres contextes de formation des dunes avec des conditions environnementales différentes de celles du contexte fluviomarin. Ainsi, le modèle conceptuel définissant l'identification des dunes à partir des saillances pourra être adapté à ces différents contextes (e.g. marin et fluvial) de même que la définition des descripteurs morphologiques utilisés pour la caractérisation des dunes et des champs. Dans cet esprit, il serait aussi envisageable d'étudier les dunes ayant subies des interventions humaines, comme le dragage. Celles-ci ne présentant plus les caractéristiques des dunes naturelles, c'est-à-dire les saillances définies dans le modèle conceptuel des dunes, elles ne peuvent plus être considérées comme des dunes. Elles nécessitent donc la proposition d'un nouveau modèle conceptuel et de descripteurs adaptés.

Contributions de la recherche

Ce travail de doctorat a contribué à l'avancement des connaissances dans le domaine du traitement des données bathymétriques. Plus spécifiquement, cette recherche a permis de confirmer l'influence de la morphologie du fond sur l'incertitude des données et d'évaluer l'ampleur de cette influence. De plus, elle a proposé une formalisation des saillances permettant d'identifier une dune sous-marine à partir d'une surface modélisant le fond marin, ce qui constitue une démarche originale pour segmenter des structures naturelles

floues. Cette formalisation élimine la subjectivité non seulement de la segmentation mais également des descripteurs morphologiques intervenant dans la caractérisation des dunes. Aussi, ce travail a mis en évidence les connaissances que la caractérisation des dunes permet d'extraire de la surface du fond, non seulement sur les dunes elles-mêmes, mais aussi sur les champs au sein desquels les dunes sont localisées.

Plusieurs contributions scientifiques sont également associées à cette recherche à savoir : un nouveau modèle d'incertitude-type composée incluant une composante associée à la morphologie du fond ; un modèle conceptuel formalisant les saillances des dunes ; une chaine de traitement complète et automatique aboutissant à l'ensemble des objets dunes segmentés individuellement ; une méthode de calcul des descripteurs morphologiques exprimée à partir des saillances des objets dunes et des objets dunes eux-mêmes. Chacune de ces contributions s'est traduite par un prototype fonctionnel implémenté dans l'environnement Matlab.

Ce travail de doctorat a également donné lieu à plusieurs initiatives de diffusion des connaissances dont des articles soumis et publiés dans des revues avec comité de lecture, des conférences révisées par les pairs avec publication d'article complet et des conférences et communications diverses destinées au milieux hydrographique et scientifique. En voici une liste détaillée :

Articles soumis et publiés dans des revues avec comité de lecture :

- Cassol, W. N., Daniel, S., Guilbert, É. and Debese, N. **An empirical study of the influence of seafloor morphology on the uncertainty of bathymetric data**. *Marine Geodesy,* 2022. https://doi.org/10.1080/01490419.2022.2075499. Article soumis le 28 septembre 2021 à la revue *Marine Geodesy* et publié le 18 mai 2022.

- Cassol, W. N., Daniel, S. and Guilbert, É. **A segmentation Approach to Identify Underwater Dunes from Digital Bathymetric Models**. *Geosciences, 2021,* 11, n°9: 361. https://doi.org/10.3390/geosciences11090361. Article soumis le 23 juin 2021 à la revue Geosciences et publié le 25 août 2021.

- Cassol, W. N., Daniel, S. and Guilbert, É. **An approach for the automatic characterization of underwater dunes in fluviomarine context**. *Geosciences, 2022,* 12, 89. https://doi.org/10.3390/geosciences12020089. Article soumis le 20 janvier 2022 à la revue Geosciences et publié le 16 février 2022.

Conférences révisées par les pairs et avec article complet:

- Cassol, W. N. and Daniel, S. **Spatial-temporal migration dynamics of submarine dunes in St. Lawrence River**. *IEEE Xplore*. Oceans 2019 Seattle.

Conférences et communications pour les milieux hydrographique et scientifique:

- Cassol, W. N., Daniel, S. and Guilbert, É. **Segmentation and characterization of underwater dunes of the Northern Traverse of the Saint-Lawrence River**. *Conférence Hydrographique du Canada (CHC) 2022,* Ottawa/Gatineau, Canada.

- Cassol, W. N., Daniel, S. and Guilbert, É. **Segmentation et classification des dunes sous-marines du Fleuve Saint-Laurent.** *89e Congrès de l'ACFAS 2022*, conférence en ligne.

- Cassol, W. N., Daniel, S. and Guilbert, É. **Underwater dunes segmentation in Northern Traverse of the Saint-Lawrence River.** *École international d'automne en levés hydrographiques et LiDAR 2021*, Québec, Canada.

- Cassol, W. N., Daniel, S. and Guilbert, É. **Underwater dunes segmentation in Northern Traverse of the Saint-Lawrence River**. *US Hydro 2021*, conference en ligne.

- Cassol, W. N. and Daniel, S. **Combined Standard Measurement Uncertainty Model to Bathymetric Data.** *Conférence Hydrographique du Canada (CHC) 2020,* Québec, Canada.

- Cassol, W. N. and Daniel, S. **Étude spatio-temporelle de la migration des dunes sous-marines en fonction d'événements réguliers ou extrêmes dans le fleuve Saint-Laurent**. *Colloque vecteur 2019*. Rimouski, Canada.

- Cassol, W. N., Daniel, S. and Guilbert, É. **Segmentation et classification des dunes sous-marines du Fleuve Saint-Laurent**. *Webinaire du CRDIG*, 30 mars 2021.

Perspectives de recherche

La complétion de ce projet de doctorat ouvre plusieurs perspectives de recherche. Ainsi, il serait possible d'élargir la solution proposée à d'autres sources de données pour la segmentation et la caractérisation des dunes sous-marines. Une telle méthode multi-source nécessiterait de mettre à jour le modèle conceptuel guidant la segmentation des dunes puisque, dans celui-ci, seules les saillances identifiées dans le MNB sont exploitées. Les informations qui pourraient compléter le modèle conceptuel sont, par exemple, la granulométrie des sédiments ou bien la vitesse du courant, compte tenu de leur influence sur la formation des structures sédimentaires. Il serait aussi possible de tirer profit des données de rétrodiffusion, que ce soit pour la segmentation ou la caractérisation des dunes. En effet, la rétrodiffusion du signal acoustique varie en fonction de la nature et de la morphologie du fond. La prise en compte d'une plus grande diversité de données multi-source (ex. granulométrie des sédiments, courants, marée, …) permettrait également d'établir des liens entre

le contexte environnemental du fond et la présence de certaines structures sédimentaires. Il serait aussi possible de réaliser une analyse plus détaillée de la corrélation entre les descripteurs morphologiques et la forme des dunes sous-marines (e.g. linéaires, sinueuses, barkhanes, etc.).

Ce projet de doctorat ouvre également de nouvelles opportunités de travaux portant sur la superposition des structures sédimentaires sur le fond marin. À titre d'exemple, les rides peuvent se superposer aux dunes sous-marines et des petites dunes peuvent se superposer sur des grandes dunes. Ces deux cas de figure n'ont pas été spécifiquement investigués dans la présente recherche. Dans le premier cas, où les rides se superposent aux dunes, une approche de segmentation multi-résolution pourrait être proposée. Dans une telle approche il serait possible d'identifier les rides à partir des données de résolution plus fine et les dunes à partir des données de résolution plus grossière. Ensuite, la superposition des structures pourrait être analysée à partir d'une hiérarchie prédéterminée de structures sédimentaires. Une approche hiérarchique similaire serait également applicable dans le deuxième cas de figure, à savoir la superposition de petites dunes sur des grandes dunes. Ici, une hiérarchie de saillance pourrait être considérée.

Ce travail de recherche ouvre de nouvelles perspectives en termes d'analyse spatio-temporelle des dunes présentes sur le fond marin. Une telle analyse pourrait être directement liée à l'étude de la migration et de l'évolution des dunes. En effet, les objets dunes segmentés et caractérisés ainsi que leurs saillances associées pourraient permettre d'identifier un même objet dune dans des levés effectués à différentes époques. Ce suivi des dunes dans le temps fournirait des connaissances importantes sur l'apport sédimentaire dans certaines zones du fleuve qui pourraient être exploitées pour la sécurisation et maintenance des chenaux de navigation. Plusieurs enjeux restent à adresser pour mener une telle recherche. Un premier concerne l'intervalle de temps optimal pour l'acquisition des données bathymétriques. En effet, l'échelle temporelle doit permettre d'identifier les dunes à chaque levé afin d'observer leur déplacement sur le fond marin. Un autre enjeu concerne le fait que ces structures sédimentaires peuvent changer de forme lors de leur déplacement ce qui complexifie l'étude de la migration des dunes.

Compte tenu de la similarité des dunes sous-marines avec d'autres structures sédimentaires présentes dans le milieu terrestre, on peut facilement envisager une adaptation de ce travail de recherche à des contextes autres que celui du domaine hydrographique. Un exemple est le contexte désertique pour lequel différentes formes de relief peuvent être identifiées, telles que des dômes de sel, des playas ou encore des dunes éoliennes (Garajeh et al., 2022). Il existe déjà plusieurs études dans la littérature concernant les dunes éoliennes visant leur identification (Ewing et al., 2006 ; Shumack et al., 2020 ; Garajeh et al., 2022), leur caractérisation (Elbelrhiti et al., 2008 ; Courrech du Pont, 2015) et l'étude de leur évolution spatio-temporelle (Yang et al., 2021).

Finalement le modèle universel de données hydrographiques S-100 proposé par l'OHI (2018) prévoit l'utilisation d'une grande variété des données numériques liées à l'hydrospatial (Hains et al., 2021). Ce modèle S-100 permet une intégration plus facile des données et applications hydrographiques, tout en considérant une diversité de sources de données, de produits et d'utilisateurs (OHI, 2018). Ainsi, on peut envisager que les dunes segmentées et caractérisées par les méthodes proposées dans ce travail de recherche puissent être intégrées dans les bases de données de navigation. Une telle intégration peut s'avérer utile pour les différents utilisateurs des données hydrospatiales, surtout dans les voies navigables achalandées comme la Traverse Nord du Saint-Laurent. Des travaux futurs pourront donc être initiés en vue de la formalisation d'une classe dune et de son intégration au sein du modèle S-100.

Bibliographie

Amante, C. J. and Eakins, B. W. Accuracy of interpolated bathymetry in digital elevation models. *Journal of Coastal Research,* **2016**, SI 76. Pp. 123-133 DOI: 10.2112/SI76-011

AML Oceanographic. Base-X Product Description, viewed 07th December **2021**, http://www.mdsys.co.kr/down/AML/Base_X.pdf

AML Oceanographic. Micro-X Product Description, viewed 07th December **2021**, https://stema-systems.nl/wp-content/uploads/2015/08/Micro-X_Brochure.pdf

Amos, C.L.; King, E.L. Bedforms of the Canadian eastern seaboard: A comparison with global occurrences. *Mar. Geol.* **1984**, *57*, 167–208.

Andreotti, B.; Claudin, P.; Devauchelle, O.; Duràn, O.; Fourrière, A. Bedforms in a turbulent stream: Ripples, chevrons and antidunes. *J. Fluid Mech.* **2012**, *690*, 94–128. DOI: 10.1017/jfm.2011.386

Applanix. POS MV OceanMaster, **2019**, 2 pages, viewed 07th December 2021, https://www.applanix.com/downloads/products/specs/posmv/POS-MV-OceanMaster.pdf

Arvor, D.; Belgiu, M.; Falomir, Z.; Mougenot, I.; Durieux, L. Ontologies to interpret remote sensing images: Why do we need them? *Giscience Remote Sens*. **2019**, 56, 911–939, doi:10.1080/15481603.2019.1587890.

Ashley, G.M. Classification of large-scale subaqueous bedforms: A new look to an old problem. *J. Sediment. Petrol*. **1990**, 60, 160–172.

Bartholdy, J.; Flemming, B.W.; Bartholomä, A.; Ernstsen, V.B. Flow and grain size control of depth-independent simple subaqueous dunes. *J. Geophys. Res.* **2005**, *110*, F04S16. https://doi.org/10.1029/2004JF000183.

Beaudoin, J., Calder, B., Hiebert, J. and Imahori, G. Estimation of sounding uncertainty from measurements of water mass variability. *International Hydrographic Review,* **2009.** November 2009. Pp. 20-38.

Benz, U.C.; Hofmann, P.; Willhauck, G.; Lingenfelder, I.; Heynen, M. Multi-resolution, object oriented fuzzy analysis of remote sensing data for GIS-ready information. *ISPRS J. Photogramm. Remote Sens*. **2004**, 58, 239–258, doi:10.1016/j.isprsjprs.2003.10.002.

Berné, S. Architecture et Dynamique des Dunes Tidales. Exemples de la Marge Atlantique Française. Ph.D. Thesis, *Université des Sciences et Techniques de Lille Flandres-Artois*, **1991**, Westhoek, France.

Berné, S. ; Castaing, P ; Le Drezen, E. and Lericolais, G. Morphology, internal structure and reversal of asymmetry of large subtidal dunes in the entrance to Gironde estuary (France). *Journal of Sedimentary Research*, **1993**, 63(5). Pp. 780-793. https://doi.org/10.1306/D4267C03-2B26-11D7-8648000102C1865D

Best, J.L. The fluid dynamics of river dunes: A review and some future research directions. *J. Geophys. Res.* **2005**, *110*, F04S02. https://doi.org/10.1029/2004JF000218

Bjorn, J. and Einar, B. Time referencing in Offshore Survey Systems. FFI/RAPPORT-2006/01666. *Forsv Arets Forskninginstitutt* (Norwegian Defence Research Establishment) **2006**. 122 pages.

Blaschke, T. Object based image analysis for remote sensing. *ISPRS J. Photogramm. Remote Sens*. **2010**, 65, 2–16, doi:10.1016/j.isprsjprs.2009.06.004.

Boggs, S. Principles of Sedimentology and Stratigraphy, 4th ed.; Chapter 4 Sedimentary structures; Chapter 9 Marginal Marine Environments; *Pearson Prentice Hall: Upper Saddle River*, NJ, USA, **2006**; pp. 74–116, 289–333, ISBN 0-13-154728-3.

Byrne, J., S. and Schmidt, V. E. Uncertainty modeling for AUV acquired bathymetry. *U. S. Hydrographic Conference (US HYDRO)* **2015**. Gaylord Hotel, National Harbor, Matyland, USA. 25 pages.

Calder, B. R. and Mayer, L. A. Automatic processing of high-rate, high-density multibeam echosounder data. *Geochemistry Geophysics Geosystems* **2003**. Vol. 4, number 6, 22 pages. DOI: 10.1029/2002GC000486

Canadian Hydrographic Service (CHS). Traitement et Analyse de Données Bathymétriques de CUBE; *Pêches et Océans Canada*, Canada, **2012**; 7 pages.

Cassol, W. N. Définition d'un modèle d'incertitude-type composée pour les Systèmes LiDAR Mobiles. Master thesis. *Université Laval,* **2018**, Québec, Canada, 111 pages.

Cassol, W.N.; Daniel, S.; Guilbert, É. A Segmentation Approach to Identify Underwater Dunes from Digital Bathymetric Models. *Geoscience* **2021**, *11*, 361. https://doi.org/10.3390/geosciences11090361.

Castilla, G.; Hay, G.J. Image objects and geographic objects. *In Object-Based Image Analysis, Lecture Notes in Geoinformation and Cartography*; Blaschke, T., Lang, S., Hay, G.J., Eds.; Springer: Berlin/Heidelberg, Germany, **2008**; Chapter 1.5, 20 pages; doi:10.1007/978-3-540-77058-9_5.

Cheng, H.Q.; Chen, W.; Li, J.F.; Jiang, Y.H.; Hu, X.; Zhang, X.L.; Zhou, F.N.; Hu, F.X.; Stive, M.J.F. Morphodynamic changes of the Yangtze Estuary under the impact of the Three Gorge Dam, of estuarine engineering interventions and of climate-induced sea level rise. *Earth Planet. Sci. Lett.* **2022**, *580*, 117385. https://doi.org/10.1016/j.epsl.2022.117385.

Cheng, H.Q.; Kostaschuk, R.; Shi, Z. Tidal currents, bed sediments, and bedforms at the South Branch and the South Channel of the Changjiang (Yangtze) Estuary, China: Implications for the ripple-dune transition. *Estuaries* **2004**, *27*, 861–866.

Comité de Concertation Navigation de Saint Laurent Vision 2000. Stratégie de Navigation Durable Pour le Saint-Laurent; Ministère des Transports du Québec et Pêches et Océans Canada: Québec, QC, Canada **2004**; 114 pages.

Courrech du Pont, S. Dune morphodynamics. *Comptes Rendus Physique*, **2015**, 6. Pp. 118-138. http://dx.doi.org/10.1016/j.crhy.2015.02.002

Debese, N. Bathymétrie. Sondeurs, traitements des données, modèles numériques de terrain. Cours et exercices corrigés. *TECHNOSUP, éditions ellipses* **2013**. 404 pages.

Debese, N.; Jacq, J.J.; Garlan, T**.** Extraction of sandy bedforms features through geodesic morphometry**.** *Geomorphology* **2016**, 267, 82–97, doi:10.1016/j.geomorph.2016.05.013.

Debese, N.; Jacq, J.-J.; Degrendele, K.; Roche, M. Toward Reliable Volumetric Monitoring of Sandbanks. In *Geomorphometry*; Elsevier Science: Boulder, CO, USA, **2018**.

Deng, Y. New trends in digital terrain analysis: Landform definition, representation, and classification. *Prog. Phys. Geogr.* **2007**, 31, 405–419.

Di Stefano, M.; Mayer, L.A. An automatic procedure for the quantitative characterization of submarine bedforms. *Geosciences* **2018**, 8, 28, doi:10.3390/geosciences8010028.

Diesing, M.; Thorsnes, T. Mapping of cold-water coral carbonate mounds based on geomorphometric features: An object-based approach. *Geosciences* **2018**, 8, 38, doi:10.3390/geosciences8020034.

van Dijk, T.A.G.P.; van Dalfsen, J.A.; Van Lancker, V.; van Overmeeren, R.A.; van Heteren, S.; Doornenbal, P.J. 13—Benthic Habitat Variations over Tidal Ridges, North Sea, the Netherlands. In *Seafloor Geomorphology as Benthic Habitat*; Elsevier: Amsterdam, The Netherlands, **2012**; pp. 241–249, ISBN 9780123851406. https://doi.org/10.1016/B978-0-12-385140-6.00013-X

Dragut, L.; Blaschke, T. Automated classification of landform elements using object-bases image analysis. *Geomorphology* **2006**, 81, 330–344, doi:10.1016/j.geomorph.2006.04.013.

Dragut, L.; Tiede, D.; Levick, S.R. ESP: A tool to estimate scale parameter for multiresolution image segmentation of remotely sensed data. *Int. J. Geogr. Inf. Sci*. **2010**, 24, 859–871, doi:10.1080/13658810903174803.

Drapeau, G. Dynamique sédimentaire des littoraux de l'estuaire du Saint Laurent. *Géographie Phys. Quat.* **1992**, *46*, 233–242. https://doi.org/10.7202/032907ar.

Dupont, V. Élaboration D'une Méthode D'extraction de Plans par Croissance de Régions Dans un Nuage de Points Bathymétriques Servant à Alimenter des Estimateurs D'erreur Hydrographique. Master Thesis, *Université Laval*, **2020,** Québec, QC, Canada. 120 pages.

Elbelrhiti, H. ; Andreotti, B. and Claudin, P. Barchan dune corridors: field characterization and investigation of control parameters. *Journal of Geophysical Research*, **2008**, 113, F02S15. 21 pages. doi:10.1029/2007JF000767

Ewing, R. C. ; Kocurek, G. and Lake, L. W. Pattern analysis of dune-field parameters*. Earth Surf. Process. Landforms*, **2006**, 31. Pp. 1176-1191. DOI: 10.1002/esp.1312

Ferret, Y. Morphodynamique de Dunes Sous-Marines en Contexte de Plate-Forme Mégatidale (Manche Orientale). Approche Multi-Échelles Spatio-Temporelles. Interfaces Continentales, Environnement. Ph.D. Thesis, *Université de Rouen*, **2011,** Mont-Saint-Aignan, France.

Franzetti, M. ; Le Roy, P. ; Delacourt, C. ; Garlan, T. ; Cancouet, R. ; Sukhovich, A. ; and Deschamps, A. Diant dunes morphologies and dynamics in a deep continental shelf environment : Example of the banc du four (Western Brittany, France). *Marine Geology 346*, **2013**. Pp. 17-30.

Garajeh, M. K.; Feizizadeh, B.; Weng, Q.; Moghaddan, M. H. R. and Garajeh, A. K. Desert landform detection and mapping using a semi-automated object-based image analysis approach. *Journal of Arid Environments*, **2022**, 199, 104721. 14 pages.

Garlan, T. Study on Marine Sandwave Dynamics. *Int. Hydrogr. Rev*. **2007**, 8, 26–37.

Garlan, T. GIS and Mapping of Moving Marine Sand Dunes. Presented at the 24th International Cartography Conference, (ICC 2009), Santiago, Chile, 15–21 November **2009**.

Godin, A. The calibration of shallow water multibeam echo-sounding systems. *Department of Geodesy and Geomatics Engineering. University of New Brunswick* **1998**. Pp. 76-120.

Goulden, T. Prediction of error due to terrain slope in LiDAR observations. Technical Repport n° 265. *Department of Geodesy and Geomatics Engineering* **2009**. *University of New Brunswick*. 150 pages.

Goulden, T. and Hopkinson, C. The forward propagation of integrated system component error within airborne LiDAR data. *Photogrammetry Engineering & Remote Sensing* **2010**, 76, n°5, pp. 589-601.

Guilbert, E.; Moulin, B. Towards a Common Framework for the Identification of Landforms on Terrain Models. *ISPRS Int. J. Geo-Inf*. **2017**, 6, 12.

Guilbert, E.; Moulin, B.; Cortés Murcia, A. A conceptual model for the representation of landforms using ontology design patterns. ISPRS Annals of the Photogrammetry, Remote Sensing and Spatial Information Sciences, Volume III-2. *In Proceedings of the XXIII ISPRS Congress*, Prague, Czech Republic, 12–19 July **2016**; 8 pages.

Gutierrez, R.R.; Abad, J.D.; Parsons, D.R.; Best, J.L. Discrimination of bed form scales using robust spline filters and wavelet transforms: Methods and application to synthetic signals and bed forms of the Rio Paraná, Argentina. *J. Geophys. Res. Earth Surf*. **2013**, 118, 1400–1419, doi:10.1002/jgrf.20102.

Hains, D.; Bergmann, M.; Cawthra, H. C.; Cove, K.; Echeverry, P.; Maschke, J.; Mihailov, M. E.; Obura, V.; Oei, P.; Pang, P. Y.; Ponce, R. and Roperez, J. Hydrospatial…A global movement. *International Hydrographic Review*, **2021**. Pp. 147-153.

Hare, R. Depth and position error budgets for multibeam sounding. *International Hydrographic Review* **1995***,* Monaco, LXXII(2), pp. 37-69.

Hare, R. Error Budget analysis for US Naval Oceanographic Office (NAVOCEANO) Hydrographic survey systems. *University of Southern Mississippi*, **2001**. 155 pages.

Hare, R., Eakins, B. and Amante, C. Modelling bathymetric uncertainty. *International Hydrographic Review* **2011**. November 2011. Pp. 31-42.

Hendershot, M. L.; Venditti, J. G.; Bradley, R. W.; Kostachuk R. A.; Church, M. and Allison, M. A. Response of low-angle dunes variable flow. *Sedimentology*, 63. **2016**. DOI : 10.1111/sed.122363

Hudon, C. and Carignan, R. Cumulative impacts of hydrology and human activities on water quality in Sr. Lawrence River (Lake Saint-Pierre, Quebec, Canada). *Canadian Journal of fisheries and aquatic sciences*, **2008**, vol. 65. Pp. 1165-1180.

Hughes Clarke, J. E. The impact of acoustic imaging geometry on the fidelity of seabed bathymetric models. *Geosciences* **2018**, 8, 109. DOI: 10.3390/geosciences8040109

International Hydrographic Organization. Standards for Hydrographic Surveys. *IHO publication n°44* **2020**. 6th edition, 49 pages.

Ismail, K.; Huvenne, V.A.I.; Masson, D.G. Objective automated classification technique for marine landscape mapping in submarine canyons. *Mar. Geol*. **2015**, 362, 17–32, DOI:10.1016/j.margeo.2015.01.006.

Jasiewicz, J.; Stepinski, T.F. Geomorphons—A pattern reconigtion approach to classification and mapping of landforms. *Geomorphology* **2012**, *182*, 147–156. DOI : 10.1016/j.geomorph.2012.11.005.

Joint Committee for Guides in Metrology. Evaluation of measurement data – Guide to the expression of uncertainty in measurement. First edition, September **2008**. 134 pages.

Kenyon, N.H. Sand Ribbons of European tidal Seas. *Mar. Geol.* **1970**, *9*, 25–39.

Knaapen, M.A.F. Sandwave migration predictor based on shape information. *J. Geophys. Res.* **2005**, *110*. DOI :10.1029/2004JF000195.

Kongsberg. EM 2040 Multibeam Echosounder, **2021** 2 pages, viewed 07th December 2021, https://www.kongsberg.com/contentassets/e8fa4f09f25f4b1e86eda52cc1355dc7/em-2040---mkii-data-sheet.pdf

Landeghem, K.J.J.; Wheeler, A.J.; Mitchell, N.C.; Sutton, G. Variations in sediment wave dimensions across the tidally dominated Irish Sea, NW Europe. *Mar. Geol.* **2009**, 263, 108–119. DOI :10.1016/j.margeo.2009.04.003

Le Bot, S. Morphodynamique de Dunes Sous-Marines Sous Influence des Marées et des Tempêtes. Processus Hydro-Sédimentaires et Enregistrement. Exemple du Pas-de-Calais. Ph.D. Thesis, *Université de Lille I*, **2001**, Villeneuve-d'Ascq, France.

Lebrec, U.; Riera, R.; Paumard, V.; O'Leary, M.J.; Lang, S.C. Automatic Mapping and Characterisation of Linear Depositional Bedforms: Theory and Application Using Bathymetry from the North West Shelf of Australia. *Remote Sens.* **2022**, *14*, 280. DOI: 10.3390/rs14020280.

Lecours, V.; Dolan, M.F.J.; Micallef, A.; Lucieer, V.L. A review of marine geomorphometry, the quantitative study of the seafloor. *Hydrol. Earth Syst. Sci*. **2016**, 20, 3207–3244, DOI: 10.5194/hess-20-3207-2016.

Lefebvre, A.; Paarlberg, A.J.; Winter, C. Characterising natural bedform morphology and its influence on flow. *Geo-Mar. Lett.* **2016**, *36*, 379–393. DOI: 10.1007/s00367-016-0455-5.

López-Ornelas, E. High resolution images: Segmenting, extracting information and GIS integration. *World Acad. Sci. Eng. Technol.* **2009**, 54, 172–177.

Lucieer, V., Huang, Z. and Siwabessy, J. Analysing uncertainty in multibeam bathymetric data and the impact on derived seafloor attributes. *Marine Geodesy*, **2016**. 42 Pages. DOI: 10.1080/01490419.2015.1121173

Lucieer, V.; Lecours, V.; Dolan, M.F.J. Charting the course for future developments in marine geomorphometry: An introduction to the special issue. *Geosciences* **2018**, 8, 477, DOI: 10.3390/geosciences8120477.

Lurton, X. Theoretical modelling of acoustical measurement accuracy for swath bathymetric sonars. *International Hydrographic Review* **2003**, pp 17-30.

Lurton, X. and Augustin, J. M. A measurement quality factor for swath bathymetry sounders. *IEEE Journal of Oceanic Engineering*, **2010**, 35, 4. Pp. 852-862.

van der Mark, C.F.; Blom, A. A New & Widely Applicable Bedform Tracking Tool; University of Twente: Enschede, The Netherlands, **2007**; 44 pages.

Masetti, G.; Mayer, L.A.; Ward, L.G. A Bathymetry- and Reflectivity-Based Approach for Seafloor Segmentation. *Geosciences* **2018**, 8, 14, DOI:10.3390/geosciences8010014.

Naankeu Wati, G., Geldof, J. B. and Seube, N. **2016**. Error Budget Analysis for surface and underwater survey system. *International Hydrographic Review*, pp 21-46.

Nguyen, T.H.; Daniel, S.; Guériot, D.; Sintès, C.; Le Caillec, J.M. Super-resolution-based snake model—an unsupervised method for large-scale building extraction using airborne LiDAR data and optical image. *Remote Sens.* **2020**, 12, 1702, DOI:10.3390/rs12111702.

Nichols, G. Sedimentology and Stratigraphy, 2th ed.; Chapter 4 Processes of transport and sedimentary structures; *Wiley-Blackwell, A John Wiley & Sons,Ltd., Publication: West Sussex, UK*, **2009**; pp. 44–68.

Ogor, J. Design of Algorithms for the Automatic Characterization of Marine Dune Morphology and Dynamics. Ocean, Atmosphere. Ph.D. Thesis, *ENSTA-Bretagne*, **2018,** Brest, France.

d'Oleire-Oltmanns, S.; Eisank, C.; Dragut, L.; Blaschke, T. An object-based workflow to extract landforms at multiple scale from two distinct data types. *IEEE Geosci. Remote Sens. Lett*. **2013**, 10, 947–951

Organisation Hydrographique Internationale. Manuel d'hydrographie. Edition 1.0.0. *Bureau Hydrographique International, Monaco*, **2011**. 31 Pages.

Organisation Hydrographique Internationale. S-100 – Universal Hydrographic Data Model. Edition 4.0.0, **2018**. Part 5 – Feature Catalogue. Pp. 215 – 237.

Parsons, D.R.; Best, J.L.; Orfeo, O.; Hardy, R.J.; Kostaschuk, R.; Lane, S.N. Morphology and flow fields of three-dimensional dunes, Rio Paranà, Argentina: Results from simultaneous multibeam echo sounding and acoustic Doppler current profiling. *J. Geophys. Res.* **2005**, *110*, F04S03. DOI: 10.1029/2004JF000231

Schaer, P.; Skaloud., J.; Landtwing, S. and Legat, K. Accuracy estimation for laser point cloud including scanning geometry. *5th International symposium on mobile mapping technology*, **2007**. Padova, Italy, May 29-31. 8 pages.

Seube, N. and Keyetieu, R. Multibeam Echo Sounders-IMU Automatic Boresight Calibration on Natural Surfaces. *Marine Geodesy* **2017**, 40:2-3, pp. 172-186, DOI: 10.1080/01490419.2017.1310156

Shumack, S.; Hesse, P. and Farebrother, W. Deep learning for dune pattern mapping with the AW3D30 global surface model. *Earth Surf. Process. Landforms*, **2020**, 45. Pp. 2417-2431. DOI: 10.1002/esp.4888

Soille, P. and Pesaresi, M. Advances in mathematical morphology applied to geosciences and remote sensing. *IEEE Trans. Geosci.* Remote Sens. **2002**, 40, 2042–2055.

Sowers, D.C.; Masetti, G.; Mayer, L.A.; Johnson, P.; Gardner, J.V.; Armstrong, A.A. Standardized Geomorphic Classification of the Seafloor within the United States Atlantic Canyons and Continental Margin. *Front. Mar. Sci*. **2020**, 7, 9, DOI:10.3389/fmars.2020.00009.

Spectra Geospatial. SP90m GNSS receiver **2020**, 3 pages, viewed 13th June 2021.

Thibaud, R.; Del Mondo, G.; Garlan, T.; Mascret, A.; Carpentier, C. A Spatio-Temporal Graph Model for Marine Dune Dynamics Analysis and Representation. *Trans. GIS,* **2013**, 17, 742–762, DOI:10.1111/tgis.12006.

Tidd, R. A. The impact of varying seafloor topographies, and object geometris on resolution for multibeam echosounders and multi-angle swath bathymetry systems. *Proceedings of OCEANS **2005** MTS/IEEE*, Washington DC, pp. 2224-2227 Vol. 3, DOI: 10.1109/OCEANS.2005.1640096.

Venditti, J.G. Bedforms in sand-bedded rivers. *Treatise on Geomorphology, Fluvial Geomorphology*, **2013.** Editor in chief Shroder, J.F. and Wohl, E, volume 3. Pp. 137–162.

Wood, J. The Geomorphological Characterization of Digital Elevation Models. Ph.D. Thesis, University of Leicester, Leicester, UK, **1996**.

Yan, G.; Cheng, H.Q.; Jiang, Z.Y.; Tengm, L.Z.; Tang, M.; Shi, T.; Jiang, Y.H.; Yang, G.Q.; Zhou, Q.P. Recognition of fluvial bank erosion along the main stream of the Yangtze River. *Engineering* **2021**. 19 pages. DOI:/10.1016/j.eng.2021.03.027

Yang, Z.; Qian, G.; Dong, Z.; Tian, M. and Lu, J. Migration of barchan dunes and factors that influence migration in the Sanlongsha dune field of the Northern Kumtagh sand sea, China. *Geomorphology*, **2021**, 378, 107615. 12 pages. DOI: 10.1016/j.geomorph.2021.107615

Annexe A

Cette annexe a pour objectif de recenser les principales fonctions disponibles dans Matlab qui ont été utilisées dans l'approche de segmentation proposée dans le chapitre 2 de la thèse. Veuillez noter que l'approche de caractérisation considère les résultats de la segmentation et utilise différentes fonctions statistiques disponibles dans Matlab. Les principales fonctions utilisées à chaque étape de l'approche de segmentation sont représentées à la Figure A.1 et A.2. L'entièreté des codes développés dans ce projet de doctorat est disponible sur le site de dépôt de données : https://github.com/wncassol/PhDCode.

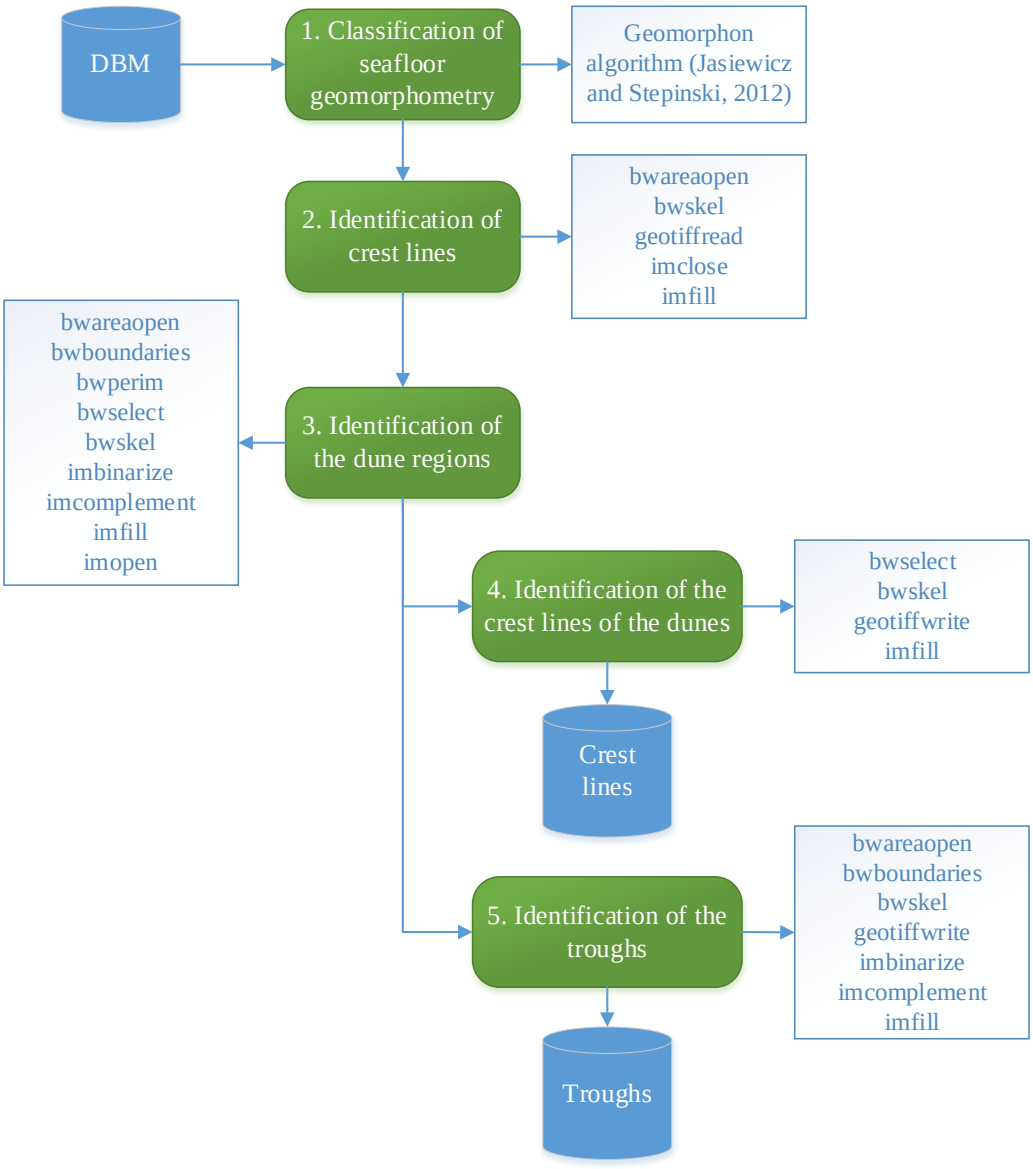

Figure A.1 –Fonctions de morphologie mathématique et de traitement d'image disponibles dans Matlab qui ont été utilisées dans la première phase de segmentation des dunes (voir la section 2.6.2.1 *Phase I – Salient*

features identification). Les données intrants et les résultants sont représentés en bleu, les différentes étapes de traitement en vert et en blanc les fonctions Matlab utilisées en chaque étape.

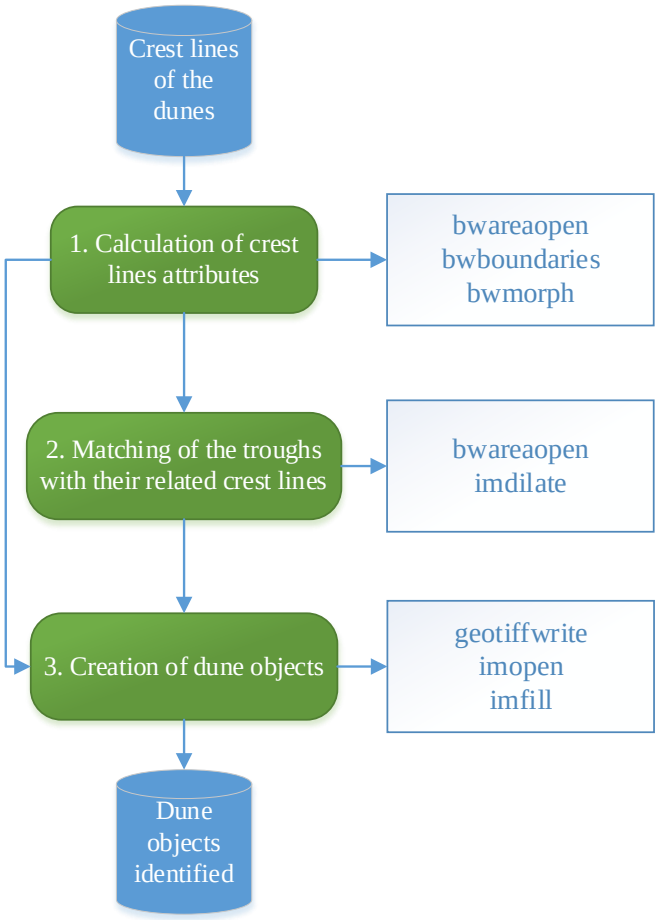

Figure A.2 - Fonctions de morphologie mathématique et de traitement d'image disponibles dans Matlab qui ont été utilisées dans la deuxième phase de segmentation des dunes (voir la section 2.6.2.2 *Phase II – Dune identification*). Les données intrants et les résultants sont représentés en bleu, les différentes étapes de traitement en vert et en blanc les fonctions Matlab utilisées en chaque étape.